Effects of Global Climate Change on the Recruitment of Anchovy in the Southern Benguela Upwelling System

Shona Linda Young

Submitted in fulfilment of the requirements for the degree of Master of Philosophy in the Faculty of Humanities (Department of Environmental and Geographical Science), University of Cape Town

Supervisors: Assoc. Prof. Bruce C. Hewitson
Dr Anthony J. Richardson

This thesis is dedicated to
Mum and Dad. Thank you both
for everything.

ACKNOWLEDGEMENTS

Firstly, I would like to thank my two supervisors for their involvement over the past three years. The financial assistance and opportunities provided to me by my supervisor, Associate Professor Bruce Hewitson are gratefully appreciated, as well as his advice and comments on my work. Thank you also to Dr Anthony Richardson in the Oceanography Department, UCT, for his constant enthusiasm and help along the way and the countless number of drafts he edited. I would also like to thank Chris Jack for all his assistance with the climate modelling and my data. Thank you to St John for all his help with formatting my thesis at the final stages.

Thanks also to Dr Alan Boyd, Dr Larry Hutchings and Dr Lynne Shannon at Sea Fisheries for their input at the initial stages of my project. I would like to thank Dr Frank Shillington in the Oceanography Department for his invaluable comments and useful discussions. Thank you to Dr Claude Roy and Dr Andrew Bakun for their useful comments. Thank you to Shirley Butcher for her GIS help and to Dr Debbie Hudson for her help with GRADS. I would also like to thank everyone in the CSAG for the help I received along the way and the tearoom chats.

I would like to thank all my friends who have been patient and supporting and let me moan about my complaints when things got tough. Those especially worth mentioning are Zoë (who went through her Masters at the same time as me but finished way before), Jax (for all the cups of coffee and sympathetic chats), Shayne (for having more faith in me than I deserved), Lindi (for helping me through the final stages), Kev, Shane, Mel, Di and Lois, as well as Scott and Bonny. A special thanks to Gailyn, my sister and friend who was always there for me.

Thank you to my parents for their constant encouragement, support and love throughout my studies.

And lastly thank you Ant. Without you I would still be sitting at my computer trying to finish. Thank you for all the encouragement and optimism, when I wasn't able to see the light at the end of the tunnel. Your constant editing of drafts, advice and motivational speeches (and eagerness to get me into the job market!!) have enabled me to finally reach the end.

ABSTRACT

Changes to global climate patterns, as predicted by many climatologists, will impact on ecosystems in numerous ways. The nutrient-rich waters of marine upwelling environments enable prolific plankton growth, which in turn supports vast shoals of pelagic fish. The nutrient supply is dependent on the strength and direction of winds, which govern the upwelling process as well as turbulence. A change in climate may thus affect the food supply and feeding conditions required by pelagic fish populations.

This thesis investigates predicted changes in wind patterns in the southern Benguela system and assesses how these changes may impact on the recruitment of the Cape anchovy, *Engraulis capensis*. A general circulation model (NCAR Climate System Model) is used to compare a future simulation under double CO_2 conditions with a simulation of the present day wind regime. Climate change effects on anchovy in the other main upwelling systems, off the coasts of California, Peru and Morocco are also examined.

Wind speeds and turbulence off the Agulhas Bank in the southern Benguela system are expected to remain suitable and potentially become even more conducive to spawning in the future. The results show similar mean wind speeds to present day values, a decrease in mean turbulence, a decrease in the frequency of extreme wind speeds and a decrease in the frequency of extreme turbulence during the anchovy spawning season (i.e. September-February). An increase in Lasker events is expected at the Eastern Bank Grid Cell, which suggests that this area may become the preferred spawning habitat in the future. The Cape Town Grid Cell also shows suitable conditions in the future simulation for anchovy spawning and may thus become an alternative spawning location. The West Coast shows an increase in alongshore wind stress and thus an increase in upwelling in the future simulation from November – February. This is likely to increase planktonic food availability and ultimately anchovy recruitment.

Future simulations from the Climate System Model show that the upwelling systems off the coasts of California, Peru and Morocco are likely to continue supporting anchovy spawning and may become even more suitable in terms of wind and turbulence regimes.

TABLE OF CONTENTS

LIST OF FIGURES

ABBREVIATIONS REFERRED TO IN THE TEXT

CSM	Climate System Model
GCM	General Circulation Model
IPCC	Intergovernmental Report on Climate Change
NCAR	National Center for Atmospheric Research
NCEP	National Center for Environmental Programming
OEW	Optimal Environmental Window
SAHP	South African High Pressure System

CHAPTER ONE

Setting the Scene

1.1 Global Climate Change

In the geological past, climates have changed radically and it is certain that they will change again in the future (Bernal 1991). The climate system consists of various components including the atmosphere, the ocean, ice and snow cover, the land surface and features associated with it, and all the interactions among these components (IPCC Report 2001) (Fig. 1.1). Climate change and variability are related to a complex set of causative and modulating factors that may be divided into two groups: external and internal forces (IPCC Report 1996). External forces act on the ocean-atmosphere system and include plate tectonics, orogenic activity, tidal forcing, solar output and orbital geometry. Internal changes exist within the system itself and include variations in the gas components of the atmosphere, changes in albedo, changes in the amount of heat stored and redistributed in the oceans and changes in the volume of polar ice.

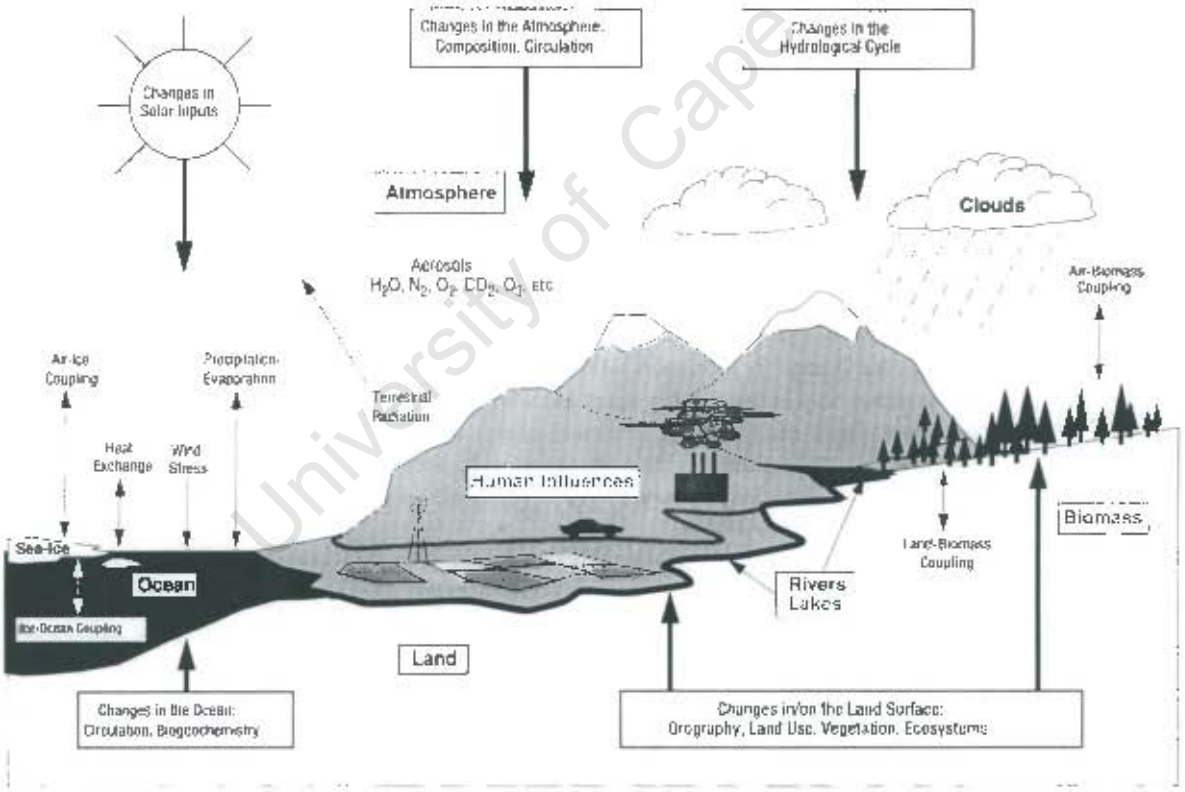

Figure 1-1 Components of the global climate system and the associated processes and interactions (IPCC Report 1996)

The major internal force causing global climate change is the amount of greenhouse gas in the atmosphere. The most important greenhouse gas is carbon dioxide (CO_2). Global

carbon dioxide concentrations have been increasing at a rate of ~1.3 parts per million by volume per year (ppmv) for the last 35 years (Fig. 1.2) (IPCC Report 1996) and have showed a 31% increase since 1750 (IPCC Report 2001). It is estimated that if CO_2 emission rates are maintained at 1994 levels, then concentrations will reach double pre-industrial values of 280 ppmv by the end of the 21st century. These increases (i.e. in the 20th century) are more rapid than any observed increases in the past (Neftel *et al.* 1988). An increase in CO_2 decreases the amount of outgoing long wave radiation, a phenomenon known as the enhanced greenhouse effect. This alters the radiative balance and the energetics of the atmosphere, which impacts numerous other factors such as wind and rainfall (IPCC Report 1996).

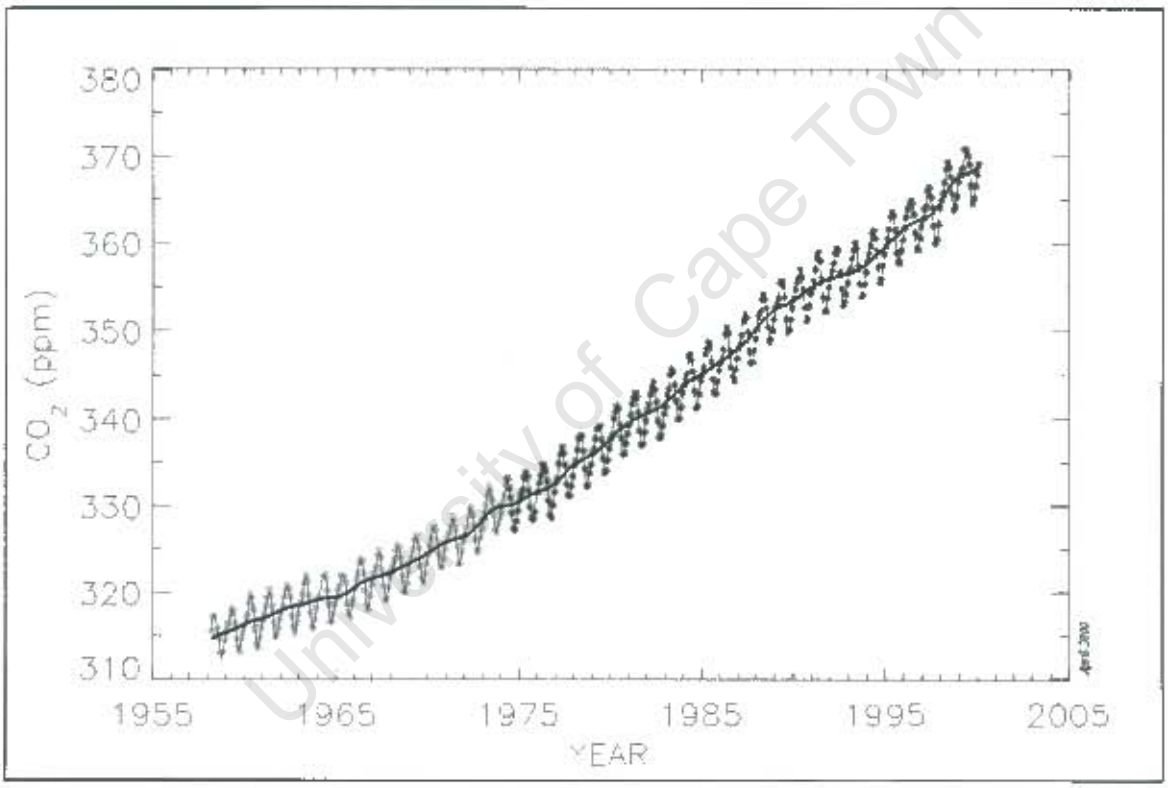

Figure 1-2 Mean monthly atmospheric carbon dioxide increases from Mauna Loa from 1958-2000 (NOAA and SIO 2000)

The increase in CO_2 emissions is thought to be directly responsible for part of the 0.3 to 0.6°C increase in global atmospheric temperatures over the last century (IPCC Report 1992). In the past 40 years, global atmospheric temperatures have increased by about 0.2 to 0.3°C (IPCC Report 1996). On a global scale it is likely that the 1990s was the warmest decade since records began (IPCC Report 2001). It is expected in all cases that the rate of

warming in the future will be greater than any changes in the last 10 000 years (IPCC Report 1996).

A rise in global sea levels is one of the principle consequences of global warming. Sea levels have risen 0.1-0.2 m over the past 100 years (IPCC Report 2001). Over the past two millennia global sea levels have been relatively constant and only varied within a range of ~20-30 cm (Varekamp *et al.* 1992). The large rise recently is a consequence of the thermal expansion of the water in the oceans and the increased melting of glaciers. As there appears to be a twenty-year lag between a rise in temperature and a rise in sea levels (Gornitz *et al.* 1982), the current rate of rising sea levels reflects the increase in temperature in the 1980s. Thus, the present increase in temperatures has yet to be reflected in sea levels (Kerr 1990). Therefore, even if there is a decrease in present day CO_2 emissions, a rise in sea levels will still take place because of lags in the climate system (IPCC Report 1990). Future estimates of sea level rise remain uncertain, although a rise of 0.09-0.88 m is projected between 1990 and 2100 (IPCC Report 2001). This rate of expected rise is more rapid than any rise in sea level in the past.

Studies by the Hadley Centre (UK Meterological Office) have shown that sea surface temperature increases along with air temperature (IPCC Report 1996). Temperature rise in the ocean is, however, not as rapid or to the same degree as in the atmosphere, owing to the greater thermal inertia of the ocean. This rise in sea temperature is likely to be the most dominant effect of climate change on the ocean.

This increase in sea surface temperature could have a profound effect on the global climate system because of the feedback from the ocean system (IPCC Report 1996). Oceanic currents driven by geographic and seasonal patterns of heat at the earth's surface and in the lower atmosphere distribute heat from the tropics to colder regions via a global heat 'conveyor belt'. Global warming of the atmosphere, however, may alter these circulation patterns. Moreover, it is unlikely that the ocean-atmosphere system will respond linearly to increasing greenhouse gases, but may undergo sharp, worldwide reorganisation, switching from one stable state to another (Bakun 1990).

Another effect of global climate change is the depletion of stratospheric ozone and the resultant increase in ultraviolet (UV) radiation (IPCC Report 1996). This expected increase in UV radiation is of great concern because of the large number of important species that spend all or part of their life cycle near the ocean surface (Bakun 1996). Increases are likely to threaten important sea-surface processes. Primary productivity, for example, decreases when exposed to UV radiation and the growth of marine micro-organisms is inhibited (Cullen and Lesser 1991, Cullen *et al.* 1992). Marine species also respond differently to UV radiation, resulting in shifts in community structures that may alter the dynamics of marine food webs (Hardy 1997, IPCC Report 1996, Karentz 1994).

1.2 Climate Change and Clupeoids

Clupeoids are small, schooling fish inhabiting the upper layers of the ocean (Shannon *et al.* 1996). Clupeoids belong to the order Clupeiformes, which is made up of two groups: clupeids (sardine, herring, round herring and sardinella) and engraulids (anchovy). Clupeoids undergo large natural fluctuations in spatial range and stock size as a result of changes in recruitment (the number of fish recruiting each year to the adult population) success caused by environmental variability (Beverton 1990, Lluch-Belda *et al.* 1992).

Fishery scientists have focussed on attempting to understand processes controlling recruitment in pelagic fish. Although a relationship between the number of spawning adults and the number of recruits is automatically assumed in stock recruitment and fisheries models, these models have been largely unsuccessful (Bakun 1996). In the past two decades it has been suggested by authors, such as Lasker and Sherman (1981), that spawner-recruit relationships cannot be examined without taking other factors (e.g. turbulence) into account. Indeed, it has been acknowledged that there is no single variable responsible for determining successful recruitment (Campbell and Graham 1991).

The sensitivity of clupeoids to environmental perturbations as well as their ecological importance (discussed in further detail in section 1.4) makes them ideal subjects for studying possible effects of climate change on the pelagic system. There are several reasons for the susceptibility of clupeoids to environmental fluctuations:

- They are an *r*-selected species, being characterised by being small, having early sexual maturity and high fecundity (Lalli and Parsons 1993).

- They feed on short, plankton-based food chains, which may be affected by changes in upwelling that may result from global climate change.
- Recruitment is controlled by egg and larval survival, which is highly dependent upon the ocean climate and could be directly influenced by increasing ocean temperature (Bernal 1991).
- Recruitment is limited by wind speeds that are too high or too weak (i.e. optimal environmental window) (see section 1.6), with reproductive success and hence recruitment highest at an intermediate wind intensity (Cury and Roy 1989).

An example of how clupeoids are susceptible to abiotic factors is the effect of small changes in water temperature, which could influence the spawning potential of adult fish (Hunter and Macewicz 1985). Firstly, a decrease in water temperature can cause female clupeoids to resorb their eggs, a condition known as ovarian atresia. Secondly, larval retention areas depend on the existence of precise circulation patterns that may be altered by sea temperature changes (Bakun 1996). Thirdly, warming of the surface layer will increase stratification and if other factors remain equal, this change may enhance the formation of high food concentration layers required for larval feeding. These stratified layers are key food resource areas for larval survival, since average concentrations of particles in the ocean do not provide enough food for maintaining a positive daily energy budget for larvae (Bakun 1990). Winds are another abiotic factor which greatly affect larval survival. In particular, strong winds can destroy the stable layer of food particles required for first feeding larvae (Lasker 1975). Strong winds can also result in larvae being transported too far offshore and thus not reaching their food-rich nursery grounds (Bakun and Parrish 1980). The changes in the climate system could thus have a direct effect on clupeoids, which in turn could affect the ecological balance in the ocean and the financial balance in the fishing industry (discussed in further detail in section 1.4).

1.3 Upwelling Systems and Clupeoids

Clupeoids feed mainly on plankton and are thus located in the shallow coastal regions of upwelling areas. The main upwelling areas of the world are on the eastern boundaries of the oceans, where there are strong equatorward winds (Huntsman and Barber 1977, Wooster and Reid 1963). Upwelling systems are found off the west coasts of Peru (Humboldt Current), California (California Current), North-West Africa (Canary Current)

and Namibia and South Africa (Benguela Current) (Cury and Roy 1989). Equatorward winds cause offshore transport of the surface layers as a result of Ekman drift (Mann and Lazier 1991). Cool water containing nutrients, particularly nitrate and phosphate then upwells into the euphotic layer, replacing the water that has moved offshore. This nutrient-rich upwelled water promotes the growth of phytoplankton, which supports large standing stocks of zooplankton. In turn, this supports large stocks of planktivorous pelagic fish (Cushing 1969). In upwelling areas high primary productivity supports large commercial fisheries (Crawford *et al.* 1987).

The Benguela system, situated along the West Coast of southern Africa, is part of the South Atlantic gyre. It extends from as far south as the area of interaction with the Agulhas Current to the tropical water regime of southern Angola, with the offshore boundary being fairly open ended (Nelson and Hutchings 1983, Shannon 1985). The oceanography of the Benguela Current (south of about 15°) is similar to other eastern boundary current regions off California, Peru and North-West Africa, in that it is dominated by coastal upwelling (Shannon 1985). Wind-induced upwelling occurs at many areas off the West Coast, with Lüderitz in Namibia being the major upwelling area. Here, a semi-permanent tongue of cool water acts as a barrier, separating the Benguela into two regions: the northern and southern Benguela. It is the latter region that forms the area of focus in this thesis. In this region, there are wind-driven upwelling centres off the Cape Peninsula, Cape Columbine and Hondeklip Bay (Nelson and Hutchings 1983).

1.4 Financial and Ecological Importance of Clupeoids

Clupeoids are of immense commercial importance. Since 1989, approximately one hundred million tons of fish and shellfish have been removed from the sea and inland waters each year (Faure and Cury 1998). Of this, 75% represents marine catch, with one third of this catch made up of pelagic fish (Fig. 1.3). Although coastal upwelling areas represent less than 0.1% of the ocean surface, they are some of the most productive oceanic regions and make a large contribution to the fisheries world-wide (Pauly and Tsukayama 1987). An average of 18.2 million tons of clupeoids were caught per year world-wide in the 1980s, amounting to 20% of the world's total marine fish catch (Armstrong and Thomas 1989).

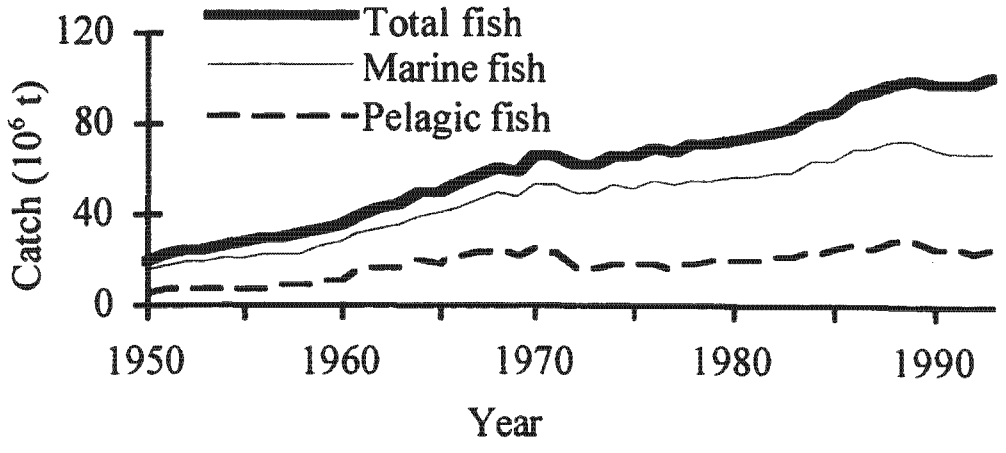

Figure 1-3 Total world fish catch showing marine and pelagic fish catches from 1950-1995 (FAO 1995)

The two most commercially important clupeoids in the southern Benguela are anchovy and sardine. Pelagic fish generate approximately R403 million per annum for the South African fishing industry (Booth and Hecht 2000). In the southern Benguela upwelling system between 2-3 million clupeoids are caught annually (Hutchings 1994). The clupeoid fishing industry is also responsible for the direct employment of approximately 6000 people (Hutchings and Boyd 1992).

In upwelling areas there is often an important intermediate level occupied by plankton-feeding pelagic fish which is dominated by one, or sometimes two, species of fish (i.e. anchovy and/or sardine) (Bakun 1996). There are usually a larger number of species at the bottom and top trophic layers (Cury *et al.* 2000). At the intermediate level, pelagic fish feed on lower trophic levels (i.e. top-down control on zooplankton) and are fed on by higher trophic layers (i.e. bottom-up control of predators). In the Southern Benguela, such predators include larger fish (e.g. hake), seabirds (e.g. Cape Gannet) and marine mammals (e.g. seals and dolphins). It is often noted that the collapse of small pelagic fish populations is accompanied by sharp declines in the marine bird and mammal populations that depend on them for their source of food (Crawford 1987, Hutchings *et al.* 2000).

Anchovy and sardine show alternating periods of dominance in most upwelling systems and exhibit high population variability (Kawasaki *et al.* 1991). In the southern Benguela system, sardine landings dominated until the mid 1960s, with the highest landing recorded in 1962 (410 200 tons) (Crawford *et al.* 1987). After 1966, however, sardine landings began to decrease and anchovy became the mainstay of the South African purse-seine fishery (Crawford *et al.* 1987). For example in 1967, sardine landings were 69 700 tons and anchovy were 270 600 tons. In 1974 a peak anchovy catch of 350 000 tons was recorded. Between 1972 and 1985 average anchovy catches were 265 000 tons, never falling below 200 000 tons (Crawford *et al.* 1987). From 1985 to 1999 anchovy and sardine catches did not exceed 17 000 and 31 000 tons respectively (Fig. 4.1). In 2000 a peak anchovy catch of 414 000 tons was recorded (MCM Unpublished data). Cape anchovy, *Engraulis capensis* thus still remains the dominant species landed in the southern Benguela system.

Fluctuations in the anchovy resource, in particular, are likely to have adverse impacts on the industry. Predicting changes that may occur in anchovy populations is consequently of importance for this industry. An assessment of possible scenarios for future wind regimes and the effects on anchovy recruitment could assist in planning fish monitoring programmes and identifying the key abiotic factors at play.

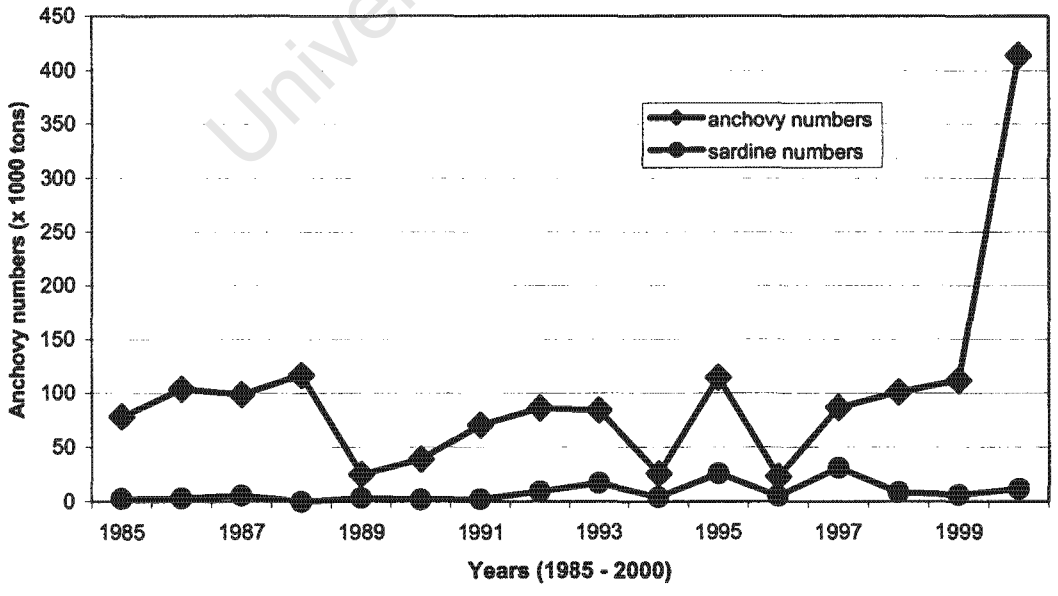

Figure 1-4 Fluctuations in anchovy numbers from recruit survey data in the southern Benguela system from 1985-2000 (MCM Unpublished data)

1.5 Life History of Anchovy

Anchovy forms the focus of this dissertation because of its economic importance, and because more is known of its general biology than any other pelagic fish in the southern Benguela upwelling system. The distribution and abundance of anchovy off South Africa has been well documented (Hampton 1987, 1992).

Well-defined age-specific, seasonal patterns of distribution and availability have been found for anchovy off the West Coast of South Africa (Crawford 1980). Unlike the reproductive process in most other upwelling systems, the spawning grounds and nursery grounds are spatially distinct in the southern Benguela system. The major spawning ground for anchovy is the area east of Cape Point to Cape Agulhas on the western Agulhas Bank (Fig. 1.5) (Shelton 1981, 1986, Crawford *et al.* 1987), although the major spawning area has shifted further east in recent years (Van Der Lingen *et al.* In press). It has been suggested that this eastward movement of anchovy is linked to age structure, with older anchovy found further east (C. Van Der Lingen 2001 pers. comm.).

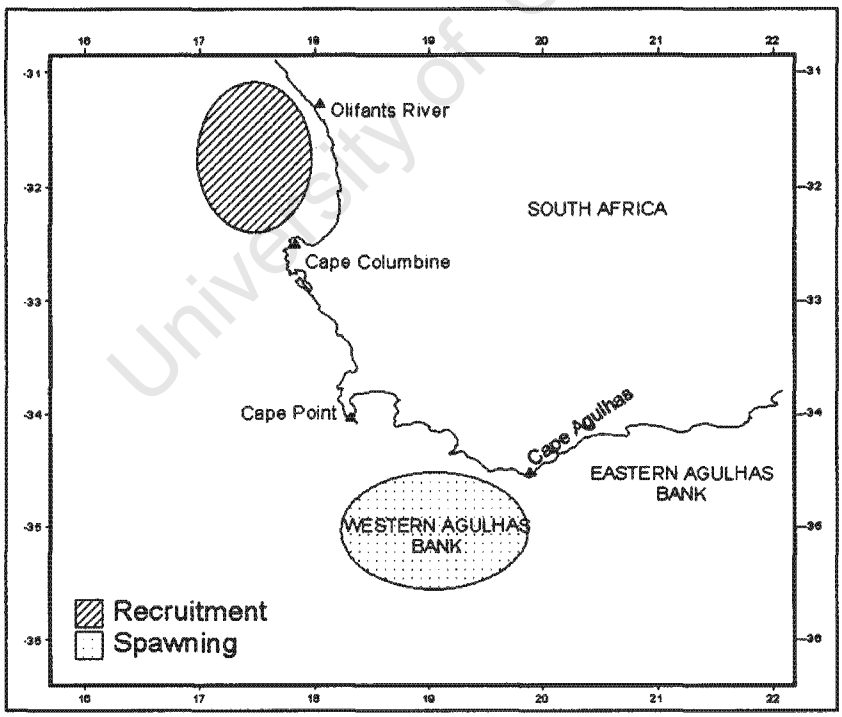

Figure 1-5 The major spawning and recruitment areas for anchovy in the southern Benguela system

Major nursery grounds are found along the West Coast, with anchovy recruits found as far north as the Orange River (Crawford *et al.* 1987). Anchovy spawn from September to February with peak spawning months from October to January (Shelton 1986, Melo 1994a). They are serial spawners and can lay up to 170 000 eggs throughout their spawning season (Melo 1994b).

Once adult anchovy have spawned, their eggs and larvae are carried in a north-westerly direction by the prevailing currents to the recruitment area (Shelton and Hutchings 1982). Pre-recruits (2-4 cm in length) are widespread offshore along the West Coast shelf region, and then migrate or are passively moved shoreward (Hutchings 1992). Inshore they continue to grow in the nursery grounds (St Helena Bay to the Orange River Mouth) where there is an abundant food supply. Anchovy are filter feeders and feed almost exclusively on large zooplankton such as euphasiids and copepods (James 1987, James and Findlay 1989). The mode of feeding for the anchovy (whether it is particulate or filter-feeding) and the consumption rate are determined mainly by the concentration and size spectrum of food particles in the water column (James and Findlay 1989). It is advantageous for anchovy to feed on larger food particles as it reduces their energetic costs (James and Findlay 1989). Anchovy thus obtain most of their energy by size-selective feeding on the largest zooplankton available. Although body reserves in anchovy account for about half of the energy required for spawning (Hunter and Goldberg 1980), the rest of the energy comes from feeding on zooplankton during the spawning period (James *et al.* 1989). Saving energy is important for the long distance they have to travel back to the spawning grounds, as well as for the spawning process itself. Also, if anchovy energy requirements are not met, or unfavourable temperatures are experienced, they can undergo ovarian astresia, which affects their potential to spawn during the current spawning season (Hunter and Macewicz 1985, Melo 1994a, 1994b).

Anchovy begin their return migration southwards back to the spawning grounds at approximately six months of age (Armstrong and Thomas 1989, Crawford *et al.* 1987, Shannon *et al.* 1996). Anchovy return to the western Agulhas Bank when they are sexually mature (one year of age) and ready to spawn (Shelton *et al.* 1985).

It is during the return migration to the spawning grounds that 0-year olds recruit to the fishery (Shelton 1981). Anchovy recruitment occurs in autumn and winter close to upwelling centres (Shelton *et al.* 1985), with anchovy most readily available to the fishery from June to September (Crawford 1980). About 70% of the catch consists of 0-year old recruits (Cochrane and Hutchings 1995). Therefore, the anchovy fishery is dependent on annual recruitment, making it highly susceptible to recruitment failure. Reproductive success of most clupeoids, which have planktonic larval stages and high larval mortality, is greatly dependent on environmental factors (Blaxter and Hunter 1982). Studies on environmental factors have consequently become increasingly important for studying pelagic fish recruitment (Kawasaki *et al.* 1991). Some of the main factors identified as being important in determining recruitment success include transport (Parrish *et al.* 1983), temperature (Armstrong *et al.* 1988), predation (Valdés *et al.* 1987), population density (Parrish *et al.* 1983), food (Lasker 1978) and turbulence (Lasker 1975) (i.e. the Optimal Environmental Window). Many of these factors are inter-related and impact on recruitment in a myriad of ways.

1.6 The Optimal Environmental Window

Until recently, linear statistics have dominated marine ecology and fisheries science. Some of the earliest work identified empirical linear relationships between pelagic fish recruitment and local wind effects in eastern boundary systems (Bakun and Parrish 1980). There has since, however, been a shift towards non-linear methods of empirical analysis (Mendelssohn and Cury 1987, Cury *et al.* 1995).

The relationship between annual pelagic fish recruitment indices and wind intensity in various upwelling areas has been analysed by Cury and Roy (1989). They found a dome-shaped relationship (Fig. 1.6), with maximum recruitment at intermediate wind speeds. The primary causes of larval mortality are predation and starvation (Blaxter and Hunter 1982) and these are influenced by wind. This optimal environmental window (OEW) is thought to be a consequence of the effect of wind on larval survival and hence on recruitment. The peak of the graph is the optimal area for larval survival and thus recruitment, with the areas to the left and right of the graph limiting larval survival and hence having a negative impact on recruitment of pelagic fish.

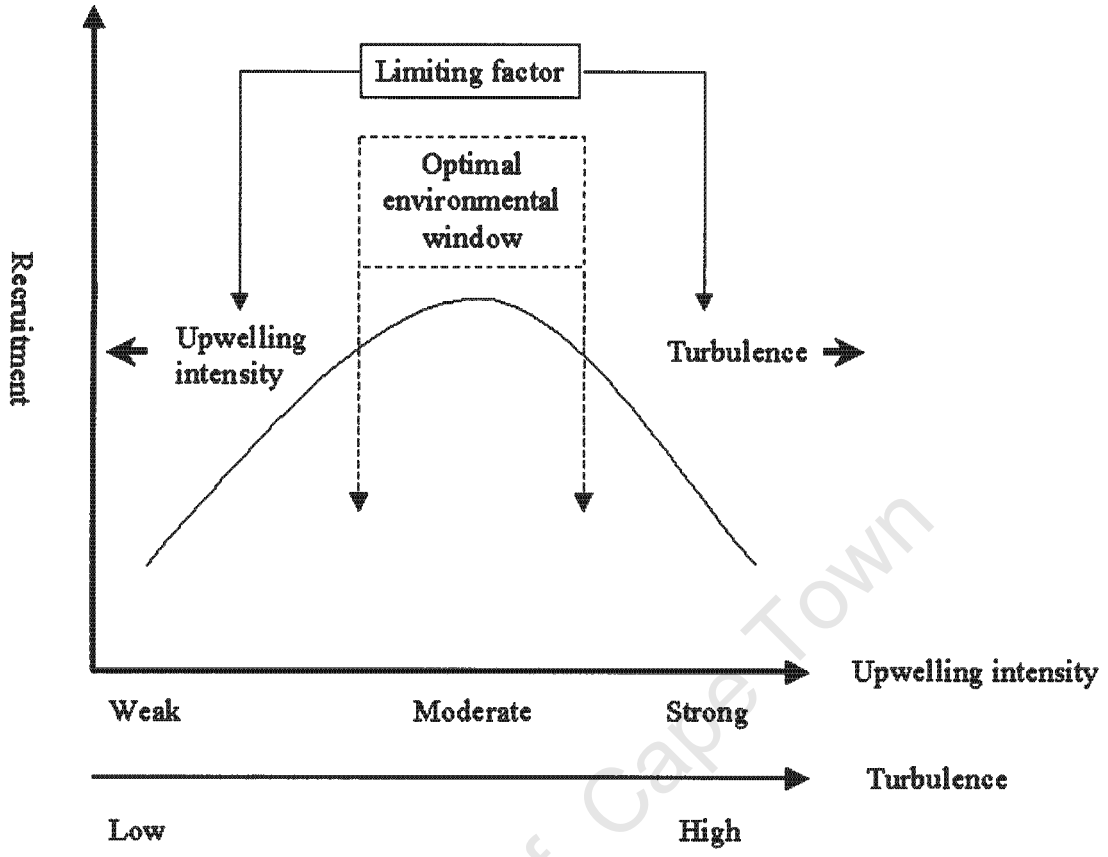

Figure 1-6 The Optimal Environmental Window (adapted from Cury and Roy 1989)

On the left side of the curve two factors limit recruitment. Firstly, low wind speeds result in weak upwelling and little nutrient enrichment of the euphotic layer. This results in low abundance of phytoplankton, the major source of food for fish larvae (Blaxter and Hunter 1982). Thus, weak upwelling can result in larval mortality (Cushing 1969). Secondly, low wind speeds result in low turbulence in the water column. This lack of mixing reduces the encounter rate between larvae and food particles (MacKenzie *et al.* 1994).

On the right side of the graph, strong wind speeds limit larval survival and thus recruitment (Cury and Roy 1989). As the dominant wind in upwelling systems is equatorward, strong winds lead to offshore movement of the Ekman layer, causing pelagic eggs and larvae to be removed from their preferred food-rich coastal habitat (Bakun and Parrish 1980, Sinclair 1988) and lost to the system. Strong winds also enhance turbulent

mixing in the surface layer (Kullenberg 1971, Serra *et al.* 1998), which causes the dispersal of patches of larval prey organisms (Lasker 1978, Theriault and Platt 1981). This makes it difficult for larvae to obtain sufficient food and increases the chance of larval mortality through starvation. Furthermore, high wind speeds and strong turbulence can inhibit the ability of larvae to capture food particles (MacKenzie *et al.* 1994). Strong turbulence can also affect primary production (Huntsman and Barber 1977) by mixing phytoplankton below a critical depth at which photosynthesis is no longer greater than respiration (Steele 1974).

The region surrounding the peak of the dome-shaped graph is termed the optimal environmental window. It is the optimal area for larval survival where the wind intensity is neither too weak (left side of the diagram) nor too strong (right side of the diagram). At this wind speed, there is both moderate upwelling and turbulence, which is ideal for larval survival and hence recruitment. The optimum wind speed for larval survival in most upwelling systems (Peru, California and North-West Africa) is 5-6 $m.s^{-1}$ (Cury and Roy 1989). In the southern Benguela system, however, the OEW Hypothesis has to date, not been tested due to insufficient data (C. Roy 2001 pers. comm.). Studies in the southern Benguela system show that peak spawning of anchovy occurs when wind speed values are 5-8 $m.s^{-1}$ (Fig. 1.7) and peak spawning of sardine occurs with wind speed values of 7-9 $m.s^{-1}$ (Fig. 1.8) (Shin *et al.* 1998). Despite average wind speeds in the southern Benguela system being higher than those observed in other upwelling systems, anchovy and sardine still spawn successfully in this system. This is thought to be due to stratification in the water column (see Section 3.2.2).

In an upwelling area, pelagic fish attempt to maximise reproductive success by optimising the physical constraints. For instance, in a weak upwelling area pelagic fish are inclined to reproduce in the most productive time-space areas. In moderate upwelling areas, fish reproduce in areas that are a compromise between the limiting factors of productivity and turbulence. Under strong upwelling conditions, areas of high offshore Ekman transport and turbulence are avoided by spawning fish (Cury and Roy 1989). Thus, changes in wind intensity may benefit or negatively impact recruitment. Furthermore, changes in wind may alter the optimal habitats for spawning and recruitment so that pelagic fish may adopt new reproductive strategies in time or space.

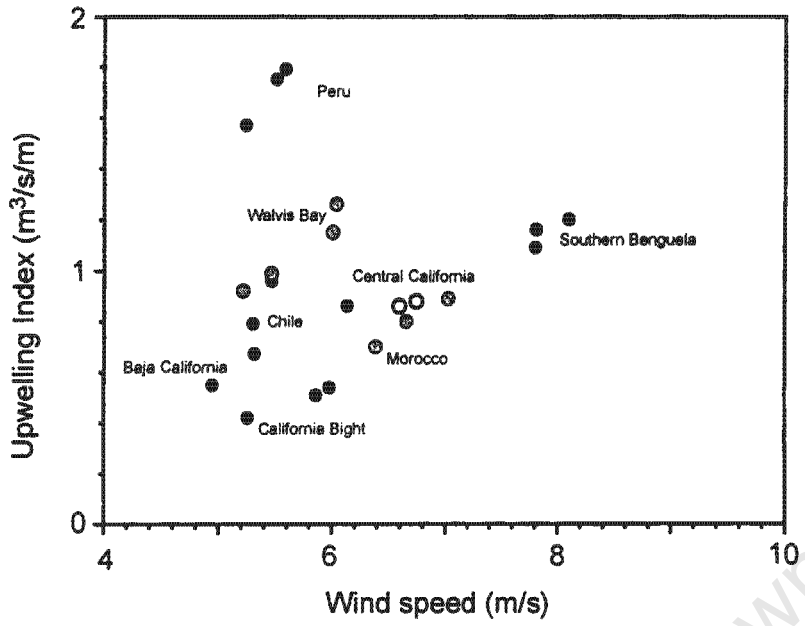

Figure 1-7 Plots of spawning peaks of anchovy against monthly means of wind speed and of coastal upwelling index by ecosystem (Shin *et al.* 1998)

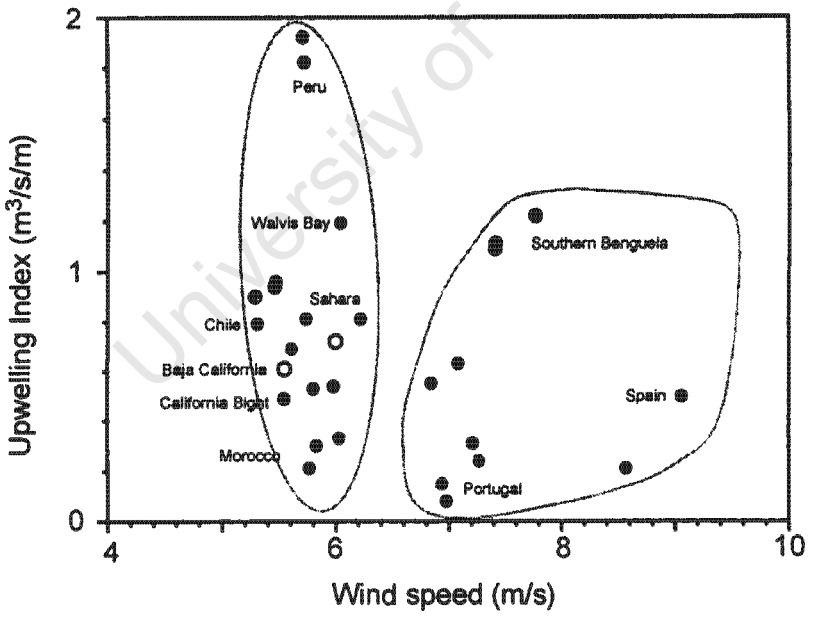

Figure 1-8 Plots of spawning peaks of sardine against monthly means of wind speed and of coastal upwelling index by ecosystem (Shin *et al.* 1998)

1.7 Turbulence

The rate of input of turbulent kinetic energy by the wind to the ocean is approximately proportional to the cube of wind speed (Elsbery and Garwood 1978). The average turbulence in most upwelling systems where anchovy and sardine spawn, is ~250 $m^3.s^{-3}$ (Bakun 1993). The turbulence, however, on the Agulhas Bank is higher than that of any other upwelling system and averages 600-650 $m^3.s^{-3}$ (Fig. 1.9) (Bakun 1996). To cope with this anchovy spawning in the southern Benguela is temporally and spatially adapted to avoid areas characterised by intense turbulent mixing and strong offshore transport (Parrish *et al.* 1983).

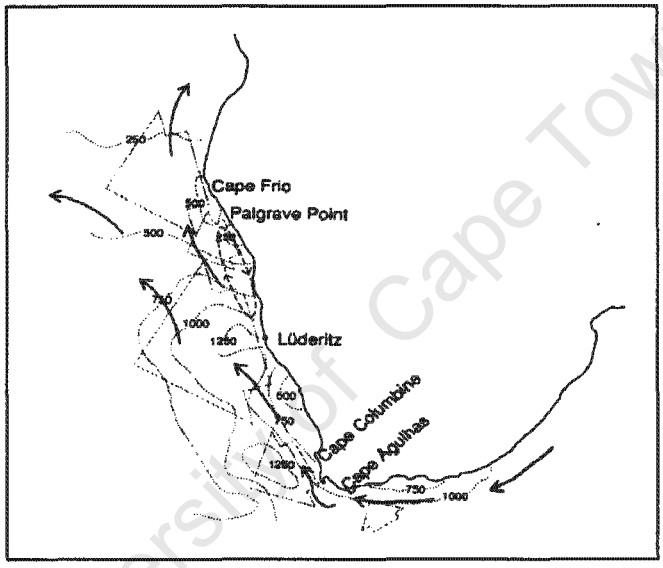

Figure 1-9 Turbulence values in the southern Benguela system (adapted from Parrish *et al.* 1983)

Anchovy in the southern Benguela system spawn predominantly on the Agulhas Bank from October to January when there is a stable layer that forms. This forms from warm Indian Ocean surface water that is transported in the Agulhas Current that flows around the tip of southern Africa and overlies water from the Benguela Current, which is both cooler and denser (Parrish *et al.* 1983). Moreover, upwelling is reduced on the Agulhas Bank as a consequence of the east-west orientation of the coastline (Bakun 1996). Therefore the shape of this coastline provides the fish with a reproductive area, which is protected from the upwelling coast.

1.8 Lasker Events

The frequency of winds also impacts survival of pelagic fish larvae (Lasker 1975). A lack of frequent winds allows the water column to stabilise and phytoplankton to form concentrated patches (e.g. layer of maximum chlorophyll). This enables enhanced feeding for first feeding larvae and increases the chances of survival. First feeding larvae are particularly susceptible to starvation and thus require high concentrations of food particles (Lasker *et al.* 1970). If these food requirements are not met it results in larvae resorbing their yolk sac (Wroblewski and Richman 1987). Frequent winds, however, produce turbulent conditions, which deepens the upper mixed layer and disperses food to below threshold concentrations (Lasker 1975, Shelton and Hutchings 1990). Therefore, the stability of the water column has been suggested to be one of the most important factors contributing to the survival of fish larvae (Lasker 1975).

The duration and number of calm periods during the early life stages of fish larvae seem to be crucial to their survival (Lasker 1975, Wroblewski and Richman 1987). The term 'Lasker event' is given to a sequence of days in which the wind speed remains low enough so that there is low wind mixing, which allows food particles to concentrate in a stratified layer. Once there is a day in which the wind speed is too high, the Lasker event is interrupted (Bakun 1996). The critical wind speed, however, and the number of days of that speed, which define a Lasker event, seem to be area dependent. A wind speed of 10 $m.s^{-1}$ has been used as the maximum wind speed in a study on anchovy in the California upwelling system (Peterman and Bradford 1987). For the Peruvian anchoveta, a wind speed of 5 $m.s^{-1}$ was chosen (Mendelssohn and Mendo 1987). For larval survival in upwelling systems, Wroblewski and Richman (1987) suggest that the optimal period between wind events is six days, whereas Mendelssohn and Mendo (1987) suggest a period of four days. Shorter, calm wind periods result in an increase in the depth of the upper mixed layer and thus a decrease in productivity. Wind periods (of low wind speed) longer than 6 days also have a negative effect on productivity. For example, calm wind periods longer than 15 days result in a depletion of the chlorophyll maximum layer and therefore starvation of the larvae as the yolk sac is resorbed (Wroblewski and Richman 1987). Although Lasker events have been investigated in other upwelling systems, there has been no study in the southern Benguela system.

1.9 Bakun's Triad

Bakun (1985) and Anderson (1988) have identified starvation, predation, physical dispersal and disease as the most important processes affecting recruitment. In a similar hypothesis, Bakun (1996) identified three main processes as favouring the reproduction of fish in a particular habitat: enrichment, concentration and retention. Maximum recruitment is predicted when these three processes are simultaneously optimal.

1.9.1 The Enrichment Process

Enrichment refers to the input of nutrients into an area that increases primary production. A number of processes, such as upwelling and advective processes, enhance input of nutrients into a particular area and lead to enrichment (Bakun 1996). According to the optimal environmental window hypothesis (Cury and Roy 1989), wind speeds of 5-6 $m.s^{-1}$ in most upwelling systems result in moderate upwelling and turbulence, which ensures larval survival and thus anchovy recruitment. This is largely because of adequate food concentrations for larvae and turbulent values that allow for a sufficient encounter rate between larvae and food particles (Cury and Roy 1989).

As the main spawning area of anchovy, the Agulhas Bank is an extension of the wind-driven coastal upwelling regime of the Benguela upwelling system (Shannon 1985). Upwelling occurs inshore and leads to large blooms of phytoplankton and high numbers of copepods during the summer months on the western Agulhas Bank (Peterson *et al.* 1992, Richardson *et al.* 1998). Upwelling is therefore of great importance in determining the spawning success of anchovy (see section 1.3) (Hutchings 1992, Richardson *et al.* 1998).

1.9.2 The Concentration Process

The concentration process ensures that food resources (e.g. phytoplankton and zooplankton) remain in a certain area (Bakun 1996). These food resources are important, as they are responsible for preventing starvation and more importantly promoting rapid growth during a critical period in the life history of the fish (i.e. first feeding larvae). Optimal turbulence, stratification and the occurrence of Lasker events are all important processes in the concentration process.

The concentration process determines the food availability for both first feeding larvae and for adult anchovy when they return to the Agulhas Bank to spawn. Relatively high food concentrations on the Bank are important to satisfy the high-energy requirements of anchovy for growth over the spawning period. During the summer months, the Agulhas Bank supports large populations of planktivorous pelagic fish (Armstrong *et al.* 1991). It is suggested that the high concentrations of food on the Agulhas Bank are a result of the stable layer, which forms during the summer months (Parrish *et al.* 1983). Also, the cool upwelled water south of Mossel Bay on the eastern Agulhas Bank supports high concentrations of copepods. This is likely to be a result of the high concentrations of chlorophyll on the Eastern Bank, which assist rapid growth of copepods and also the semi-closed circulation pattern of the cyclonic feature that retains copepods in the area (Peterson *et al.* 1992). It has been suggested that copepods are then transported at thermocline depths in a westerly direction to the western Agulhas Bank (Largier *et al.* 1992).

1.9.3 The Retention Process

This process refers to the need for fish to remain in certain areas that are productive and thus increase their chances of survival. In the southern Benguela system the spawning grounds and nursery grounds are spatially separate from one another. As a result anchovy larvae need to be transported from one area to another. Anchovy eggs and larvae depend on currents to transport them from the spawning grounds on the Agulhas Bank to the nursery grounds on the West Coast. This is aided by the presence of a frontal jet, which rounds Cape Point from the western Agulhas Bank and moves northwards past Cape Columbine (Shelton and Hutchings 1982) (Fig. 1.10). The jet current strengthens in the spring and summer months (Bang and Andrews 1974, Boyd and Nelson 1998), which coincides with the months of peak anchovy in the southern Benguela system (Shelton 1986, Melo 1994b). Both anchovy eggs and larvae are present in the frontal jet current (Shelton and Hutchings 1990, Huggett *et al.* 1998). As phytoplankton and zooplankton are also entrained in the jet current, it is thought that there is sufficient food for first feeding larvae (Armstrong *et al.* 1987).

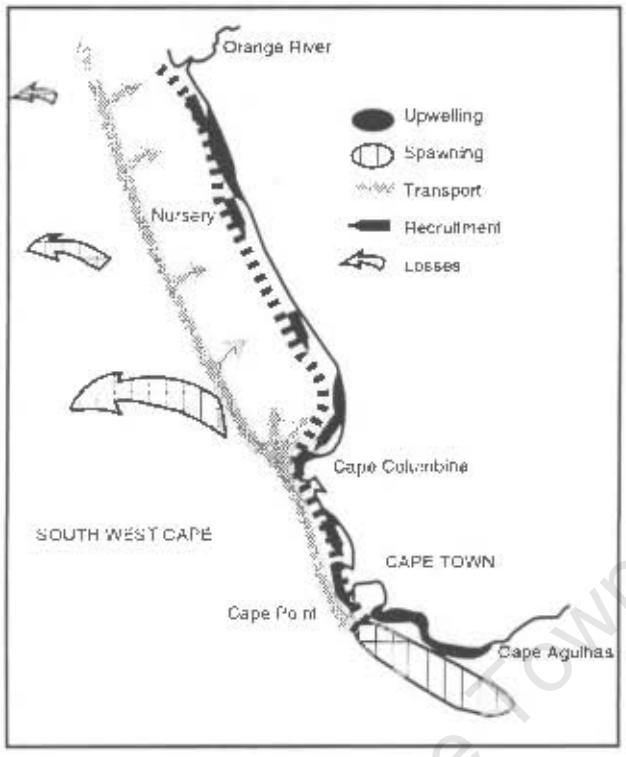

Figure 1-10 Transport of anchovy eggs and larvae to the nursery grounds on the West Coast via the north flowing frontal jet (Hutchings and Boyd 1992)

The frontal jet bifurcates at Cape Columbine (Shannon 1985), with a major arm on the outer shelf (often with an offshore component of flow) and a smaller northward arm further inshore (Fowler and Boyd 1998). It has been suggested that the outer branch of the Columbine jet is the most obvious area of potential losses of eggs and larvae on the West Coast because of its strong offshore component (Fowler and Boyd 1998). Strong upwelling intensity often results in the offshore transport of eggs and larvae. This can result in eggs and larvae being removed from their preferred environment and cause larval mortality (Bakun and Parrish 1980, Parrish *et al.* 1983). There are a number of areas between the spawning grounds and the nursery grounds where eggs and larvae could be lost to the system (Boyd *et al.* 1992). There is, however, evidence to suggest that they may be transported back to the jet current by onshore currents and thus be returned to the system and be able to continue their route northwards to the nursery grounds (Agenbag 1992, Fowler and Boyd 1998).

1.10 Predation

Predation is not analysed in this thesis as how it may be influenced by global climate change is difficult to predict. Although not included in Bakuns Triad, predation has been identified as one of the important factors regulating recruitment success (Bakun 1985 and Anderson 1988). It is important that food resources and anchovy remain in a certain area so as to reduce the chances of predation. Anchovy eggs that are spawned too far east will be exposed to increased predation and cannibalism as they have to travel westwards through high concentrations of fish (Valdés *et al.* 1987). Predators of anchovy include larger fish, seabirds and marine mammals (Crawford *et al.* 1987). In the early 1980s, it was estimated that predators consumed about 800 000 tons of anchovy per annum off South Africa's Western Cape (Crawford *et al.* 1987). Of this amount, about 656 000 tons were eaten by larger fish such as snoek, chub mackerel and other predatory fish, about 96 000 tons by marine animals (e.g. the Cape Fur seal) and about 49 000 tons by seabirds (Crawford *et al.* 1987). Natural mortality was estimated to account for up to 73% of all mortality (Bergh *et al.* 1985).

1.11 Thesis Outline

The broad objectives of this study are to examine the changes in wind regimes in the southern Benguela system from the present to the future, and to use this information to examine how such changes may affect pelagic fish recruitment in the region. There is a great deal of literature available in the separate disciplines of climate change and fisheries. There is a paucity, however, of literature and research that combine these two fields of climatology and fisheries science. In order to assess the impacts of climate change on anchovy, a cross disciplinary approach has been taken in this thesis. Chapter One has reviewed available literature on global climate change. Although the focus of this dissertation is on the influence of wind on recruitment, other climate change variables have also been included. There are two main hypotheses that have been identified as crucial to the success of recruitment. These are the Optimal Environmental Window Hypothesis (OEW) and Bakun's Triad, which have been outlined in Chapter One.

The specifications of the National Center for Atmospheric Research's (NCAR) Climate System Model (CSM), used to predict the expected changes in the future, are outlined in Chapter Two. This model is used to compare a future simulation under double CO_2

conditions with a simulation of the present day wind regime and sea level pressure. There is no consensus at present as to which coupled ocean-atmospheric general circulation model (GCM) is better at predicting future climates (IPCC Report 1996). The justification for using the Climate System Model instead of other existing models is included in Chapter Two. The NCAR model was validated by comparing its output with reanalysis data from the National Center for Environmental Prediction (NCEP) model.

In Chapter Two, results of the Climate System Model for the future scenario are also presented. Data include changes in the pressure system over the southern Benguela region, as changes at this scale can aid interpretation and give support for smaller scale changes such as wind. Data also include expected changes in the u and v wind components. Using these data, wind speed, alongshore wind stress, turbulence, the occurrence of Lasker events and the number of extreme wind speed and turbulence events are calculated. Five grid cells were selected in the region and the data reflect areal averages for each grid cell. The results focus on spring and summer months as this encompasses the spawning season of anchovy in the southern Benguela system. Non-spawning months, however, are also included in order to show comparisons in the wind speed and turbulence values from the present to future simulation. Moreover, spawning behaviour in clupeoids is sufficiently plastic that they may change their timing of spawning if conditions were to become more favourable at a different time of year.

Chapter Three examines the effect that projected climatic changes may have on the spawning and ultimately the recruitment of anchovy. Variables identified as important in the spawning process include wind speed, wind direction, alongshore wind stress, turbulence, stratification, the number of Lasker events and the number of extreme events. At each of the five grid cells the changes in these variables from the present to future simulations are discussed as well as the effect that these changes are likely to have on anchovy spawning. The role of a frontal jet for the transportation of eggs and larvae from the western Agulhas Bank to the West Coast is also examined, although the effect of changes in wind direction and wind speed in relation to the frontal jet is speculative.

Chapter Four examines other major upwelling systems in the world. These include the California Current, the Humboldt Current (off the coast of Peru) and the Canary Current

(off the coast of North-West Africa). Predicted changes in wind speed, turbulence and the frequency of Lasker events projected in the CSM future simulation are discussed in relation to anchovy spawning in these systems. The Optimal Environmental Window (OEW) has been used to identify optimal spawning conditions. The OEW identifies a dome-shaped relationship in which reproductive success appears highest at intermediate wind intensities and decreases at both higher and lower intensities. Chapter Five presents conclusions from the previous chapters and explores some of the findings and shortcomings of this study.

CHAPTER TWO

Methods and Results

2.1 General Circulation Models

2.1.1 Introduction

General Circulation Models (GCMs) have been developed to simulate past climate change, by attempting to understand the processes that produce climate, and to project future trends (Henderson-Sellers and McGuffie 1987, Peixoto and Oort 1992). They model the atmosphere three dimensionally and attempt to predict the effects of changes and interactions. By incorporating the primary components of the climate system (the atmosphere, ocean, cryosphere and land surface) climate models can simulate many of the large-scale features of the observed climate (IPCC Report 1996). These models can be used to explore the effects on climate of changes in exogenous factors such as greenhouse gases, small aerosol particles from anthropogenic and volcanic sources, and solar output. In addition to these external factors, climate varies annually because of endogenous mechanisms from year to year on its own accord, and this internal variation is also captured in the models. For the purposes of this dissertation, the GCM used is the National Center for Atmospheric Research's (NCAR) Climate System Model.

2.1.2 Climate System Model

The NCAR Climate System Model (CSM) is a global coupled ocean-atmosphere model. This model includes both a land surface and sea-ice sub model (Boville and Gent 1998). The CSM project began in 1994 with the objectives of building, maintaining and continually improving a comprehensive model of the climate system. A CSM configuration consists of four independent models for the basic system components, namely the atmosphere, ocean, land surface and sea-ice. Each of these components communicates with a flux coupler. The component models are driven mainly by fluxes at the Earth's surface.[1]

The atmosphere model is the NCAR Community Climate Model version 3, which has T42 horizontal resolution (~2.5° x 2.5°) and 18 levels in the vertical (Meehl *et al.* 2000). The ocean model is the NCAR CSM Ocean Model[1] which has 2.4 ° x 2.4 ° resolution but reduces to 1.2° in latitude in the tropics (Gent *et al.* 1998). The model that incorporates the sea ice component is the CSM Sea Ice Model and the land model is the Land Surface Model[1], which includes vegetation types and various surface processes (Meehl *et al.* 2000).

[1] http://www.cgd.ucar.edu/csm/

The CSM has been used for a number of studies. These include studies relating to the ocean (Doney *et al.* 1998, Gent *et al.* 1998), SST variability (Saravanan 1998), wind driven circulation (Danabasoglu 1998) and tropical cyclones (Tsutsui and Kasahara 1996, Tsutsui *et al.* 1999). There are also a number of evaluation studies that have analysed the formation and structure of the model (Boville *et al.* 2000, Williamson *et al.* 1995, Zhang *et al.* 1998).

The fully coupled simulations using the CSM include a 300-year present day run and a run with a 1% yr^{-1} increase of CO_2 tripling near year 125 (Maruyama *et al.* 1997). The simulation of climate change using an idealised forcing scenario with atmospheric CO_2 increasing at a rate of 1% yr^{-1} has become a standard experiment to assess the response characteristics of coupled climate models (Meehl *et al.* 2000).

2.2 Methods

2.2.1 General Methods Employed

In this dissertation, the data available for this research was derived from a model which used a 1% per year increase in atmospheric CO_2 and did not allow for sulphate forcing. The resolution of the spectral model is ~2.8 °. Ten years of daily data for the present-day period and doubled atmospheric CO_2 concentrations have been analysed. Accurate prediction of the year when double CO_2 will occur is dependent on the global response to the warnings associated with increased atmospheric CO_2.

The focus of the analysis is the spring and summer months in which anchovy spawn in the southern Benguela system, from September to February (Shelton 1986). These months are separated into those in spring (September, October and November) and summer (December, January and February). For each of the months there is a present and future simulated climate state and an anomaly. The anomaly maps represent the change in sea level pressure and wind patterns from the present to the future under doubled CO_2 (i.e. 2 x CO_2 minus 1 x CO_2). Analyses of the pressure maps have been performed over a window extending from 15°S to 42.5°S and from 0° to 40°E, in order to cover South Africa, as well as pertinent portions of the surrounding oceans.

Synoptic scale sea level pressure maps are used to identify overall features in the pressure system. Anomaly sea level pressure maps highlight the major changes in the pressure systems, as well as identifying locations where changes in wind direction and wind speed are likely to occur. Specific data are obtained from five grid cells in the southern Benguela system (Fig. 2.1), namely the Eastern Bank Grid Cell (34.883°S 22.500°E) located on the eastern portion of the Agulhas Bank; the Western Bank Grid Cell (34.883°S 19.688°E) located on the western portion of the Agulhas Bank south of the continent; the Cape Town Grid Cell (34.883°S 16.875°E) off Cape Town; the Lamberts Bay Grid Cell (32.092°S 16.875°E) and the Port Nolloth Grid Cell (29.301°S 14.063°E) situated further up the west coast in the Atlantic Ocean. These grid cells are all located in the ocean. These grid points were selected as they cover the southern Benguela upwelling system and the area in which anchovy spawn and recruit. Data from a grid cell are representative of the grid area (~2.8° x 2.8°).

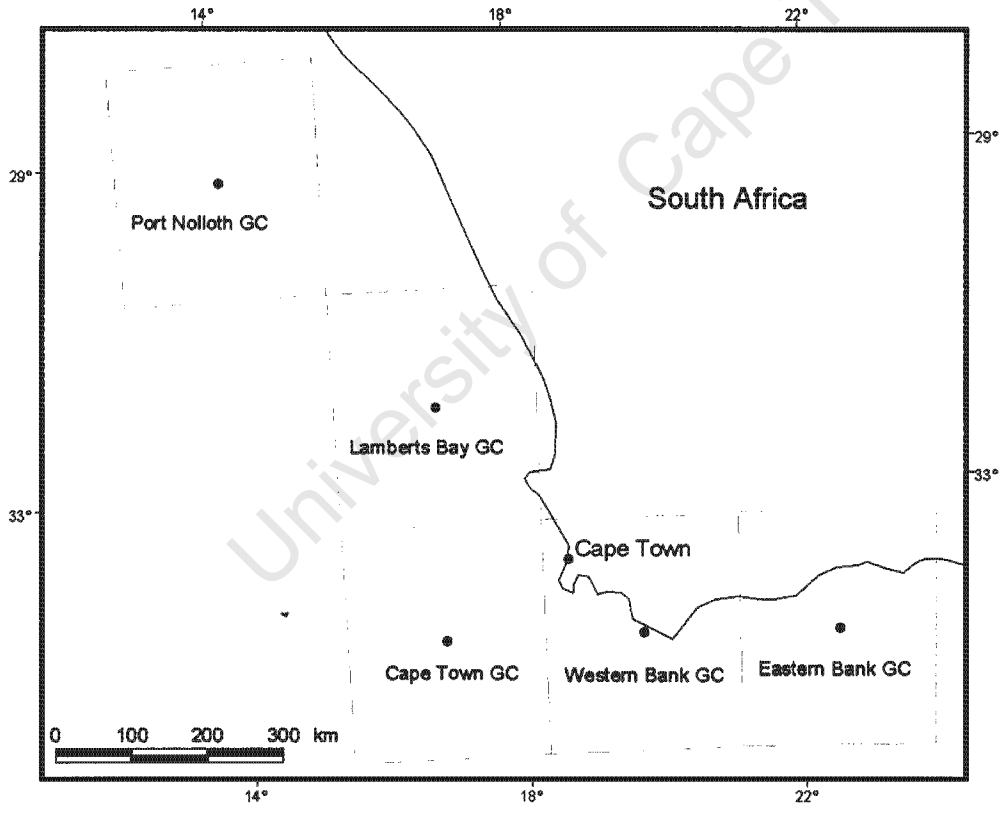

Figure 2-1 The five grid cells investigated in the southern Benguela system

U and v components of wind were obtained from model output data at each of the five grid cells. Wind speed and turbulence were then derived from the data. Wind speed was derived from the square root of the sum of the u component squared and the v component squared. Turbulence

was derived by cubing the wind speed value. For each of these variables both present and future results are presented graphically. The average values have been represented with a symbol and the standard deviation has been included to indicate the variation in values from the mean. The data presented are control run results. Each graph shows the spawning months (September - February) and the non-spawning months (March - August). A series of *t*-tests have been performed on the mean wind speed and turbulence values for the spawning season using Statistica (version 5.0). At all five grid cells the number of days showing extreme wind speeds (i.e. wind speeds >15 $m.s^{-1}$) and extreme turbulence (i.e. turbulence values >5000 $m^3.s^{-3}$) for the spawning period in both the present and future simulations have been identified

At each of the grid cells in the southern Benguela system, the number of Lasker events in the present and future simulations for the spawning period was identified. No studies on Lasker events have been conducted in the southern Benguela system and as a result, two definitions of Lasker events have been included in this study. These are: 5 consecutive days with wind speeds less than 6 $m.s^{-1}$ (referred to as Type A for the purposes of this thesis) and 6 consecutive days with wind speeds less than 6 $m.s^{-1}$ (referred to as Type B for the purposes of this thesis). The wind speed value of 6 $m.s^{-1}$ has been selected as it falls within the average wind speed range for anchovy spawning in the southern Benguela system (i.e. 5-8 $m.s^{-1}$). At each of the five grid cells the frequency of south-easterly winds was identified for the spawning season in the present and future simulations.

The alongshore wind stress has been calculated for each of the five grid cells as a proxy for upwelling. The equation used for the calculation of the alongshore wind stress is as follows:

$$\tilde{\tau} = C_D \rho_a |\tilde{U}| \tilde{U}$$

Where: $\tilde{\tau}$ is the vector wind stress at the sea surface
C_D is the drag coefficient (here assumed to be unity)
ρ_a is the density of air (here assumed to be unity)
$|\tilde{U}|$ is the magnitude of the wind velocity
$\tilde{U}$ is the wind velocity

An approximation of the angle of coastline has been calculated for each grid cell using a Mercator projection, which is an angle preserving projection. The following angles of coastline were calculated: Eastern Bank Grid Cell (200°), Western Bank Grid Cell (150°), Cape Town Grid Cell (135°), Lamberts Bay Grid Cell (110°) and Port Nolloth Grid Cell (110°). The

alongshore wind stress is compared in the present and future simulation for the spawning months.

2.2.2 Validation of the Climate System Model

It is invalid to compare the output of a GCM with data from a point source because of scale differences. Therefore, the Climate System Model (CSM) has been validated by comparison with the National Center for Environmental Prediction (NCEP) reanalysis data set. In general, CSM data compare well with the NCEP data, bearing in mind the limitations of both data sets (B. Hewitson 2001 pers. comm.). The months identified in the validation are the spawning months of anchovy in the southern Benguela system (September-February). Considering the area of study (i.e. the South and West Coasts of South Africa), the anomaly maps show relatively small differences in wind speeds (the month of November being a noticeable exception). Anomalies between the two models are discussed below.

In the spring months (September-November) the CSM shows a stronger ridging of the South Atlantic High Pressure System (Figs 2.2 and 2.3). In the summer months (December-February), however, the anomaly becomes smaller and the wind speed and wind direction are comparable with that of the NCEP output (Figs 2.3 and 2.4). In October and November on the south coast, the CSM output has a stronger southerly flow than the NCEP output. The NCEP output shows more easterly winds over this region. On the West Coast, however, the wind direction is predominantly southerly in both simulations in October and November (Figs 2.2 and 2.3).

In December (Fig 2.3) the anomaly map shows a range of about 20% of wind speed when comparing the wind speed data in the CSM to that of the NCEP data. In November the anomalies are, however, greater (Fig. 2.3). The CSM output appears to show a much stronger ridging of the South Atlantic High Pressure System resulting in high wind speed anomalies between the CSM and the NCEP data.

Considering the above anomaly information, the CSM simulation for the area of study in the southern Benguela system for the spawning months in general is comparable with that of the NCEP data. The CSM thus appears to be sufficient at simulating winds in the region and will be used to evaluate the possible effect of global climate change on fish recruitment.

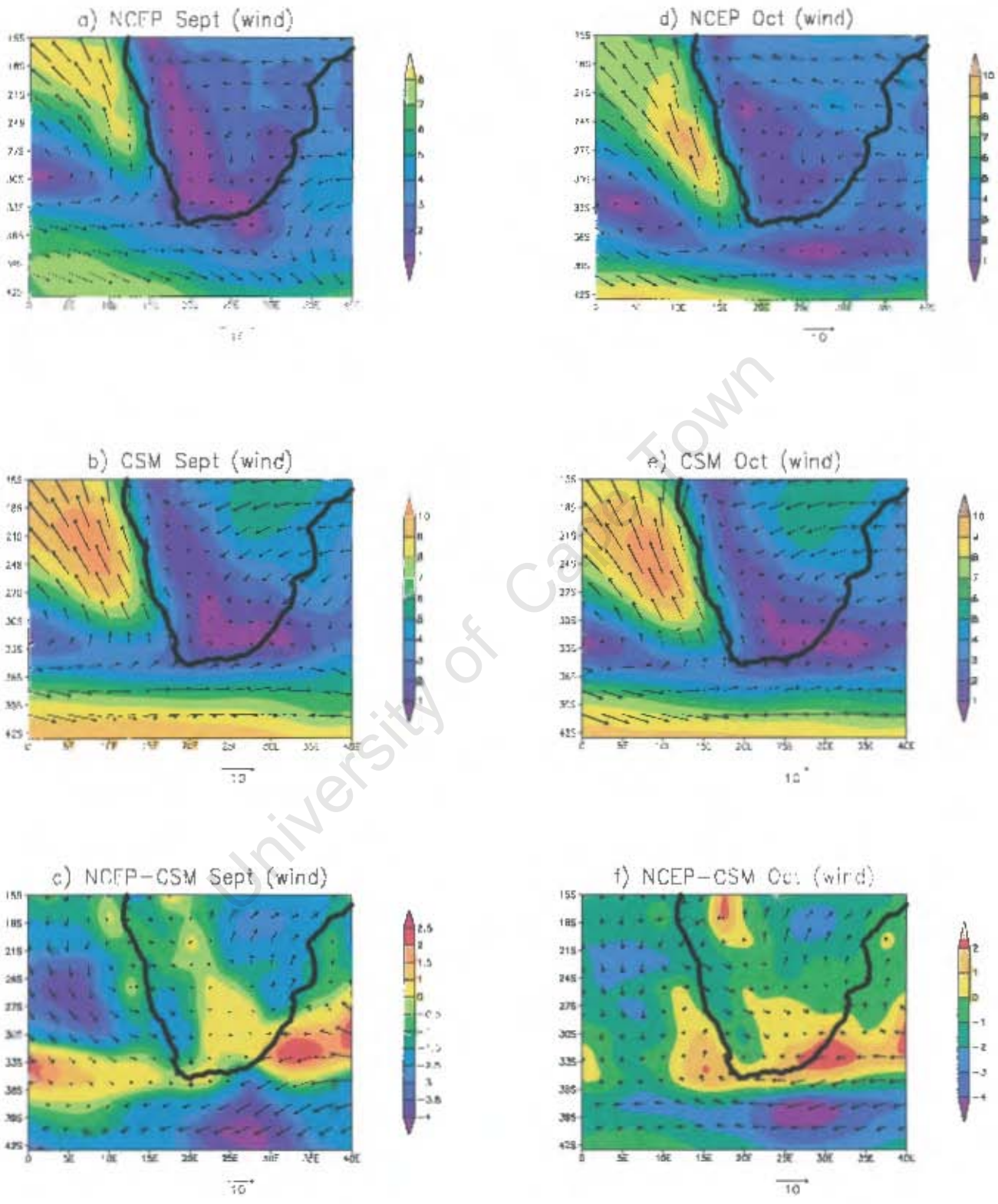

Figure 2.2 Wind vectors for the present (i.e. 1 x CO_2 simulation) with the NCEP data (a,d), the CSM data (b,e) and the anomaly (i.e. NCEP data-CSM data) (c,f) for September and October.

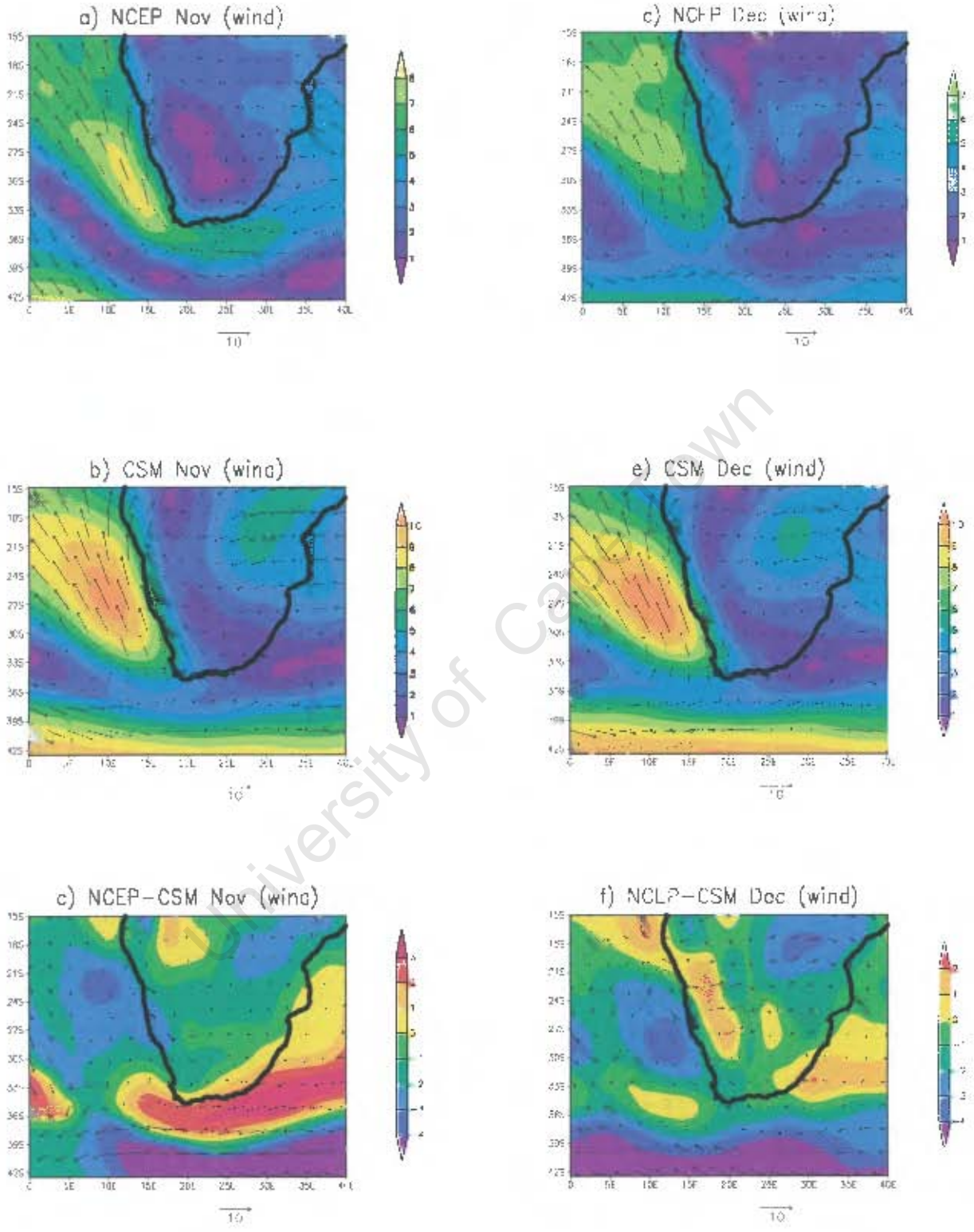

Figure 2.3 Wind vectors for the present (i.e. 1 x CO_2 simulation) with the NCEP data (a,d), the CSM data (b,e) and the anomaly (i.e. NCEP data-CSM data) (c,f) for November and December.

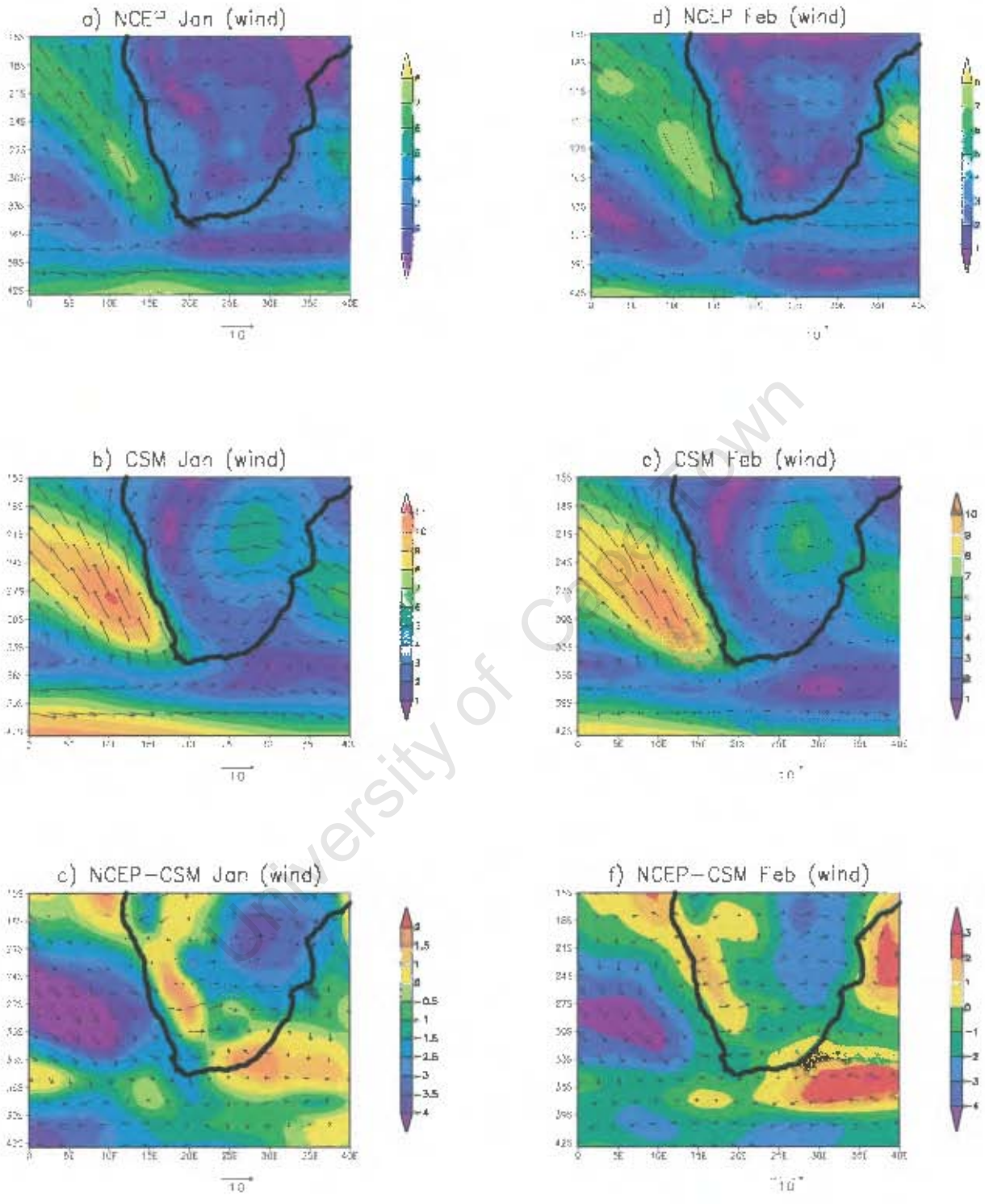

Figure 2.4 Wind vectors for the present (i.e. 1 x CO_2 simulation) with the NCEP data (a,d), the CSM data (b,c) and the anomaly (i.e. NCEP data-CSM data) (c,f) for January and February.

2.3 Results

2.3.1 Seasonality in the Pressure System

The sea level pressure maps show marked changes in seasonal characteristics in the future (see Figs 2.5, 2.6 and 2.7). The major influence on the seasonal wind regime within the present simulation is the movement of the South Atlantic High Pressure System (SAHP). The pressure changes from early to late summer in the simulation of the present are related to a decrease in the intensity of the SAHP. The South Atlantic anti-cyclone of the subtropical high pressure belt influences the entire area over summer. The SAHP system is most intense in September (Fig. 2.5a) and shows a decrease in intensity towards late summer (Fig. 2.7d). There is a westerly shift of the SAHP at present from early to late summer months.

The second major shift in the pressure system is that of the continental trough. It displays a southward movement over the interior from early to late summer in the present simulation (Figs 2.5, 2.6 and 2.7). The trough deepens as it moves further south towards the end of summer. The southerly movement and intensification of the low pressure system in the simulation of the present from early to late summer has implications for the pressure gradient over the west coast of southern Africa. The southerly movement of the continental thermal trough results in an increase in the pressure gradient over the West Coast. This increase results in an increased magnitude of south-easterly winds along the West Coast. Thus, there is a greater magnitude and frequency of south-easterly winds in the late summer months (January and February) as opposed to the early summer months (September and October) (see Figs 2.31-2.34).

Pertinent to this dissertation are the changes in the pressure system from early to late summer in the future simulation. In early summer months such as September, the South Indian High Pressure system shows a westward shift in its position in the future simulation compared with its position in the present simulation (Fig. 2.5).

The CSM simulation indicates that the SAHP system remains in its present position from September - December in the future. November is the only month in the early summer months (i.e. September - November) that displays a positive pressure anomaly with a 0.05% expected increase in pressure from the present simulation over the interior and surrounding oceans (Fig. 2.6c). This results in a stronger pressure gradient over the West Coast region. September,

October and December show a negative pressure anomaly of approximately 0.05% for the West Coast region. This results in a weaker pressure gradient in the region.

The primary anomaly is located in the late summer months, with the largest changes projected for January (Fig. 2.7c). In January and February there is a projected increase in sea level pressure of approximately 0.1% from the present simulation to the future resulting in a stronger pressure gradient. There is a projected movement of the SAHP south and east of the continent. There is also an expected intensification of the pressure cell (Fig. 2.7e).

The simulation of the future projects an intensification of the continental thermal trough and an extension to the east, which has implications for rainfall in the region. The trough, however, does not display any major movement in its position from the present simulation. The CSM output for the sea level pressure therefore indicates a northward shift of the low pressure system in the region from the present to the future. There are observed differences in the sea level pressure anomalies over the interior of South Africa over the summer months.

In January the anomaly map displays a general SW - NE pressure gradient extending across the region (Fig. 2.7c). The anomaly geostrophic vector would thus be directed from the south-east. This suggests that over the West Coast there would be a greater south-east component compared to the general flow, in the future. An increase in south-easterly winds on the West Coast will affect ocean dynamics, such as upwelling and turbulence.

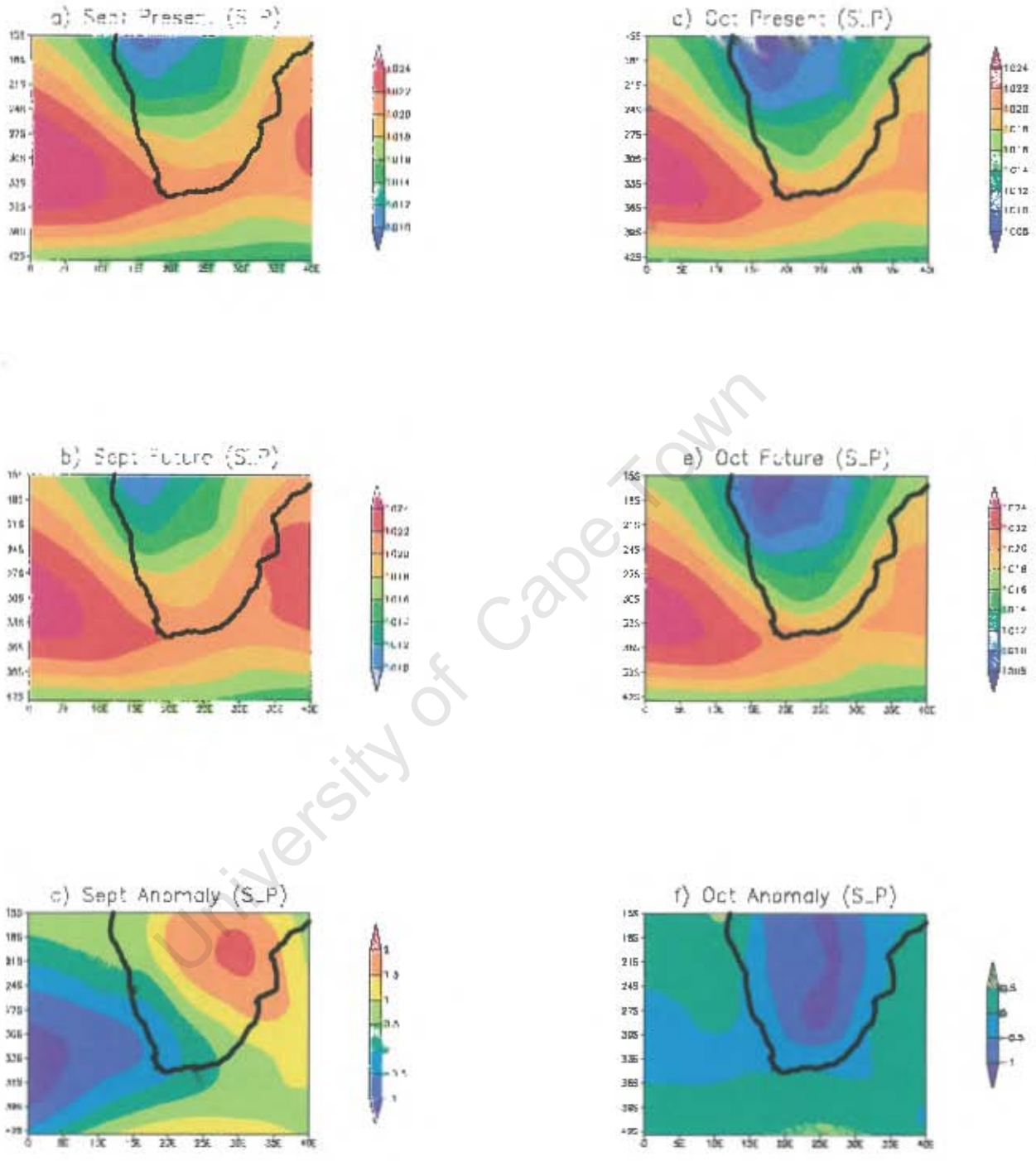

Figure 2.5 Mean sea level pressure (hPa) for the 1 x CO_2 simulation (a,d), the future simulation (b,e) and the future anomaly (i.e. 2 x CO_2 minus 1 x CO2 (c,f) for September and October.

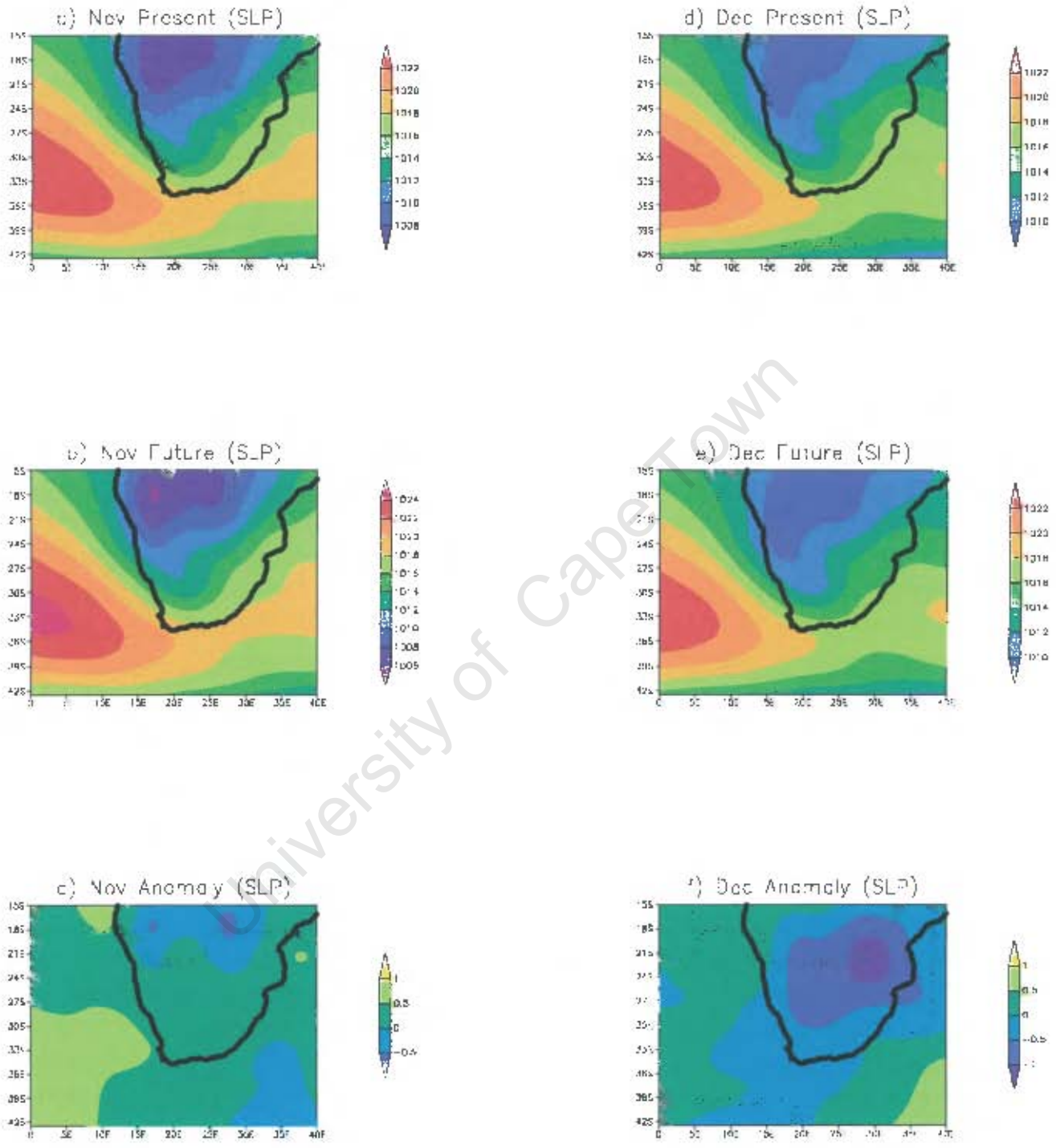

Figure 2.6 Mean sea level pressure (hPa) for the 1 x CO_2 simulation (a,d), the future simulation (b,e) and the future anomaly (i.e. 2 x CO_2 minus 1 x CO2 (c,f) for November and December.

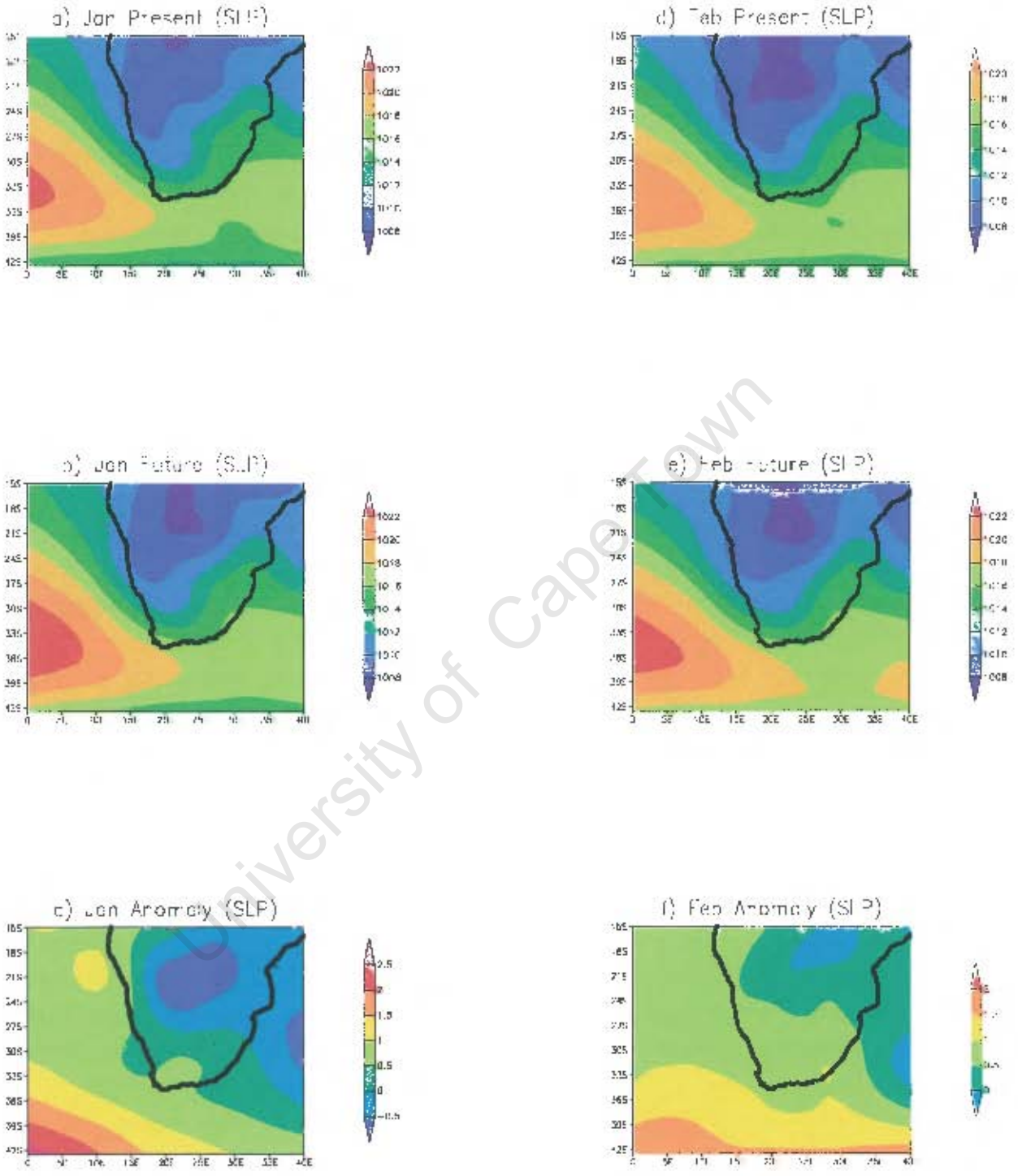

Figure 2.7 Mean sea level pressure (hPa) for the 1 x CO_2 simulation (a,d), the future simulation (b,e) and the future anomaly (i.e. 2 x CO_2 minus 1 x CO2 (c,f) for January and February.

2.3.2 Wind Speed

Mean Wind Speeds

The Eastern Bank Grid Cell has future wind projections that are very similar to those in the present simulation (Fig. 2.8). There is an overall decrease of 1.7% in mean wind speeds from the present to future over the spawning period (September - February), although this is not significant ($p > 0.05$). January is the only month in the spawning period that displays an increase in the future (i.e. an average increase of 3.9%). December shows the largest decrease (8.8%) in mean wind speeds, where mean wind speed values are 6.6 $m.s^{-1}$ in the present and 6 $m.s^{-1}$ in the future. The mean wind speed values for the spawning months (i.e. September - February) fall within the 5-8 $m.s^{-1}$ range for both the present and future simulations.

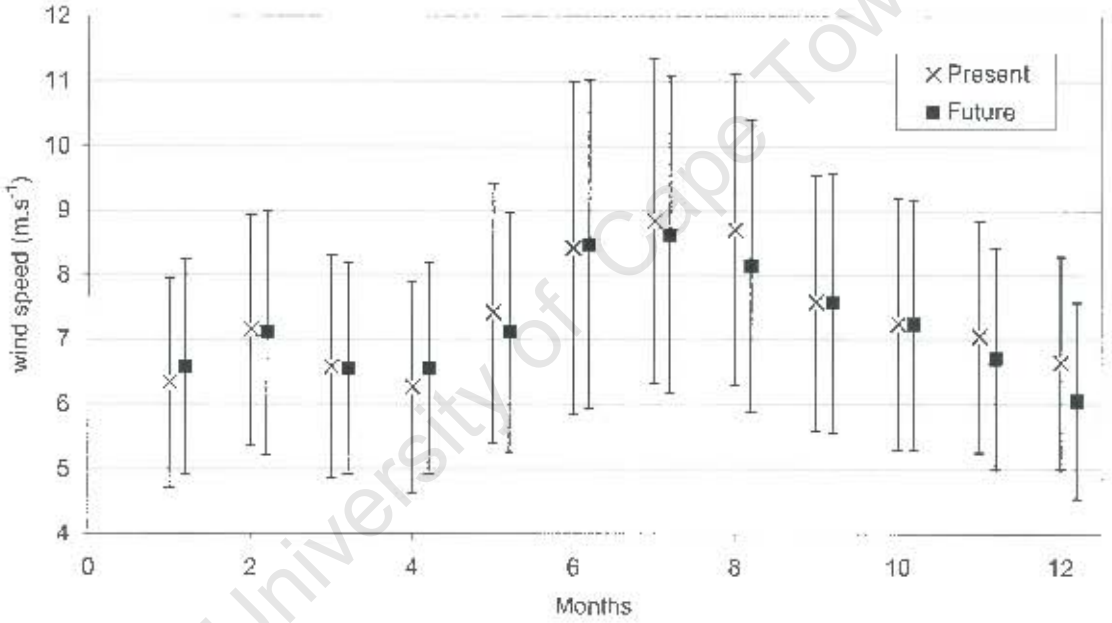

Figure 2-8 The difference between present and future wind speed ($m.s^{-1}$) monthly averages (+- standard deviation) at the Eastern Bank Grid Cell

The Western Bank Grid Cell shows an overall decrease in mean wind speeds (1.4%) in the spawning season (September - February) from the present to the future simulation (Fig. 2.9). As on the Eastern Bank, this decrease does not show a significant change from the present to the future simulation ($p > 0.05$). January is the only month in the spawning season that displays a positive mean wind speed anomaly (an increase of 5.9% from the present to the future). The only months that do not fall within the wind speed range of 5-8 $m.s^{-1}$ in both the present and

future simulation are June - August, although this is outside the present spawning season.

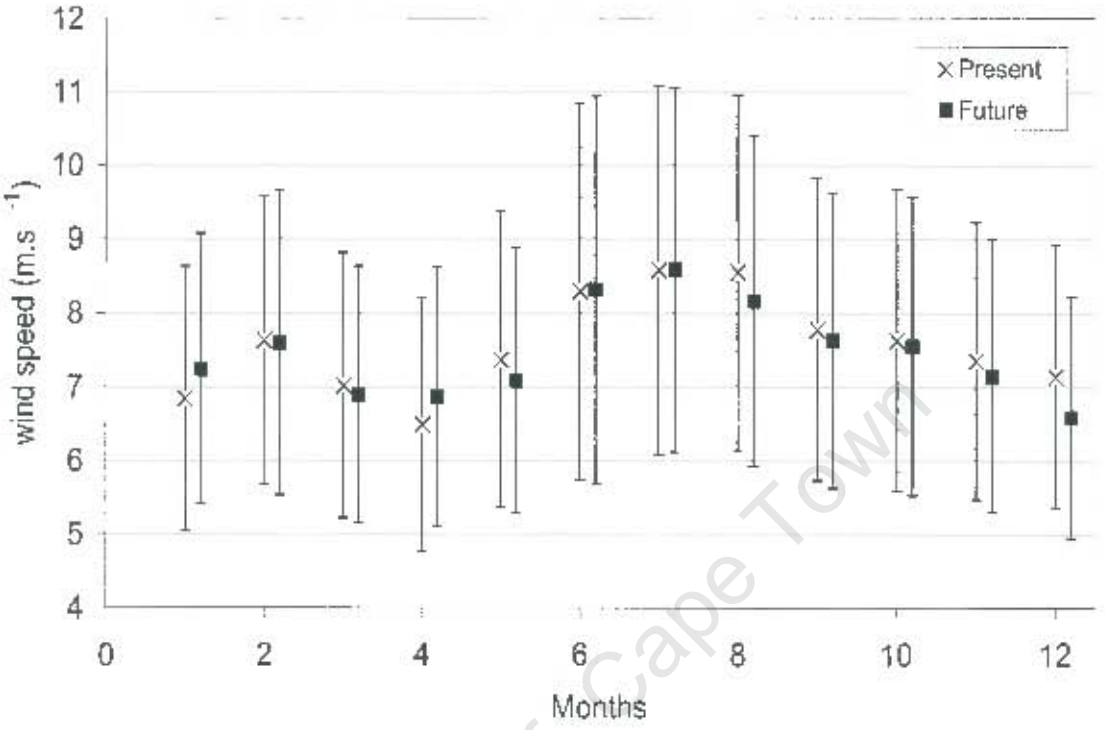

Figure 2-9 The difference between present and future wind speed ($m.s^{-1}$) monthly averages (+- standard deviation) at the Western Bank Grid Cell

At both the Eastern Bank and Western Bank Grid Cells the vector maps (Figs 2.10-2.12) show absolute wind vectors that are small in magnitude compared to the absolute wind vectors observed on the West Coast. The magnitude of the vectors for both the present and future simulations increases from the early to late summer months over the spawning season at the Eastern Bank and Western Bank Grid Cells. For example, in the early summer months (September and October) the vector maps show a value of ~0-1 $m.s^{-1}$ (Figs 2.10a, 2.10b, 2.10d and 2.10e). In November and December the vectors show a value of ~2-3 $m.s^{-1}$ at the Eastern Bank Grid Cell and ~3-4 $m.s^{-1}$ at the Western Bank Grid Cell (Figs 2.11a, 2.11b, 2.11d and 2.13c). At the end of the spawning season (February) the vectors show values of ~3-4 $m.s^{-1}$ at the Eastern Bank Grid Cell and ~4-5 $m.s^{-1}$ at the Western Bank Grid Cell (Figs 2.12d and 2.12e).

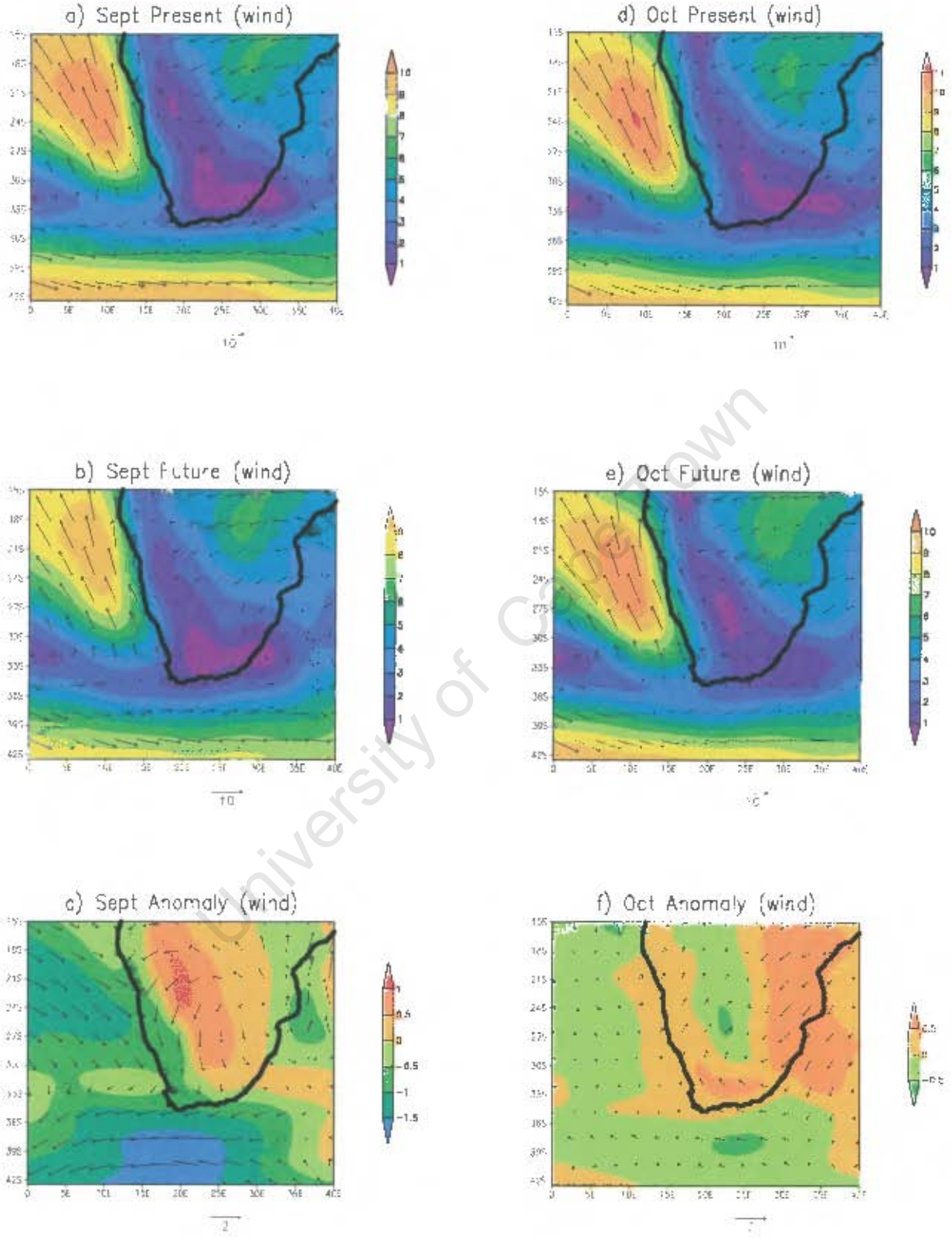

Figure 2.10 Wind vectors for the 1 x CO_2 simulation (a,d), the 2 x CO_2 simulation (b,e) and the change in magnitude and direction of the wind (c,f) i.e. 2 x CO_2 minus 1 x CO2 for September and October.

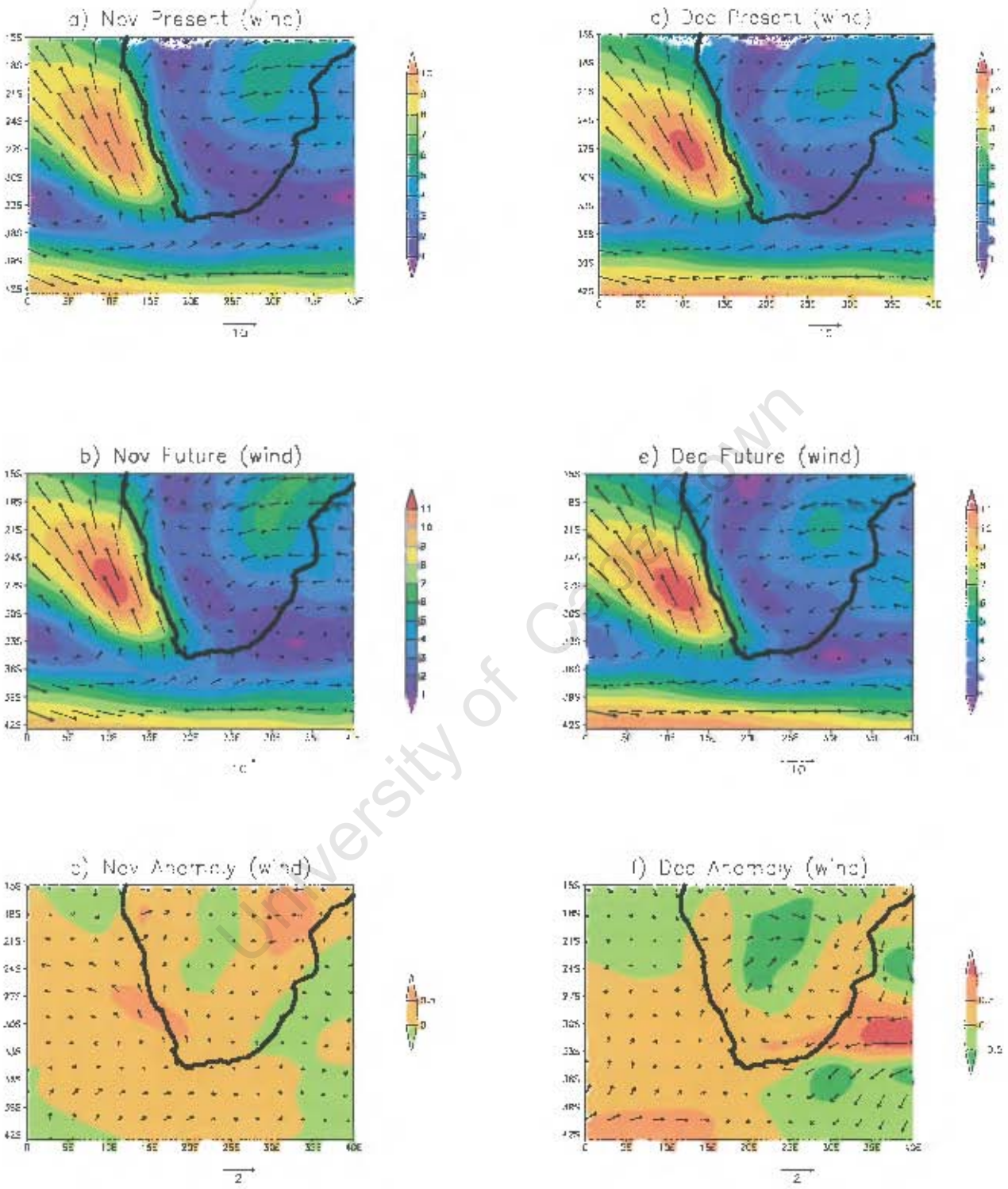

Figure 2.11 Wind vectors for the 1 x CO_2 simulation (a,d), the 2 x CO_2 simulation (b,e) and the change in magnitude and direction of the wind (c,f) i.e. 2 x CO_2 minus 1 x CO2 for November and December.

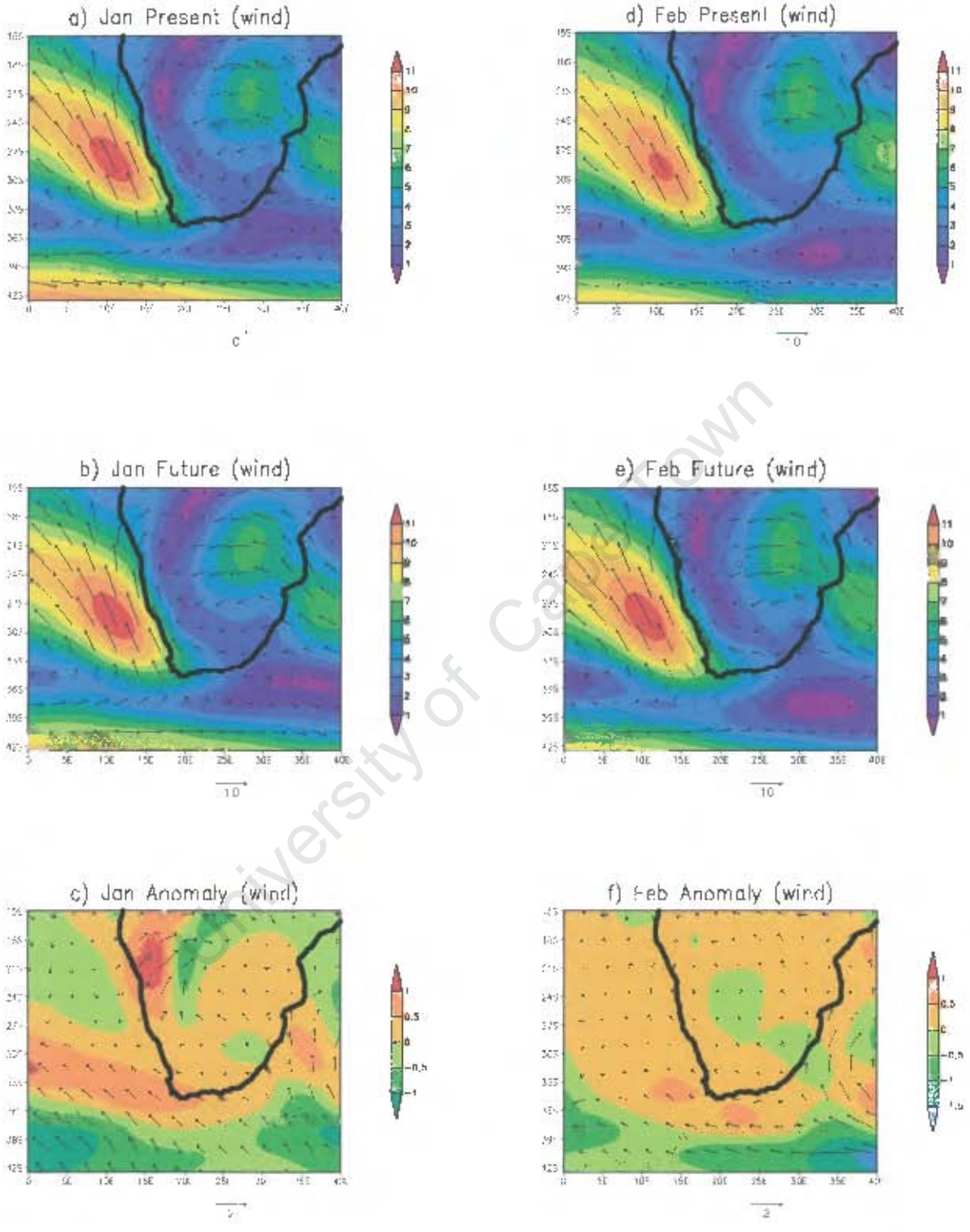

Figure 2.12 Wind vectors for the 1 x CO_2 simulation (a,d), the 2 x CO_2 simulation (b,e) and the change in magnitude and direction of the wind (c,f) i.e. 2 x CO_2 minus 1 x CO2 for January and February.

The Cape Town Grid Cell shows an overall decrease of 1.8% in mean wind speeds in the spawning season from the present to the future, although this difference is non-significant ($p > 0.05$) (Fig. 2.13). For the spawning season, all months show a decrease in mean wind speed values in the future, except for January. The wind speed anomaly for January shows an increase in mean wind speeds of 8.1% (Fig. 2.13). All months in the spawning season in both the present and future simulation fall within 5-8 $m.s^{-1}$, except for February. The mean wind speeds in February, however, only slightly exceed 8 $m.s^{-1}$ (the present and future values for February are both 8.2 $m.s^{-1}$). June - August exceed the range of 5-8 $m.s^{-1}$ in both the present and future simulations.

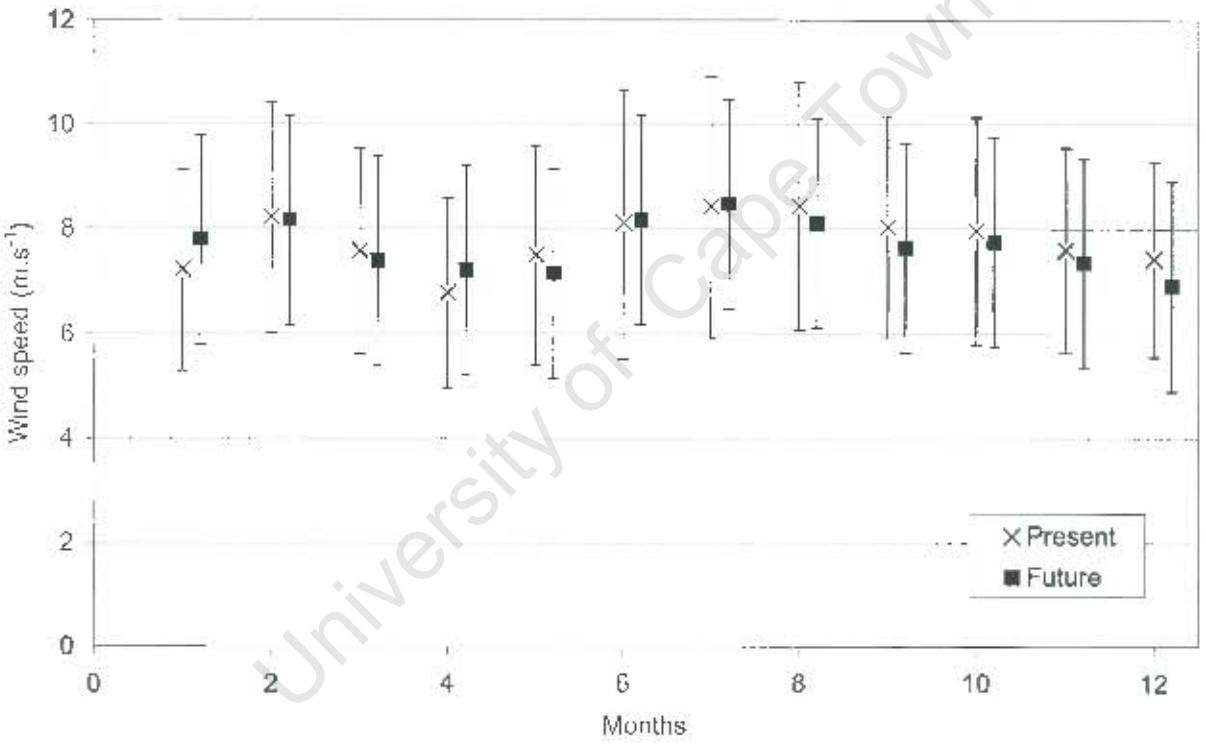

Figure 2-13 The difference between present and future wind speed ($m.s^{-1}$) monthly averages (+- standard deviation) at the Cape Town Grid Cell

The wind vector maps for the Cape Town Grid Cell in the present and future simulations show vectors that are of a greater magnitude than those observed at the Eastern Bank and Western Bank Grid Cells (Figs 2.10-2.12). The magnitude of the vectors at the Cape Town Grid Cell increases in strength from the early to late summer months. For example, in September the vectors in the present and future simulations show a strength of ~2-3 $m.s^{-1}$ (Figs 2.10a and

2.10b). By the end of the spawning season (February) the strength of the vectors in the present and future simulations increases to ~6-7 $m.s^{-1}$ (Figs 2.12d and 2.12e).

At the Lamberts Bay Grid Cell there is an overall increase in mean wind speeds from September - February in the future of 2.0% (Fig. 2.14), although the increase is non-significant ($p > 0.05$). All months in the spawning season show an increase in mean wind speeds from the present to future simulation, except October. The largest increases in mean wind speeds are November and January, which show an increase of 4.2%. Results show an expected increase in wind speeds from 8 $m.s^{-1}$ in the present simulation to 8.4 $m.s^{-1}$ in the future for November and from 8.6 $m.s^{-1}$ to 9 $m.s^{-1}$ for January (Fig. 2.14). Most of the spawning months exceed the range of 5-8 $m.s^{-1}$ in both the present and future simulations. The non-spawning months (March - August), however, all fall within this range in both the present and future simulations.

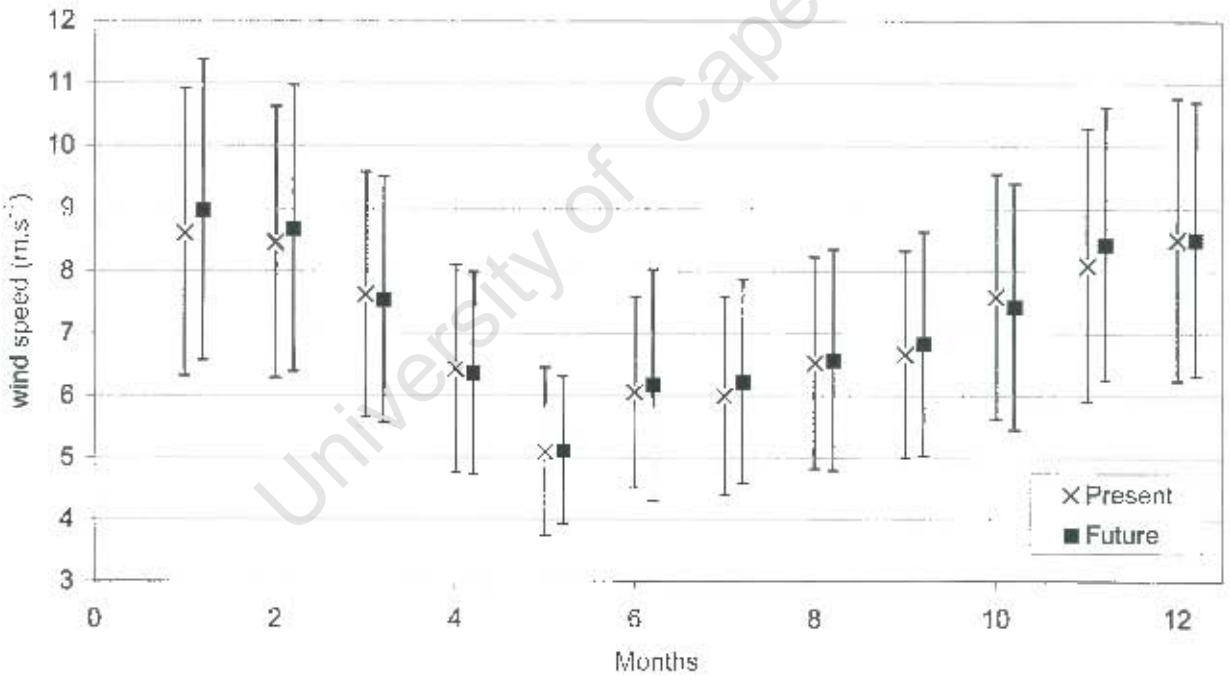

Figure 2-14 The difference between present and future wind speed ($m.s^{-1}$) monthly averages (+- standard deviation) at the Lamberts Bay Grid Cell

At the Port Nolloth Grid Cell there is an overall increase in mean wind speeds for the spawning period in the future of 1.4% (Fig. 2.15), although this increase is not significant ($p > 0.05$). September and October show a mean decrease in wind speeds in the future. The remainder of

the spawning months (November - February), however, show an increase in mean wind speeds. None of months in both the spawning and non-spawning season show a significant difference from the present to the future. The calculated mean wind speeds in the present and future simulations during the months September - February are greater than 8 $m.s^{-1}$. The mean wind speed values for the non-spawning months (April - August) in both the present and future simulations fall within the range of 5-8 $m.s^{-1}$.

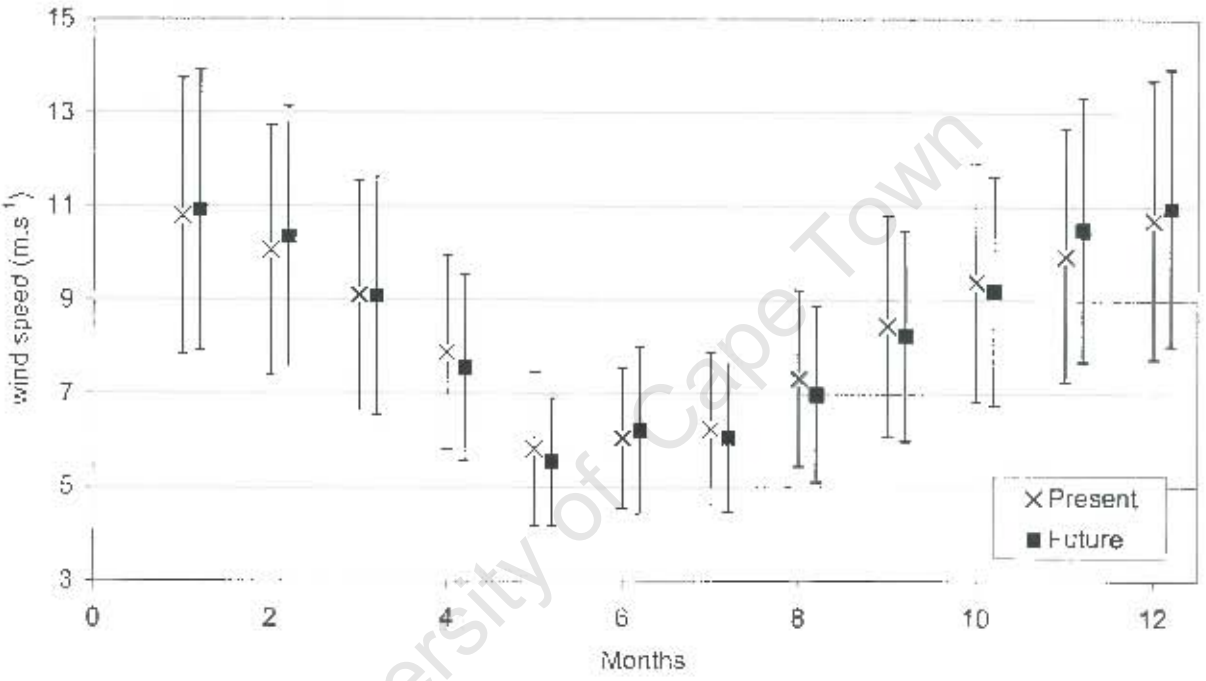

Figure 2-15 The difference between present and future wind speed ($m.s^{-1}$) monthly averages (+- standard deviation) at the Port Nolloth Grid Cell

Wind vectors maps for the Lamberts Bay and Port Nolloth Grid Cells (Figs 2.10-2.12) show wind vectors that are larger in magnitude than those at the Eastern Bank, Agulhas and Cape Town Grid Cells. As at the Cape Town Grid Cell, the vectors show an increase in magnitude from the early to late summer months. For example at the Lamberts Bay Grid Cell in September the vectors show a strength of ~3-4 $m.s^{-1}$ for the present and future simulations (Figs 2.10a and 2.10b). The late summer months (e.g. February) show values of ~7-9 $m.s^{-1}$ (Figs 2.12d and 2.12e). At the Port Nolloth Grid Cell in September the wind vectors show a strength of ~6-7 $m.s^{-1}$ for the present and future simulations (Figs 2.10a and 2.10b) and ~9-10 $m.s^{-1}$ in February (Figs 2.12d and 2.12e).

Days of Extreme Wind Speeds

At the Eastern Bank Grid Cell there is a 7.7% increase in the number of days showing extreme wind speeds (i.e. wind speeds defined as >15 $m.s^{-1}$, hereafter referred to as 'extreme wind speeds') over the spawning period (Fig. 2.16). There is an increase from 12 days of extreme wind speeds in the present simulation to 13 days in the future. At the Western Bank Grid Cell there are more days of extreme wind speeds in the present simulation than in the future (Fig. 2.17). For example in the present simulation there are 23 days where the wind speed exceeds 15 $m.s^{-1}$ whereas in the future simulation there are only 16 days. In the present simulation 2 days exceed 20 $m.s^{-1}$ whereas in the future there are no days that exceed this value. At the Cape Town Grid Cell the number of days showing extreme wind speeds in the present and future simulations are comparable (Fig. 2.18), with 17 days in both simulations showing extreme wind speeds.

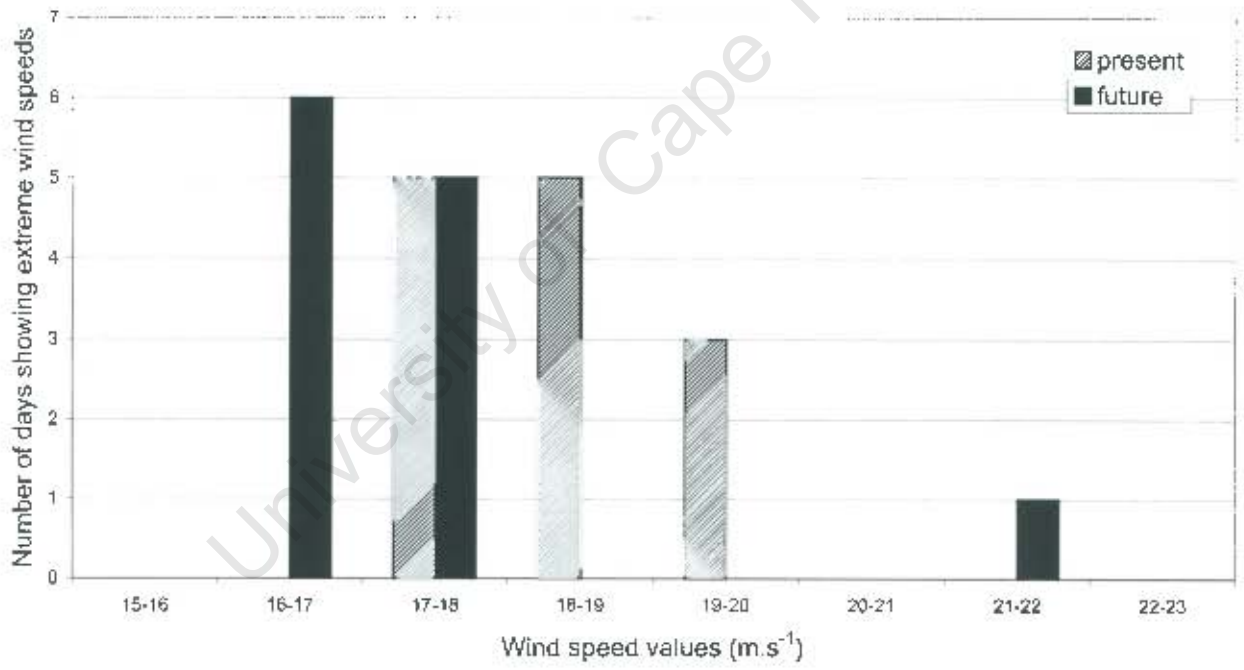

Figure 2-16 The number of days showing extreme wind speeds (defined as > 15 $m.s^{-1}$) for the spawning season in the present and future simulations at the Eastern Bank Grid Cell

At the Lamberts Bay Grid Cell there is a 50% increase in the number of days showing extreme wind speeds (Fig. 2.19). At the Port Nolloth Grid Cell there are more days of extreme wind speeds in the present simulation than in the future (Fig. 2.20). For example in the present

simulation there are 17 days where the wind speed exceeds 15 $m.s^{-1}$ whereas in the future simulation there are only 11 days.

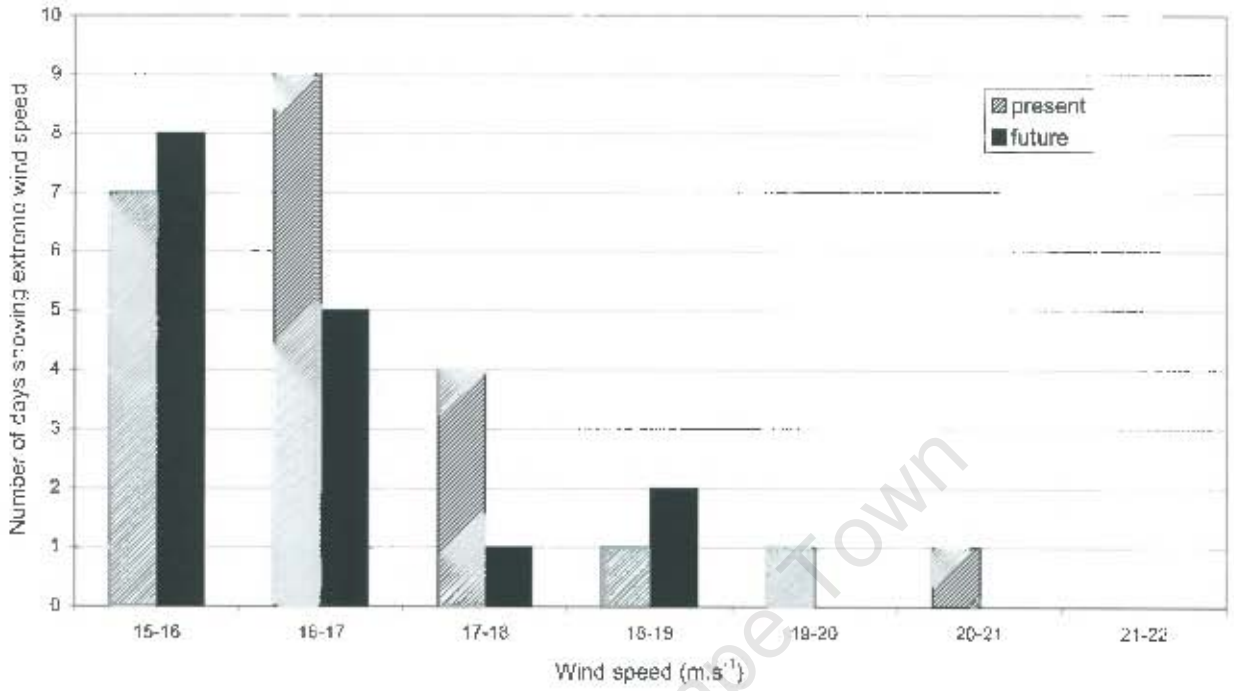

Figure 2-17 The number of days with extreme wind speeds (defined as > 15 $m.s^{-1}$) for the spawning season in the present and future simulations at the Western Bank Grid Cell

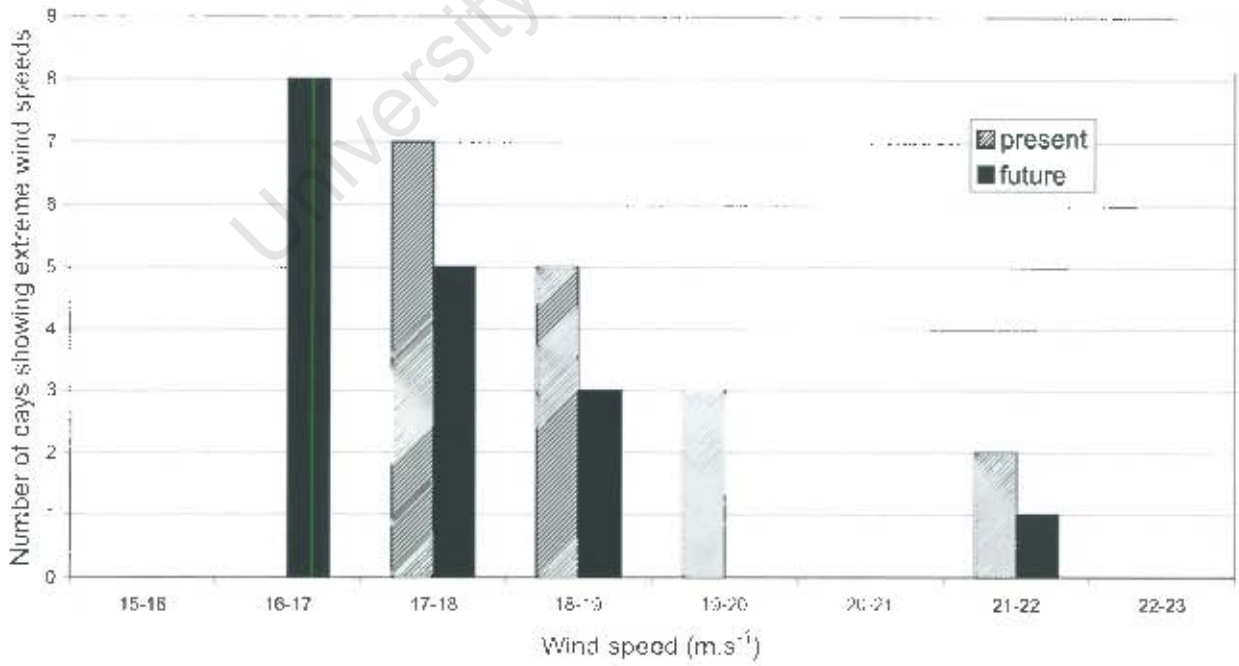

Figure 2-18 The number of days showing extreme wind speeds (defined as > 15 $m.s^{-1}$) for the spawning season in the present and future simulations at the Cape Town Grid Cell

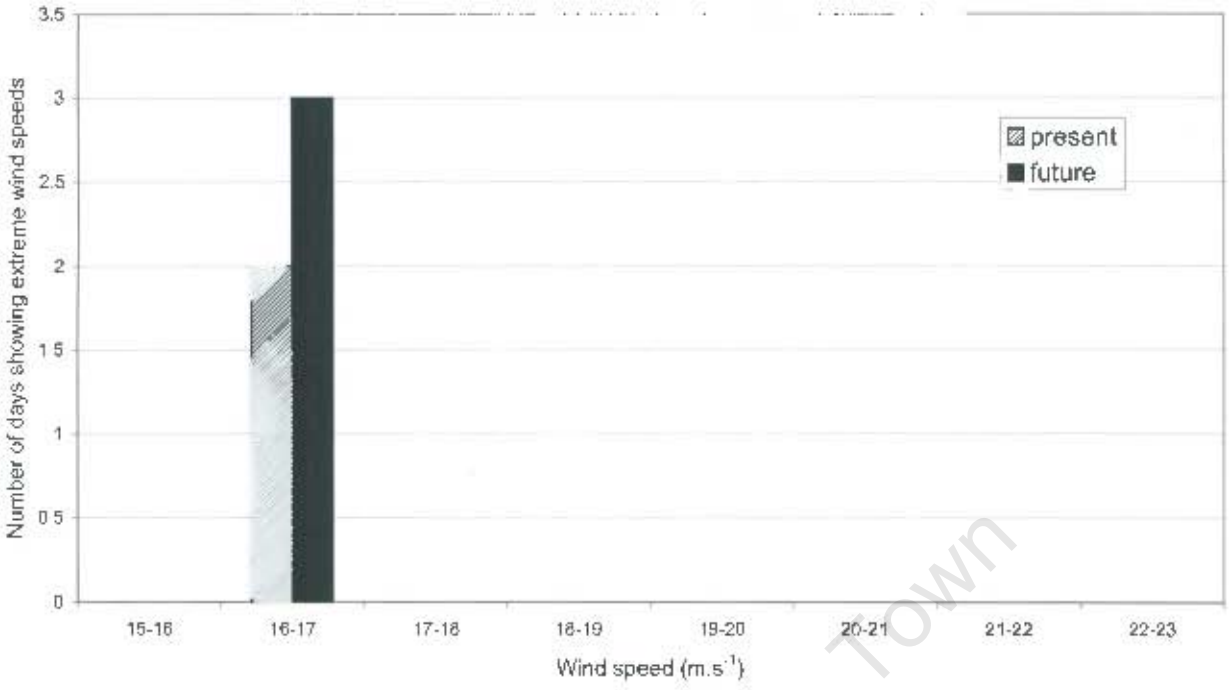

Figure 2-19 The number of days showing extreme wind speeds (defined as > 15 m.s^{-1}) for the spawning season in the present and future simulations at the Lamberts Bay Grid Cell

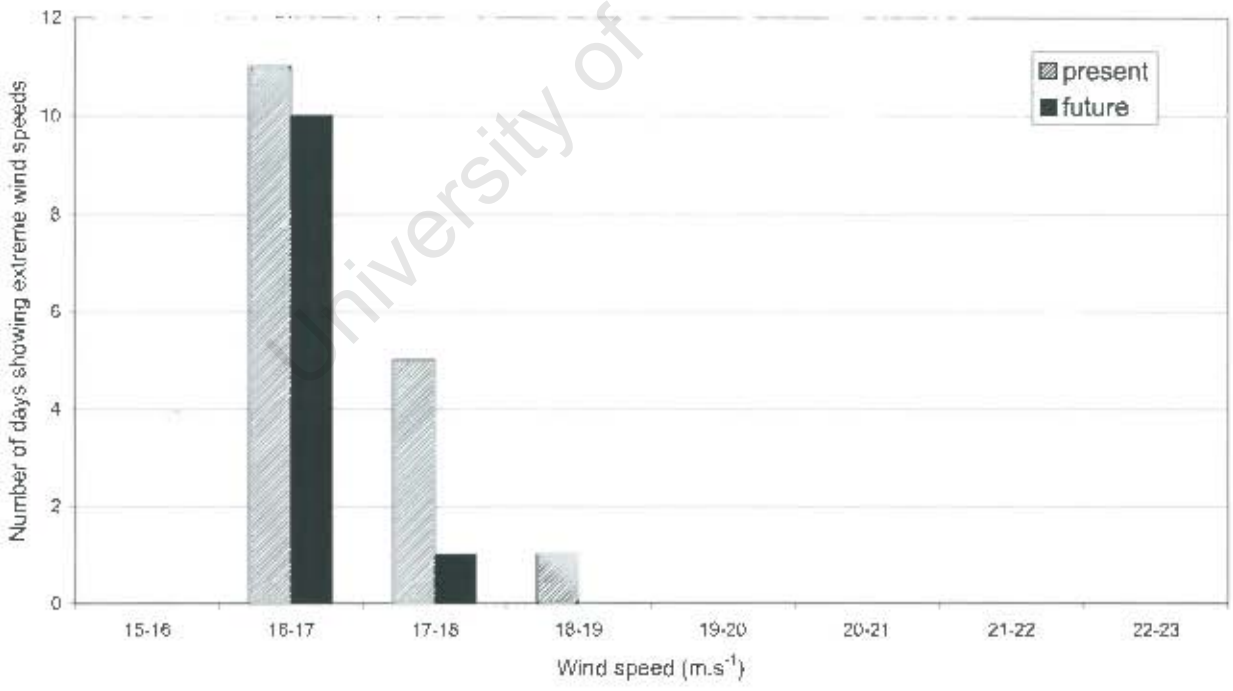

Figure 2-20 The number of days showing extreme wind speeds (defined as > 15 m.s^{-1}) for the spawning season in the present and future simulations at the Port Nolloth Grid Cell

2.3.3 Wind Direction

At the Eastern Bank Grid Cell the predominant wind is south-easterly in the spawning months in the present simulation (Fig. 2.21). In the future there is an increase in the frequency of south-easterly winds (Fig. 2.21). In September the average wind direction is south-westerly in both the present and future simulations (Figs 2.22 and 2.23). October shows an average south-westerly wind in the present and a south-easterly wind in the future. For the non-spawning months (i.e. May - August), the average winds are north-westerly in the present and future simulations.

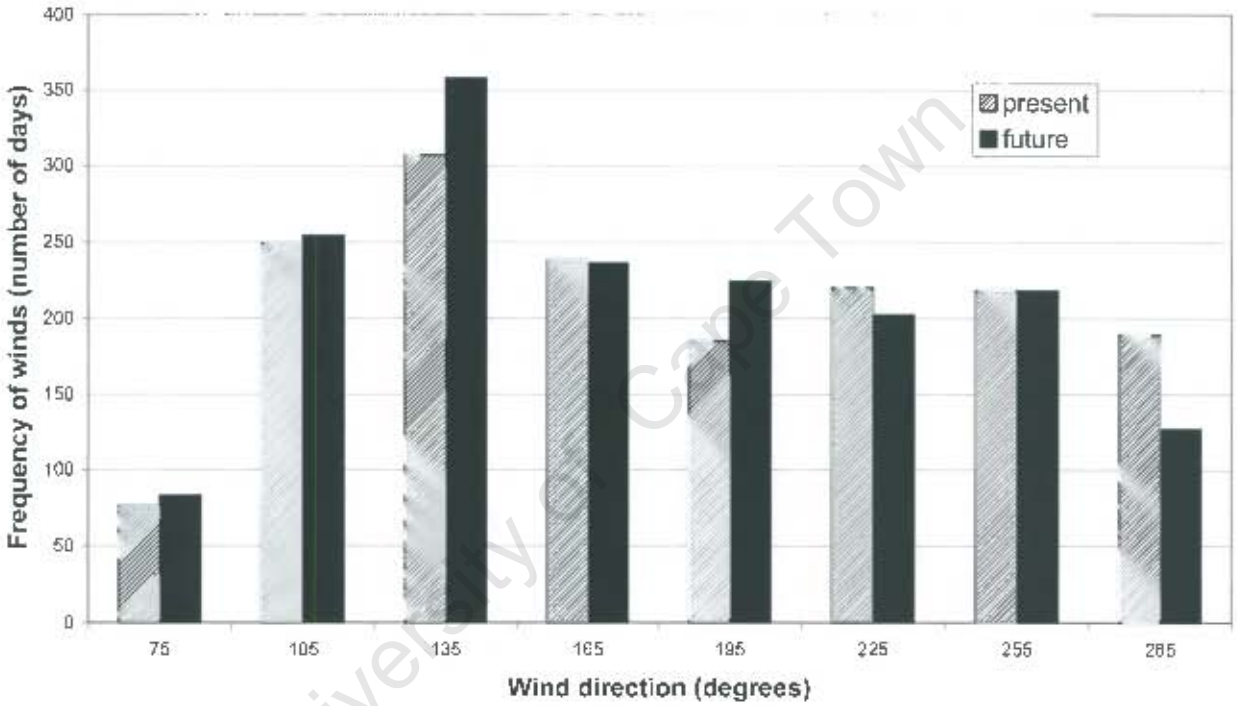

Figure 2-21 Histogram of wind direction for the range 75-285 degrees at the Eastern Bank Grid Cell for the spawning season in the pesent and future simulation

The predominant wind direction at the Western Bank Grid Cell is south-easterly in the spawning season in both the present and future simulations (Fig. 2.24). The future simulation shows an increase in the frequency of south-easterlies from September - February. There is an expected increase in the magnitude of south-easterly winds in the future as a result of the ridging of the South Atlantic High Pressure System south and east of the continent in the future (see Figs 2.5-2.7). The average wind direction in September is south-westerly in the present and future simulations (Figs 2.25 and 2.26). In October the average wind direction changes from a south-westerly wind in the present to a south-easterly wind in the future. For the non-spawning

months (i.e. May - August) the average wind direction is north-westerly in both the present and future simulations.

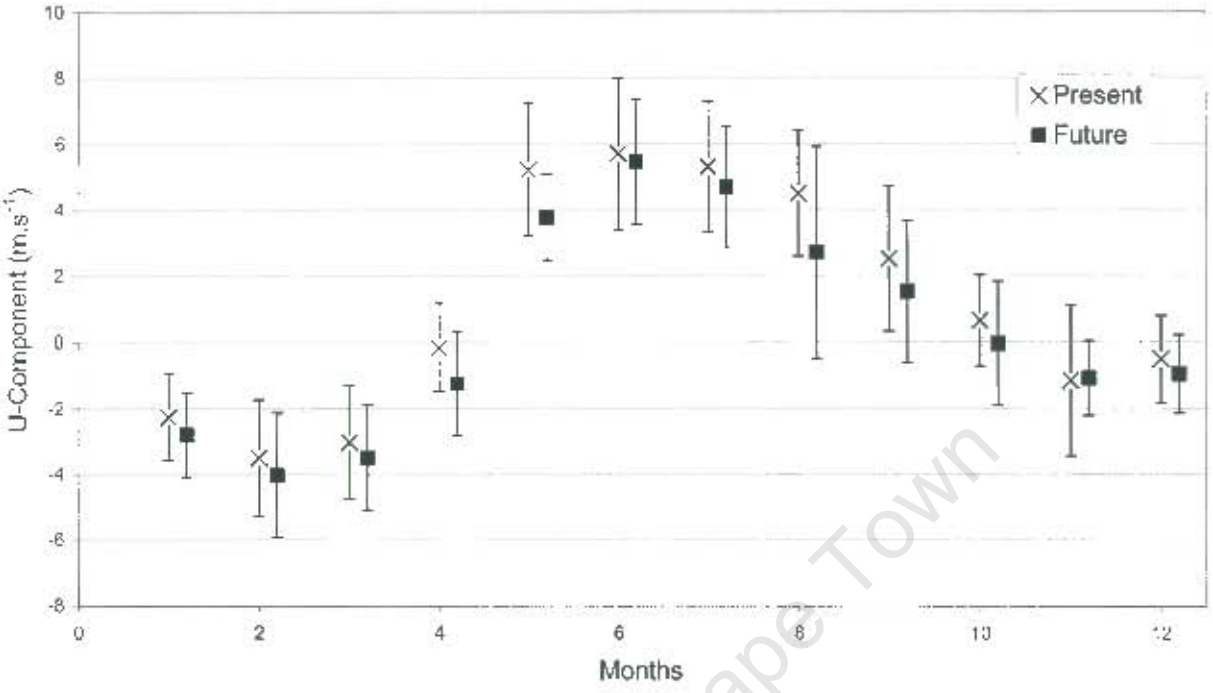

Figure 2-22 The difference between present and future monthly u component averages (+- standard deviation) at the Eastern Bank Grid Cell

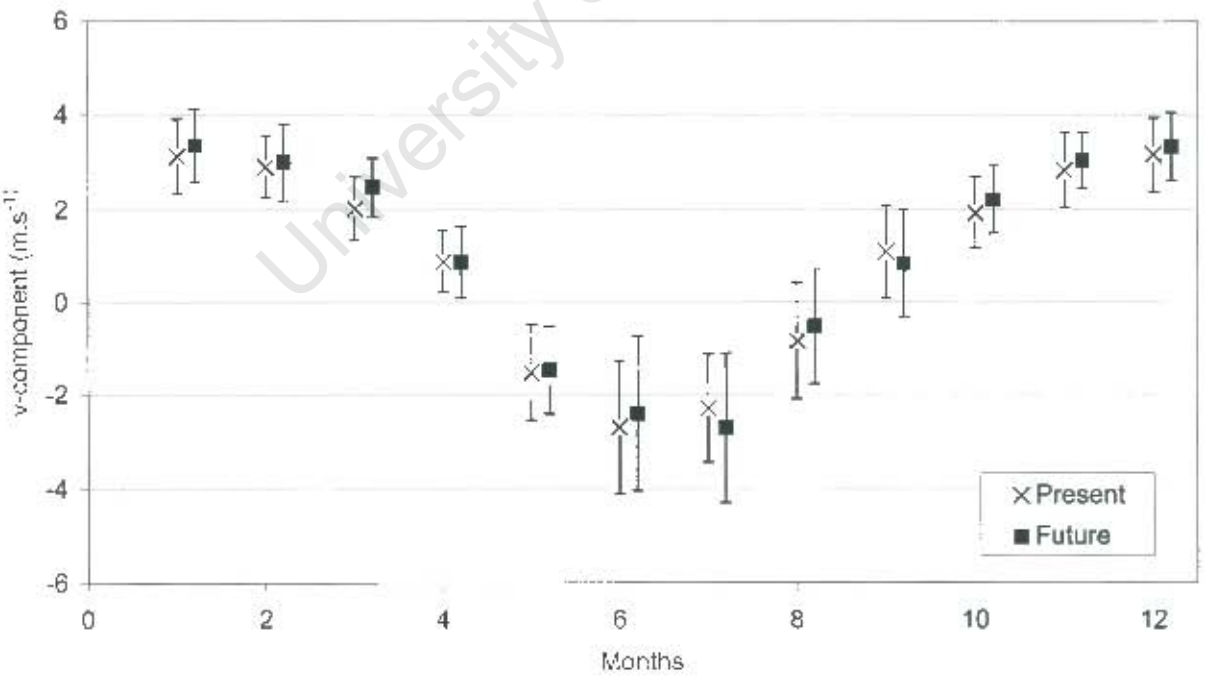

Figure 2-23 The difference between present and future v component monthly averages (+- standard deviation) at the Eastern Bank Grid Cell

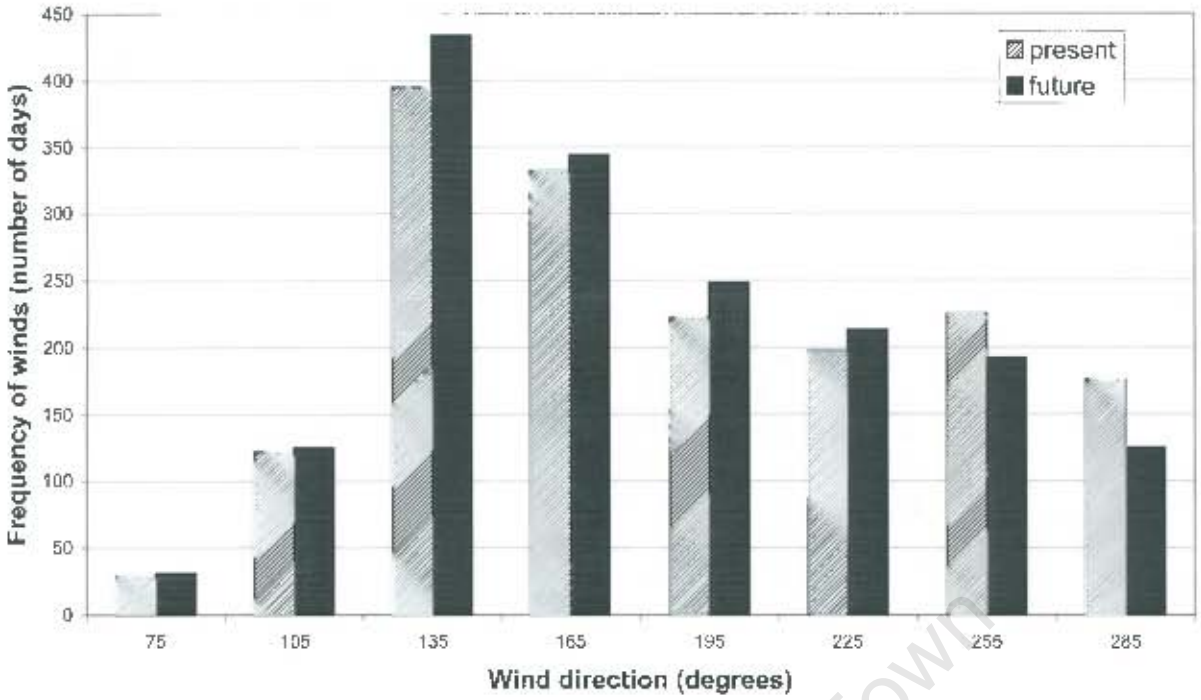

Figure 2-24 Histogram of wind direction for the range 75-285 degrees at the Western Bank Grid Cell in the spawning season in the present and future simulation

At the Cape Town Grid Cell average winds are southerly-easterly in direction for the spawning season in both the present and future simulation (Fig. 2.27). The future simulation shows an increase in the frequency of south-easterly winds for the spawning months (Fig. 2.27). September and October, however, show south-westerly winds in the present and future (Figs 2.28 and 2.29). In the future simulation the average winds from December - February have a greater south-easterly component. May - July show average winds in a north-westerly direction in the present and future and August shows average winds in a southerly-westerly direction.

The average wind direction at the Lamberts Bay Grid Cell in the spawning season is south-easterly in the present simulation (Fig 2.30). In the future the average wind direction shows an increase in the frequency of south-easterly winds (Fig. 2.30). Winds that presently average an easterly direction in the spawning period, remain easterly in the future but are stronger (Fig. 2.31). For the non-spawning months at the Lamberts Bay Grid Cell, the month of May has south-westerly winds in the present and future simulations (Figs 2.31 and 2.32). June and July have average north-westerly winds in the present and future, whereas August displays average winds in a south-westerly direction in both simulations.

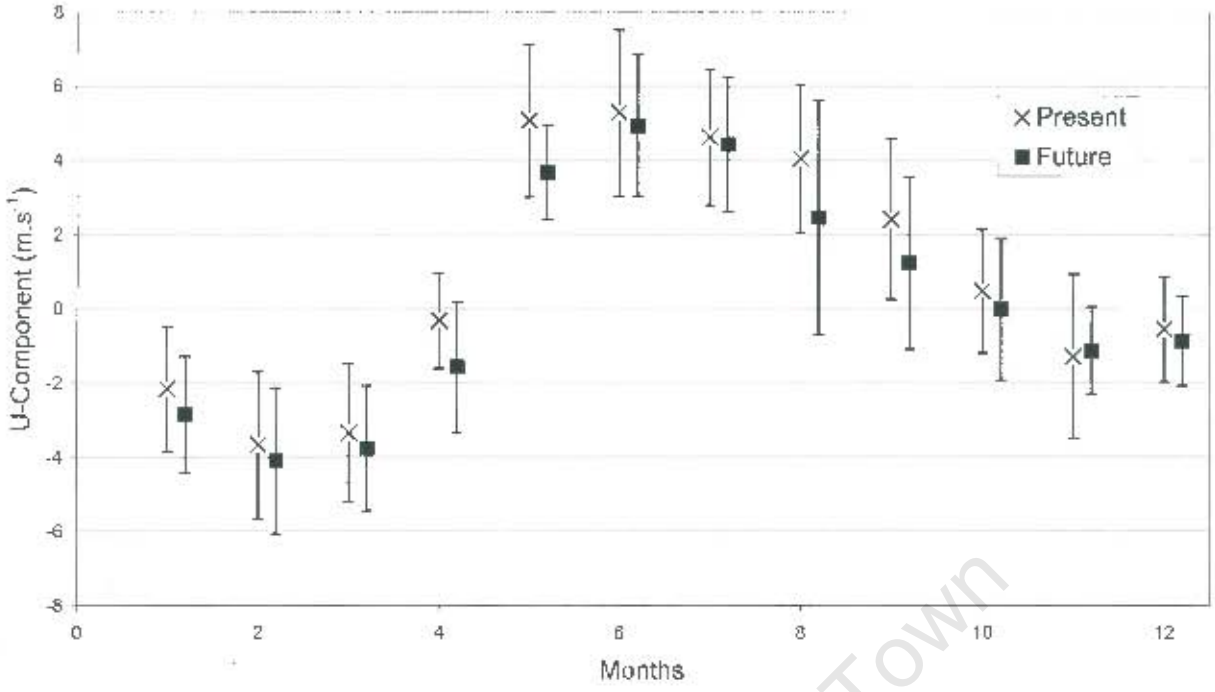

Figure 2-25 The difference between present and future monthly u component averages (+- standard deviation) at the Western Bank Grid Cell

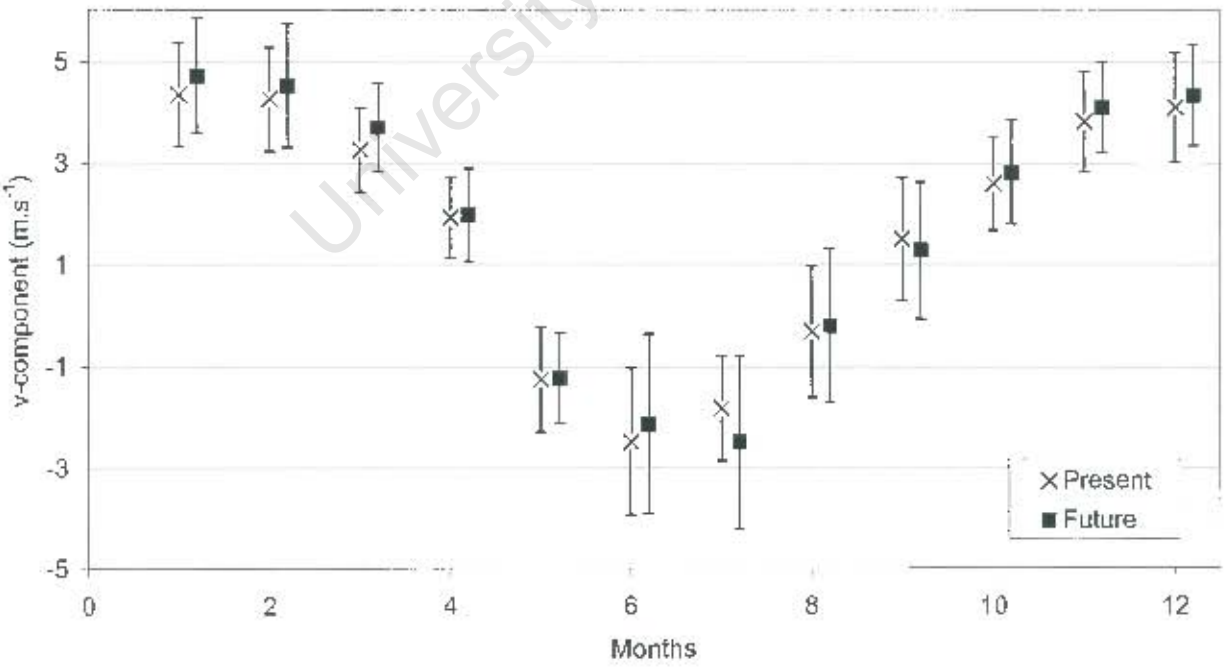

Figure 2-26 The difference between present and future v component monthly averages (+- standard deviation) at the Western Bank Grid Cell

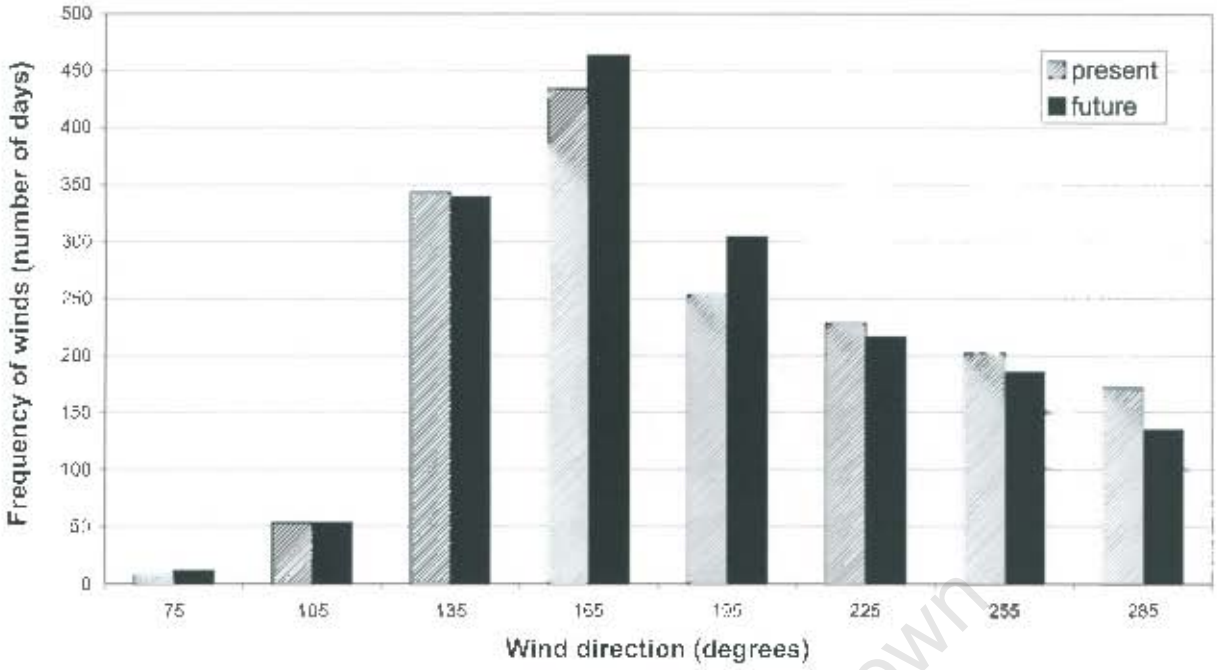

Figure 2-27 Histogram of wind direction for the range 75-285 degrees at the Cape Town Grid Cell for the spawning season in the present and future simulation

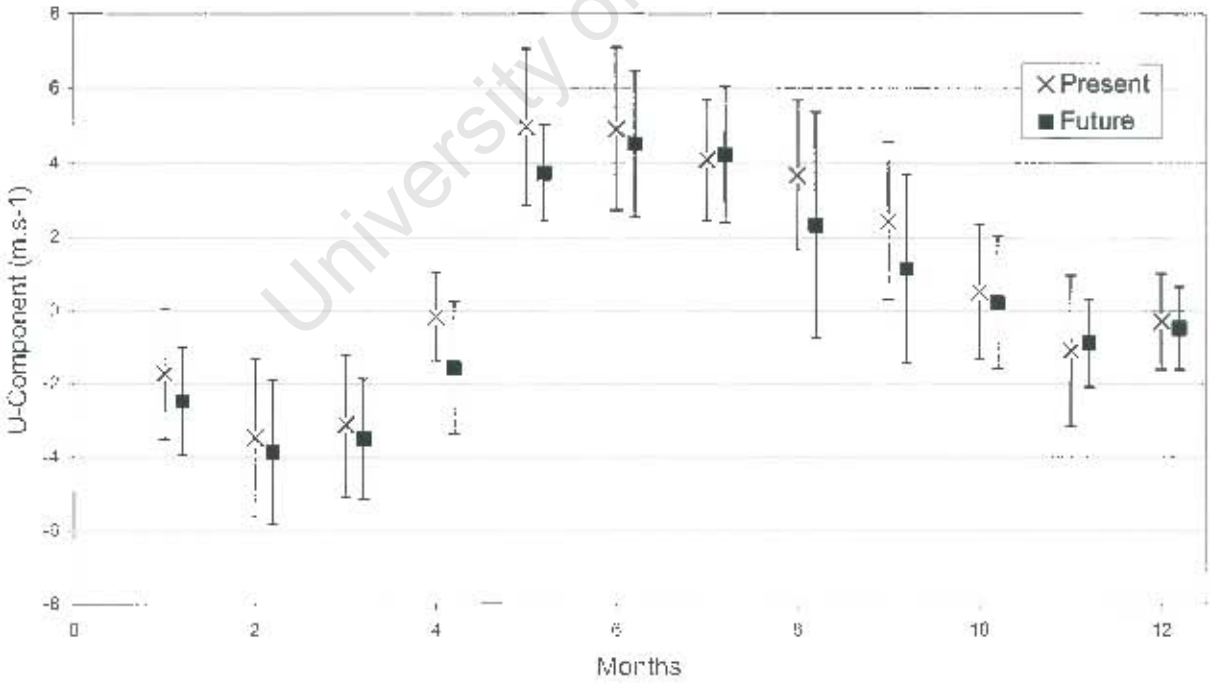

Figure 2-28 The difference between present and future monthly u component averages (+- standard deviation) at the Cape Town Grid Cell

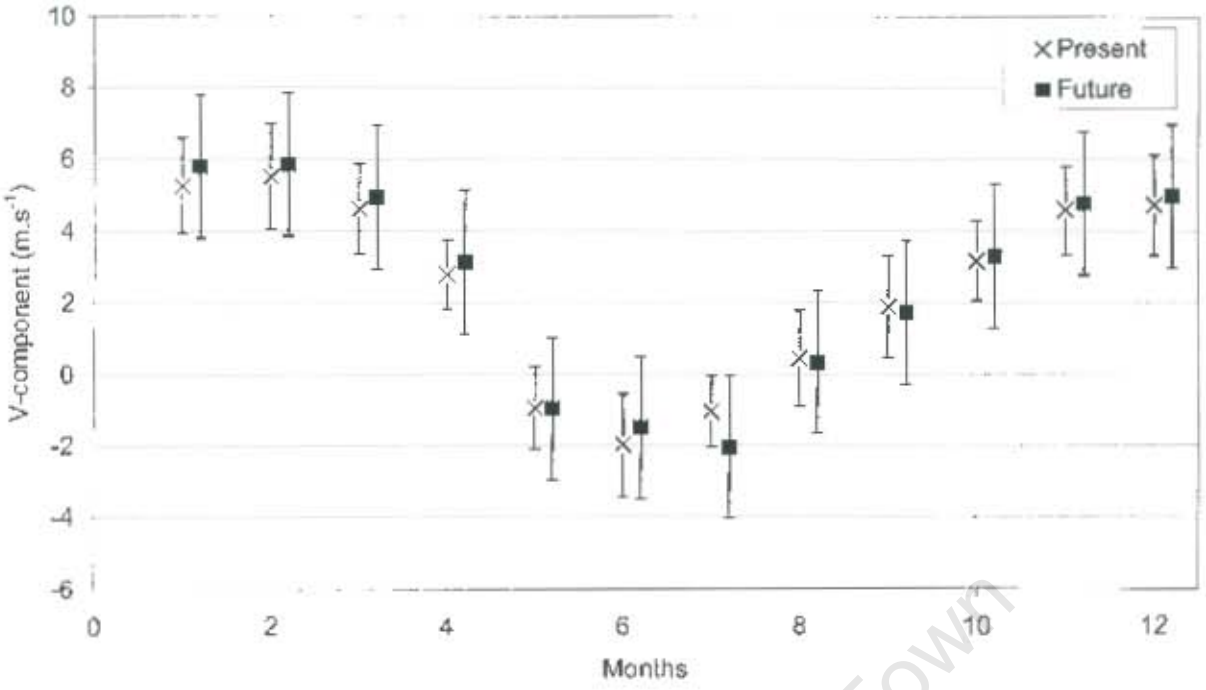

Figure 2-29 The difference between present and future monthly v component averages (+- standard deviation) at the Cape Town Grid Cell

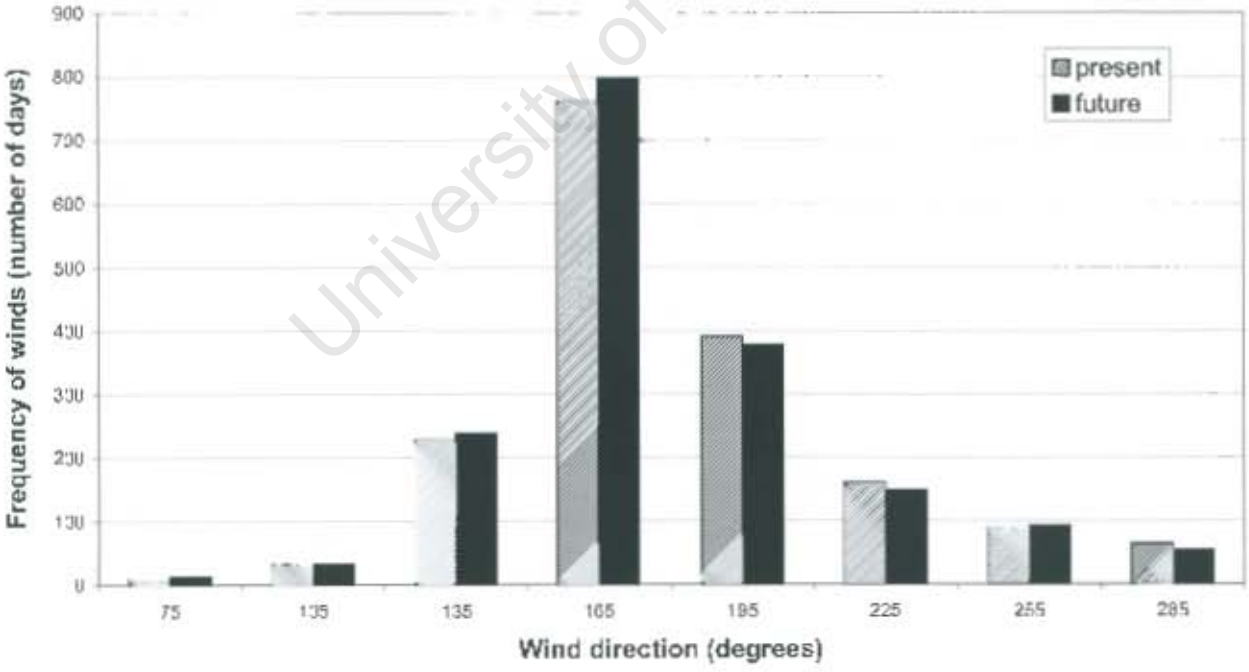

Figure 2-30 Histogram of wind direction for the range 75-285 degrees at the Lamberts Bay Grid Cell for the spawning season in the present and futue simulation

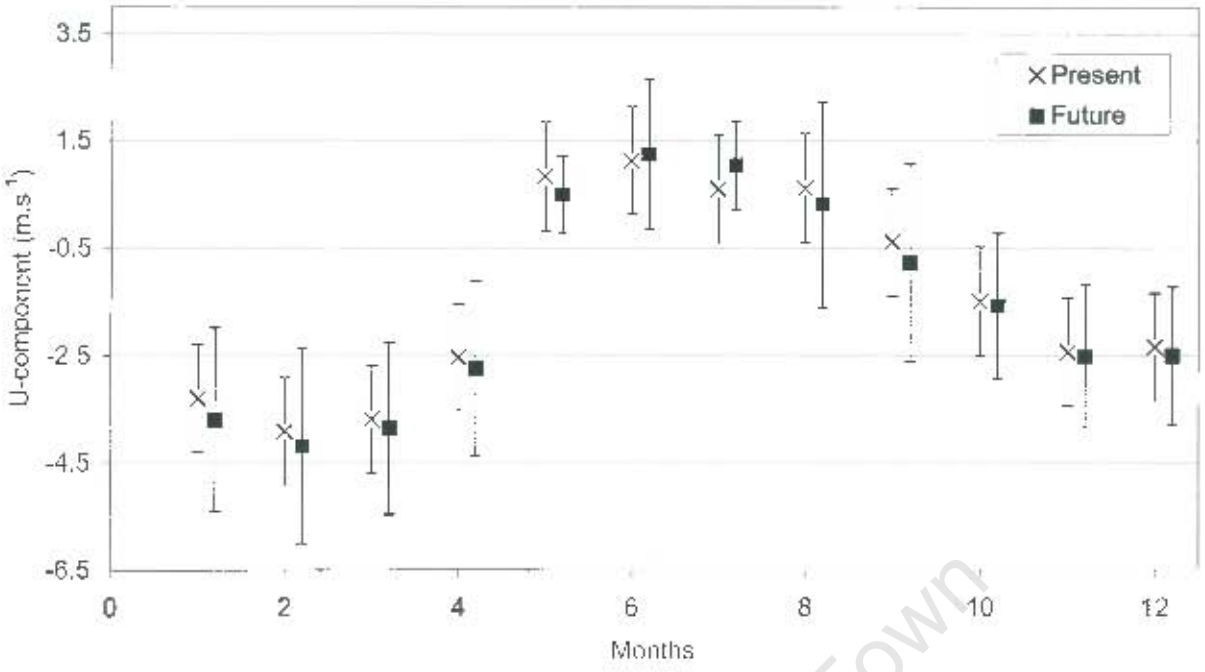

Figure 2-31 The difference between present and future u component monthly averages (+- standard deviation) at the Lamberts Bay Grid Cell

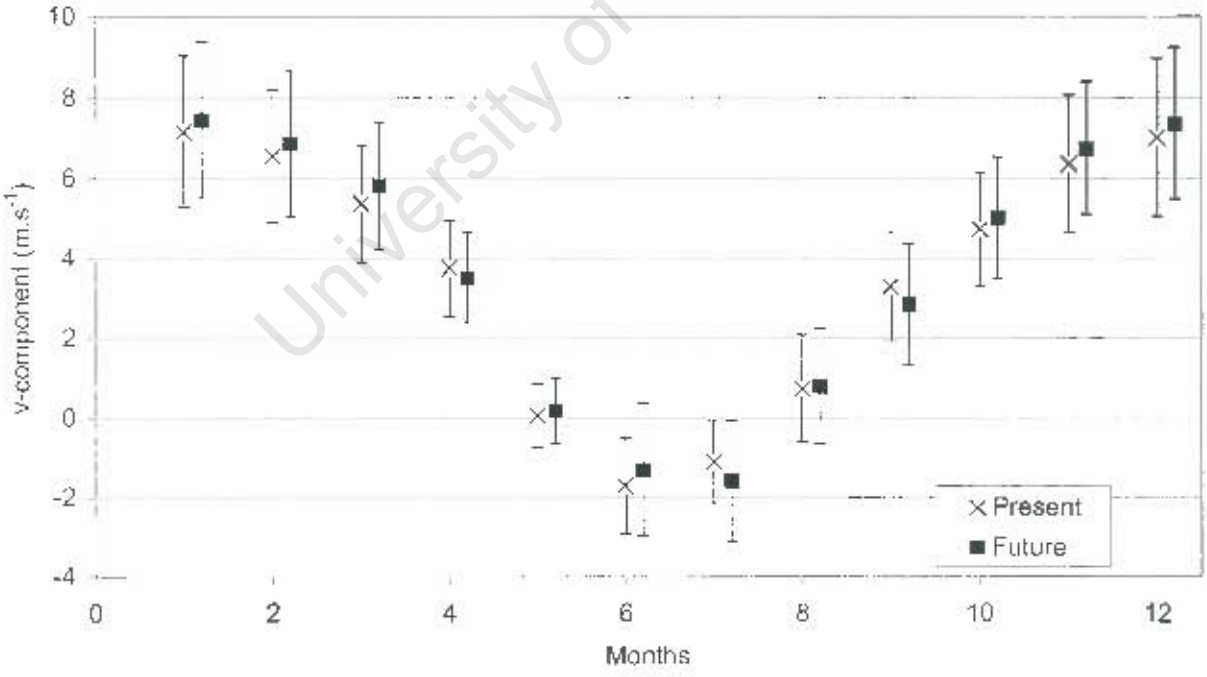

Figure 2-32 The difference between present and future v component monthly averages (+- standard deviation) at the Lamberts Bay Grid Cell

At the Port Nolloth Grid Cell, all months of the year display average winds in a south-easterly direction in the present simulation (Figs 2.33 and 2.34). In the future these winds are expected to remain south-easterly in direction, yet change in magnitude. The greatest magnitude of south-easterly winds in both the present and future simulations is for the spawning months (September - February). For the spawning months, there is a decrease in the frequency of south-easterly winds in the future (Fig. 2.35). November and February show an average decrease in easterly winds in the future (Figs 2.33 and 2.34). March and April also display strong average south-easterly winds in the present and future. The non-spawning months display average south-easterly winds in the present and future simulations, which are weaker in magnitude than the south-easterly winds shown in the spawning months (Figs 2.33 and 2.34).

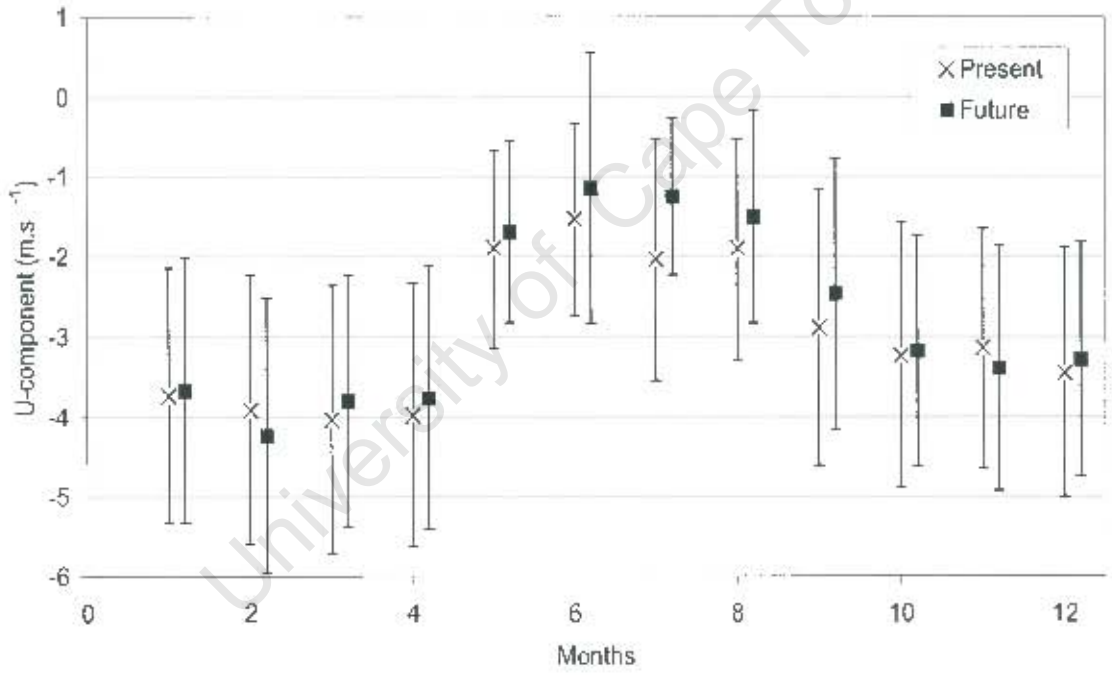

Figure 2-33 The difference between present and future u component monthly averages (+- standard deviation) at the Port Nolloth Grid Cell

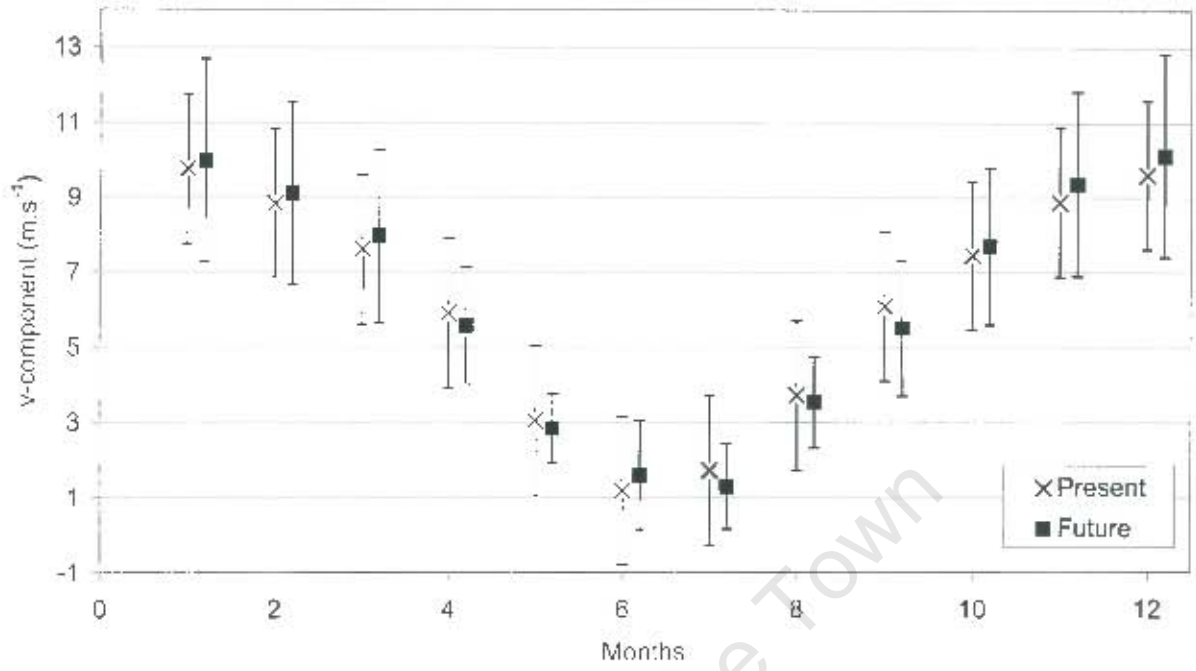

Figure 2-34 The difference between present and future v component monthly averages (+- standard deviation) at the Port Nolloth Grid Cell

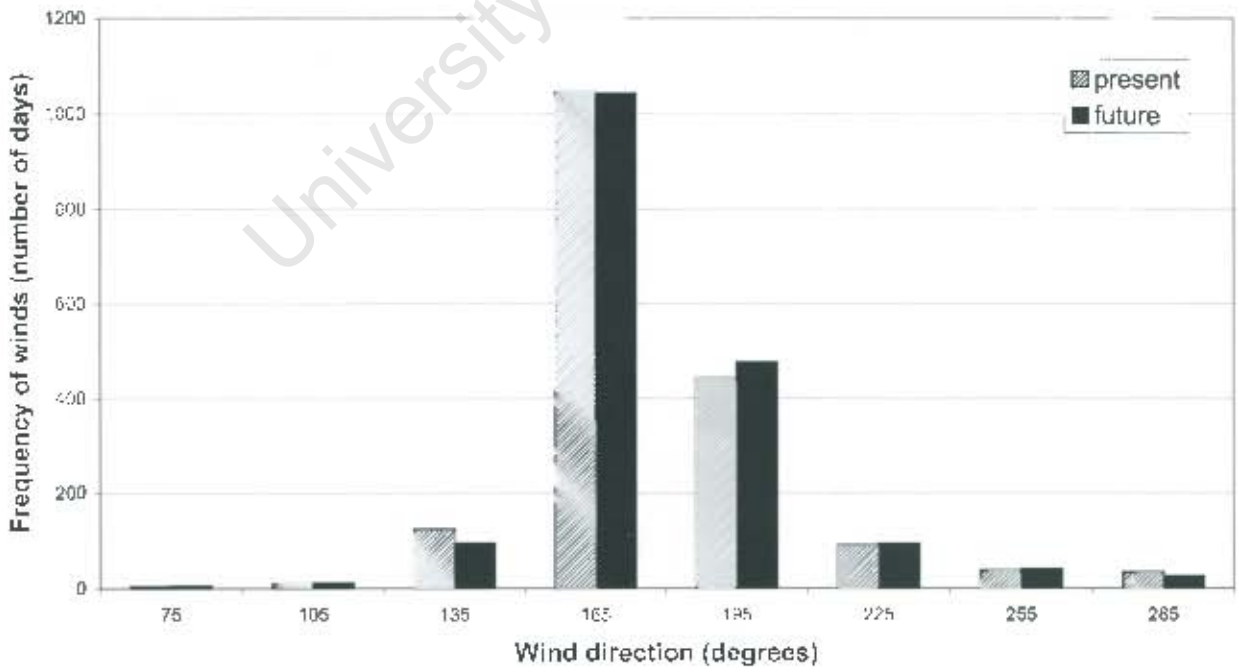

Figure 2-35 Histogram of wind direction for the range 75-285 degrees at the Port Nolloth Grid Cell in the spawning season in the present and future simulation

2.3.4 Turbulence

Mean turbulence values

At the Eastern Bank there is an expected decrease in average turbulence values for the spawning season from the present to the future (Fig. 2.36). The average turbulence for the whole spawning period in the present simulation is 587 $m^3.s^{-3}$ and in the future is 528 $m^3.s^{-3}$. For the non-spawning months (March - August) the average turbulence in the present simulation is 886 $m^3.s^{-3}$ and 819 $m^3.s^{-3}$ in the future. The average decrease in turbulence in the spawning season is 10% and shows a significant difference ($p < 0.05$). January is the only month in the spawning season that displays an increase in turbulence (i.e. from 337 $m^3.s^{-3}$ to 409 $m^3.s^{-3}$). The most notable decrease (23%) in turbulence for the spawning period in the future is for December, which shows a decrease from 469 $m^3.s^{-3}$ to 362 $m^3.s^{-3}$.

An analysis of the model output data shows that there is a 9% decrease in mean turbulence from September - February at the Western Bank Grid Cell from 658 $m^3.s^{-3}$ in the present to 596 $m^3.s^{-3}$ in the future for the spawning season (Fig. 2.37). There is a significant difference between present and future turbulence values ($p < 0.05$). January is the only month in the spawning season that shows an increase in average turbulence values from the present to the future simulation. January shows a 13.2% increase in turbulence in the future. The predicted average turbulence for the whole non-spawning period is 879 $m^3.s^{-3}$ in the present and 844 $m^3.s^{-3}$ in the future.

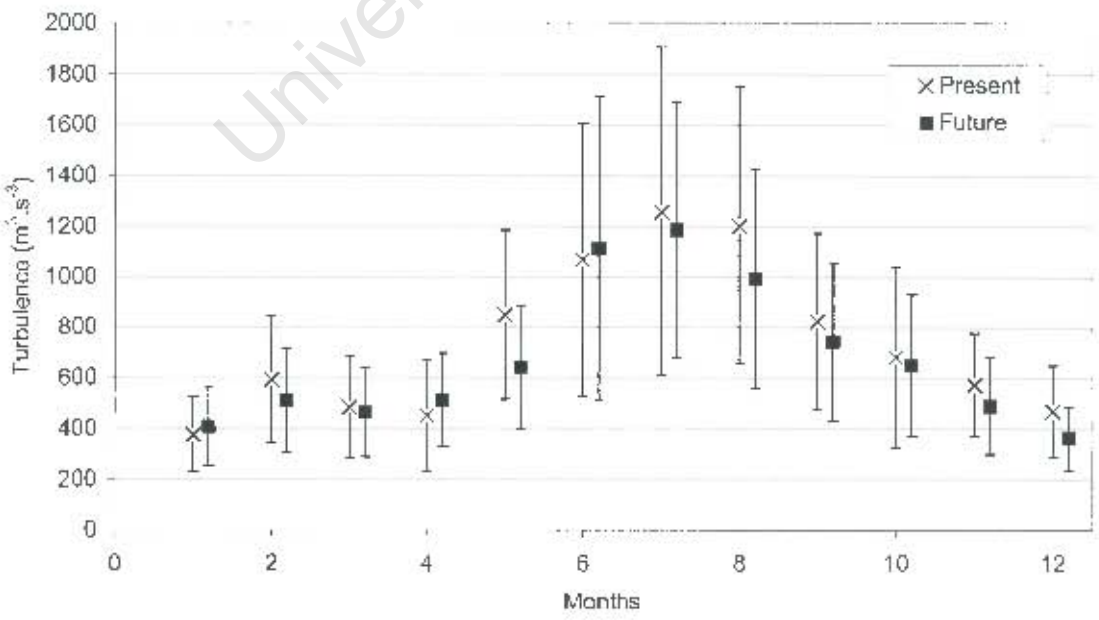

Figure 2-36 The difference between present and future turbulence ($m^3.s^{-3}$) monthly averages (+- standard deviation) at the Eastern Bank Grid Cell

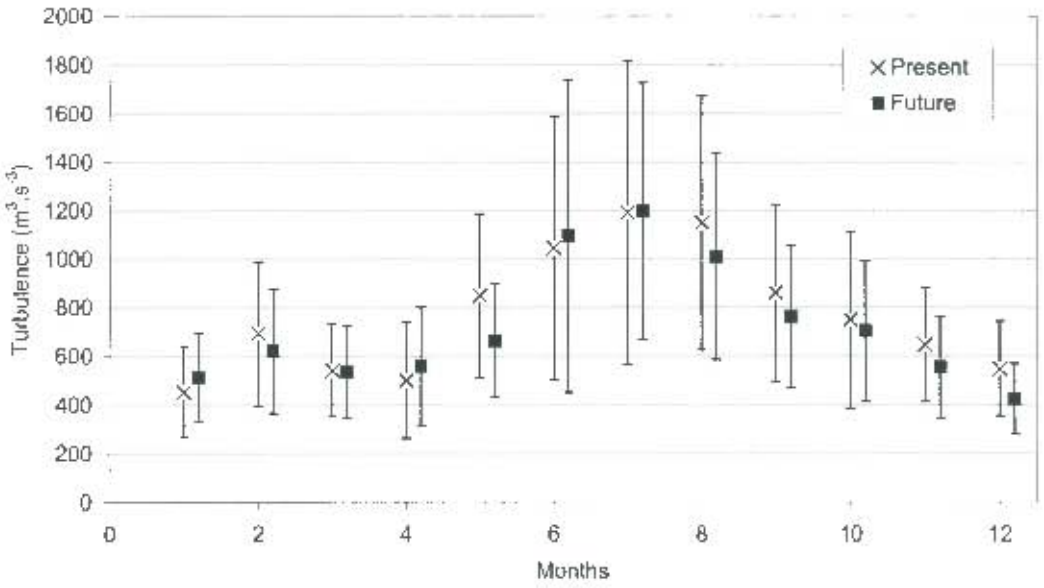

Figure 2-37 The difference between present and future turbulence ($m^3.s^{-3}$) monthly averages (+- standard deviation) at the Western Bank Grid Cell

At the Cape Town Grid Cell the spawning months show an overall decrease in turbulence from 739 $m^3.s^{-3}$ in the present to 670 $m^3.s^{-3}$ in the future (a 9.3% decrease) (Fig. 2.38). The difference between present and future turbulence is significant ($p < 0.05$). The only month in the spawning season to display an increase in turbulence from the present to future is January (19% increase) (Fig. 2.39). December shows the largest decrease in turbulence in the spawning season from 601 $m^3.s^{-3}$ in the present to 482 $m^3.s^{-3}$ in the future (a decrease of 20%). The non-spawning months also display an overall decrease in average turbulence from 874 $m^3.s^{-3}$ in the present to 860 $m^3.s^{-3}$ in the future.

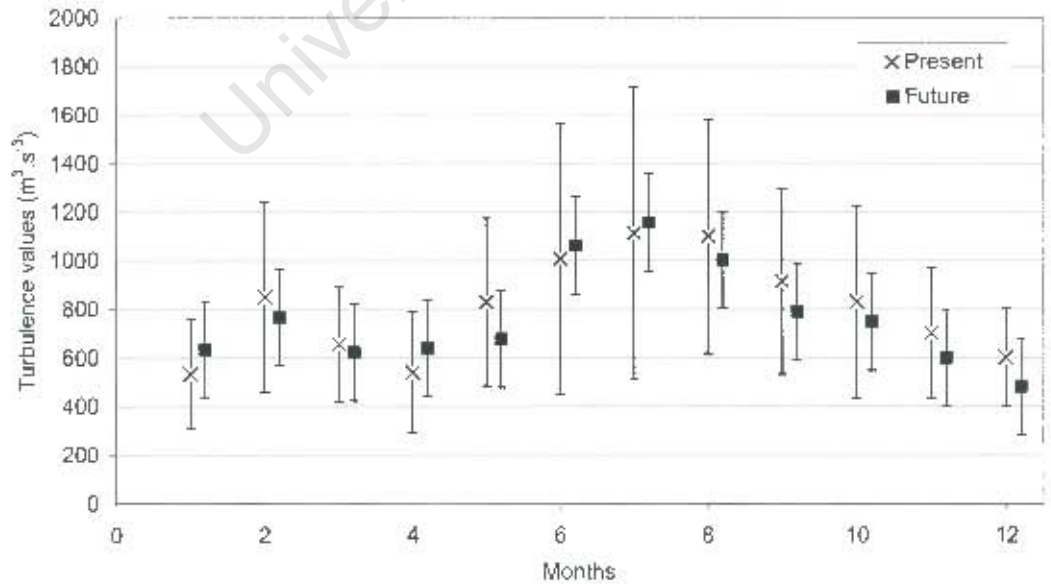

Figure 2-38 The difference between present and future turbulence ($m^3.s^{-3}$) monthly averages (+- standard deviation) at the Cape Town Grid Cell

At the Lamberts Bay Grid Cell there is an overall increase in average turbulence in the spawning season from 694 $m^3.s^{-3}$ in the present to 713 $m^3.s^{-3}$ in the future (Fig. 2.39). This increase (2.6%), however, is not significant ($p > 0.05$). The results show an increase in turbulence for all months in the spawning period except October and December. For the non-spawning months there is an average increase in turbulence from 426 $m^3.s^{-3}$ in the present to 446 $m^3.s^{-3}$ in the future.

At the Port Nolloth Grid Cell the model output displays an increase in turbulence for the spawning season from 1235 $m^3.s^{-3}$ in the present simulation to 1267 $m^3.s^{-3}$ in the future (i.e. an increase of 2.7%) (Fig. 40). This increase, however, is not significant ($p > 0.05$). Within the spawning season, November - February show an increase in turbulence values, whereas September - October display decreases in average turbulence. The results show a decrease in turbulence for the non-spawning months from 585 $m^3.s^{-3}$ in the present to 561 $m^3.s^{-3}$ in the future.

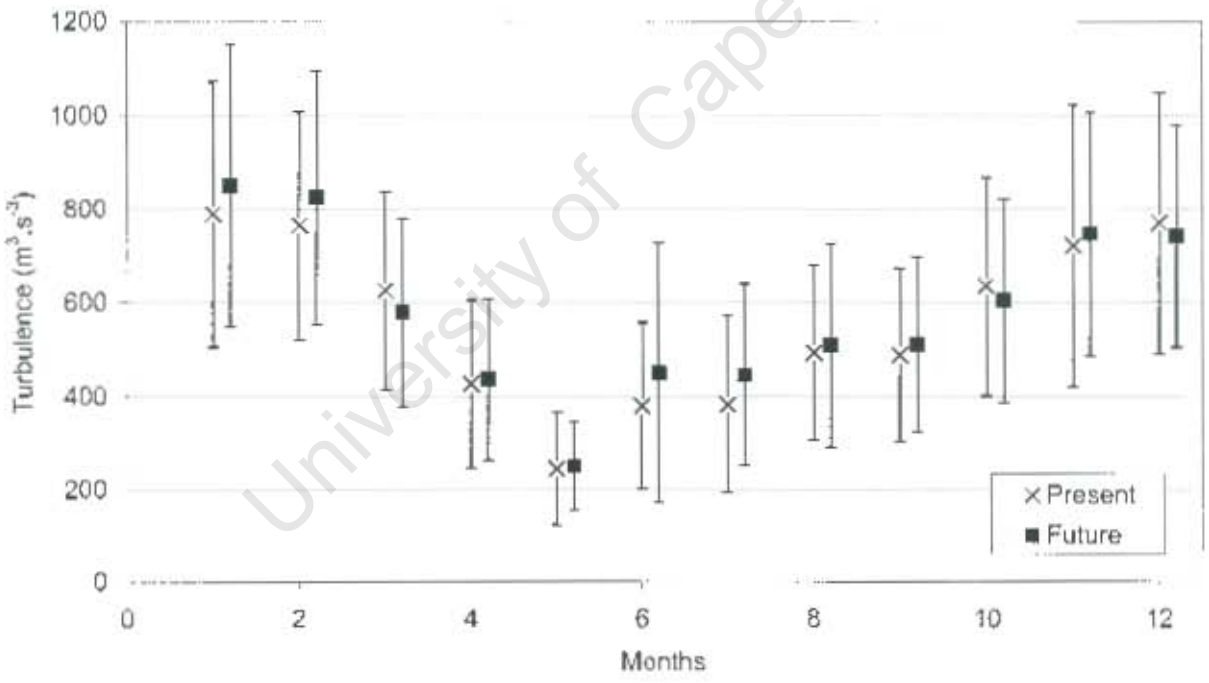

Figure 2-39 The difference between present and future turbulence ($m^3.s^{-3}$) monthly averages (+- standard deviation) at the Lamberts Bay Grid Cell

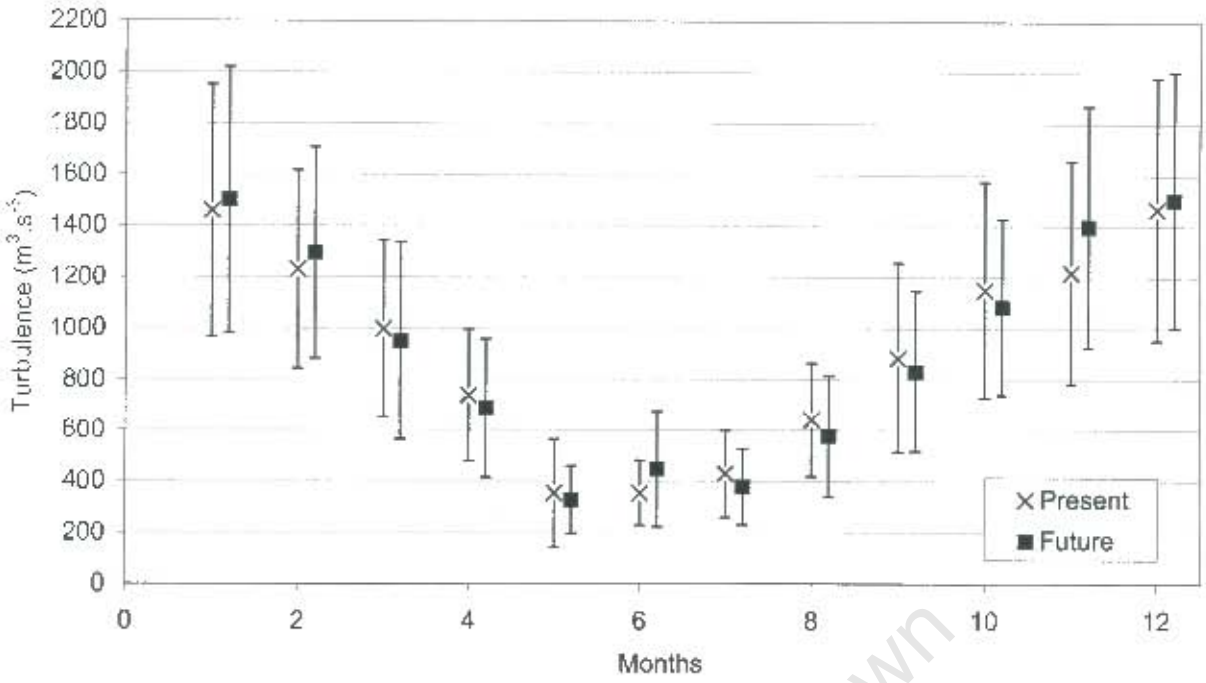

Figure 2-40 The difference between present and future turbulence ($m^3.s^{-3}$) monthly averages (+/- standard deviation) at the Port Nolloth Grid Cell

Days of Extreme Turbulence Values

At the Eastern Bank Grid Cell there are fewer days in the future than the present that display extreme turbulence (i.e. turbulence > 5000 $m^3.s^{-3}$, hereafter referred to as 'extreme turbulence') (Fig. 2.41). For example, in the present simulation there are 16 days showing extreme turbulence whereas in the future simulation there are only 6 days (a decrease of 63%). In the present simulation 8 days exceed 6000 $m^3.s^{-3}$ whereas in the future there is only 1 day that exceeds this value.

At the Western Bank Grid Cell there is a 57% decrease in the number of days showing extreme turbulence in the future simulation for the spawning months (Fig. 2.42). For example, in the present simulation there are 16 days where the turbulence exceeds 5000 $m^3.s^{-3}$, whereas in the future simulation there are only 7 days.

At the Cape Town Grid Cell there are fewer days in the future than the present that display extreme turbulence (Fig. 2.43). For example, in the present simulation there are 17 days where the turbulence exceeds 5000 $m^3.s^{-3}$ whereas in the future simulation there are only 7 days (a decrease of 59%).

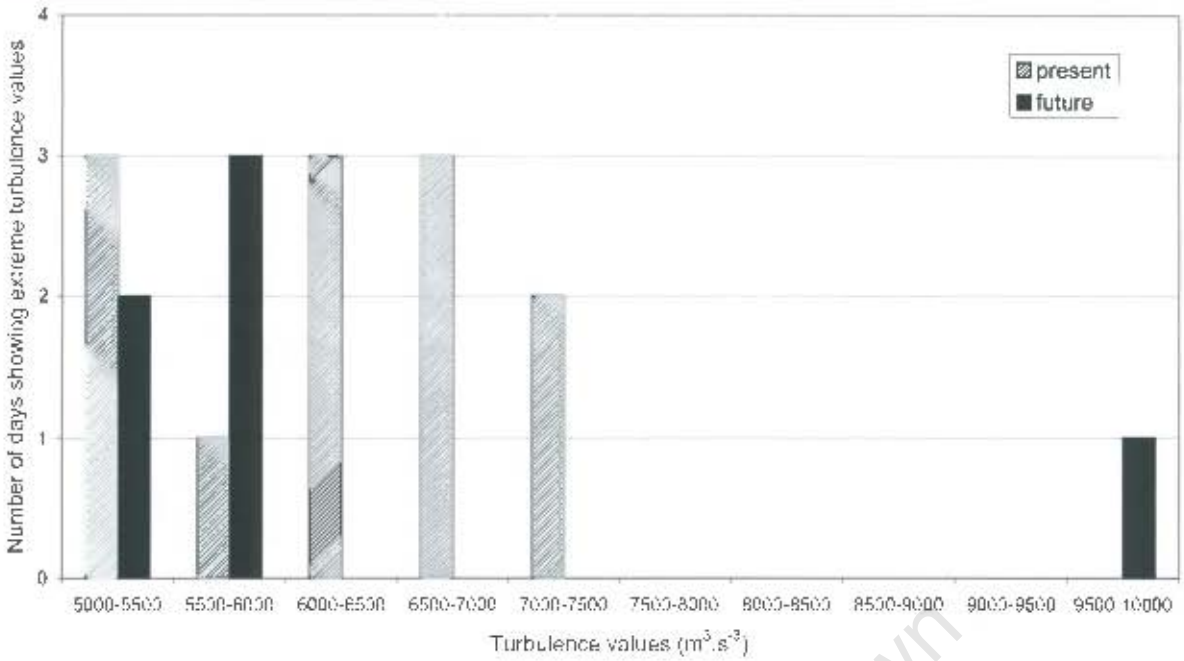

Figure 2-41 The number of days showing extreme turbulence values (defined as > 5000 $m^3.s^{-3}$) for the spawning season in the present and future simulations at the Eastern Bank Grid Cell

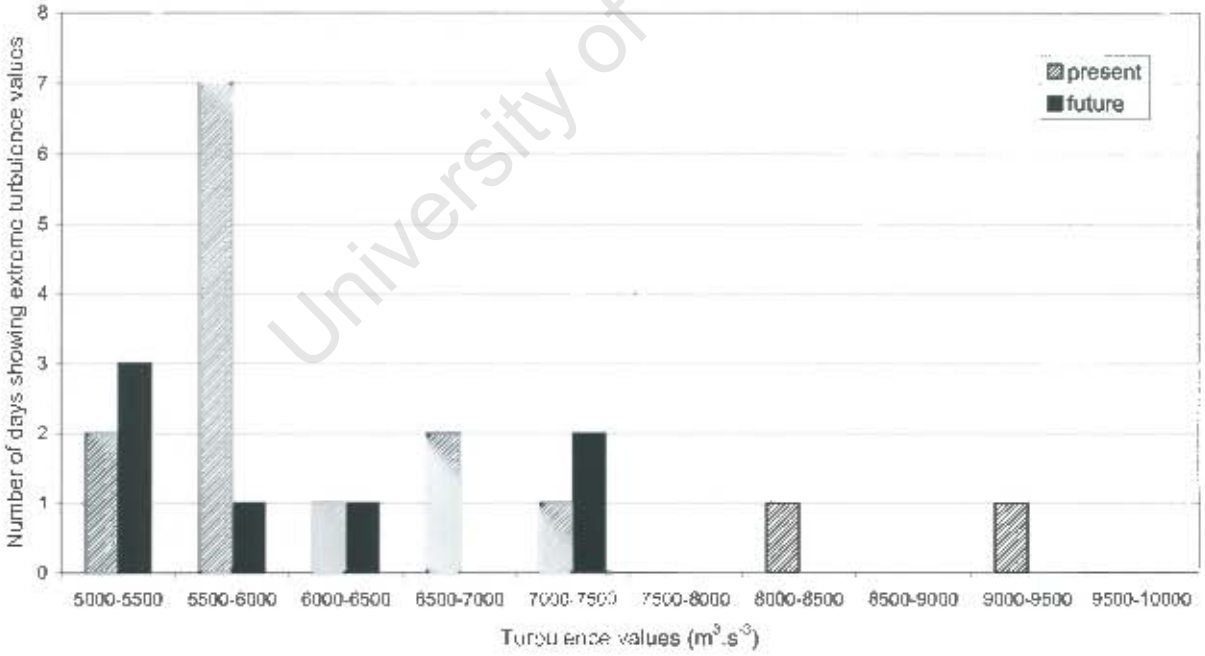

Figure 2-42 The number of days showing extreme turbulence values (defined as > 5000 $m^3.s^{-3}$) for the spawning season in the present and future simulations at the Western Bank Grid Cell

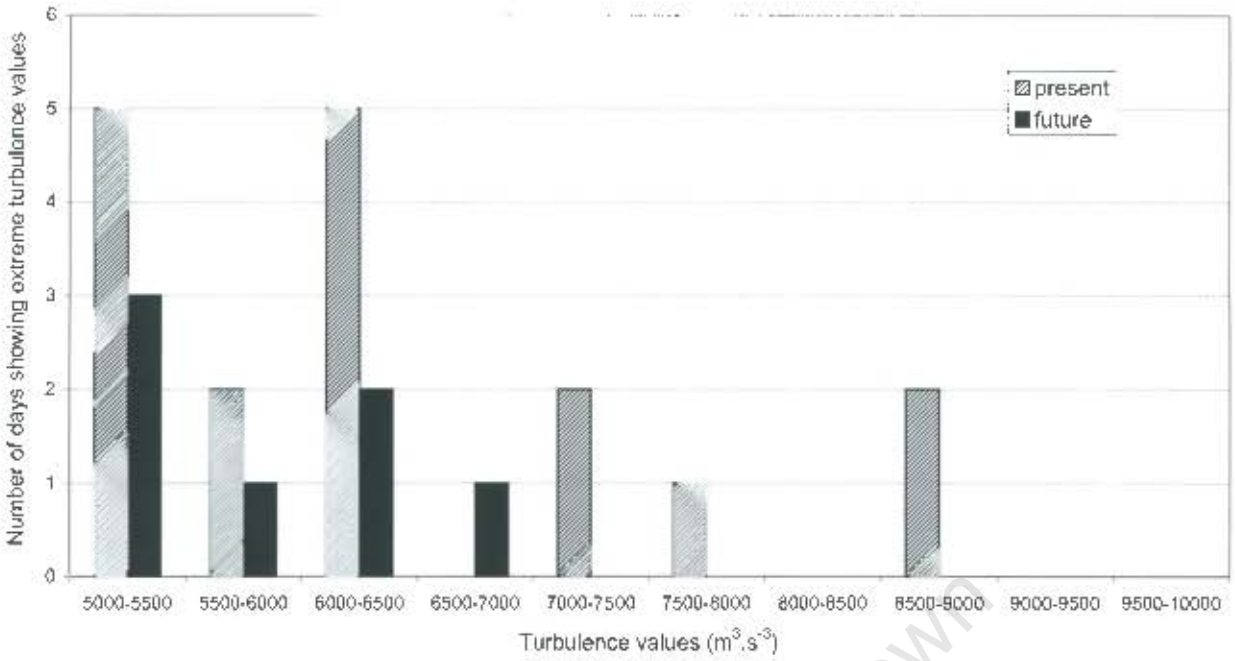

Figure 2-43 The number of days showing extreme turbulence values (defined as > 5000 $m^3.s^{-3}$) for the spawning season in the present and future simulation at the Cape Town Grid Cell

At the Lamberts Bay Grid Cell there are no days in both the present and future simulations that show extreme turbulence values. At the Port Nolloth Grid Cell there is a 50% decrease in the number of days showing extreme turbulence (Fig. 2.44).

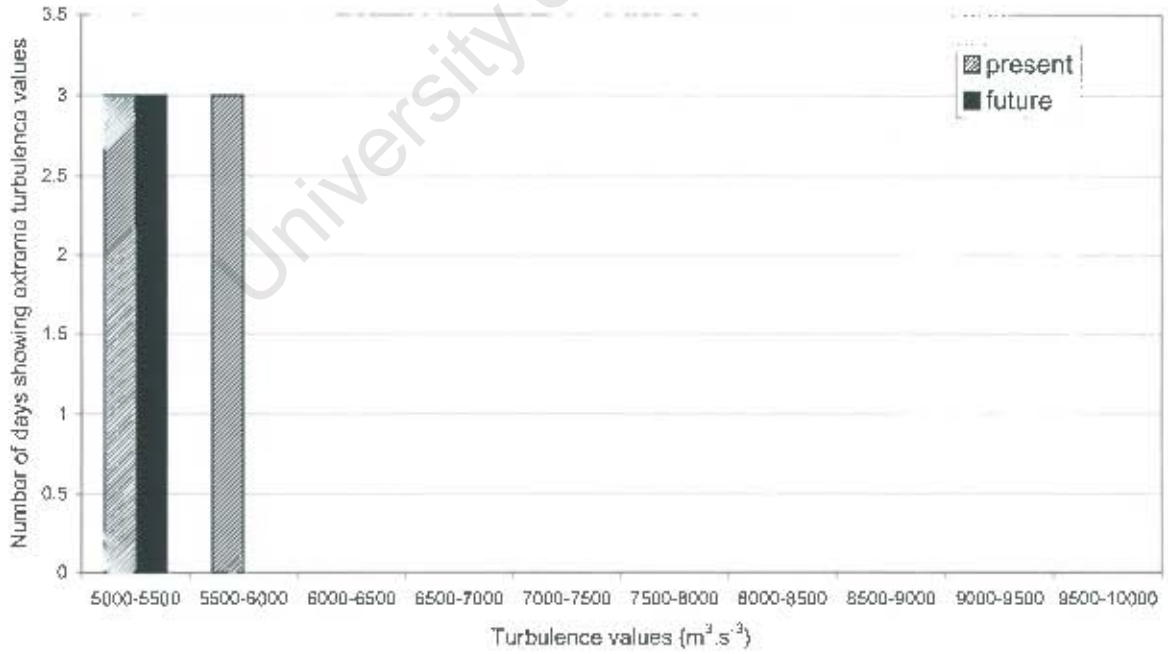

Figure 2-44 The number of days showing extreme turbulence values (defined as > 5000 $m^3.s^{-3}$) for the spawning season in the present and future simulations at the Port Nolloth Grid Cell

2.3.5 Lasker Events

There is an increase in the number of Lasker events from the present to the future simulation at the Eastern Bank Grid Cell for the spawning period (Figs 2.45 and 2.46). There is an 81% increase in the number of Type A Lasker events from 16 events in the present to 29 in the future (Fig. 2.45). There is an 86% increase in Type B Lasker events from 7 events in the present simulation to 13 in the future (Fig. 2.46). For the spawning period, the largest increase in the number of Lasker events is projected for December. December shows a 300% increase in Type A Lasker events and a 600% increase in Type B events in the future simulation. In the early summer months, September and October show a 60% and 80% projected decrease in Type A Lasker events in the future.

The Western Bank Grid Cell shows an overall decrease in the number of Lasker events over the spawning season in the future (Figs 2.47 and 2.48). There is a 27% decrease in Type A Lasker events from 22 events over a ten year period in the present simulation to 16 over the same period in the future (Fig. 2.47). There is a 20% decrease from 10 Type B Lasker events in the present simulation to 8 in the future (Fig. 2.48). In the spawning months, the only month that shows an increase in Lasker events in the future is November, which shows a 67% increase. The remainder of the spawning months show either similar values or a decrease in the future (i.e. September and December show a decrease of 60% and 33% respectively in the future for the number of Type A events).

At the Cape Town Grid Cell over the spawning period the number of Type A Lasker events show an 8% increase from 12 events over a ten-year period in the present simulation to 13 events for the same period in the future simulation (Fig. 2.49). There is a 33% increase from 6 Type B events in the present simulation to 8 events in the future (Fig. 2.50). At the Cape Town Grid Cell, the months in the spawning season that show an increase in the number of Type A events in the future are October, December and February. October and December show a 100% increase and February shows a 33% increase in the number of Type A Lasker events in the future. The rest of the spawning months show a decrease in the number of Type A Lasker events in the future.

The Lamberts Bay Grid Cell shows an 88% increase in the number of Lasker events from 8 Type A events over a ten year period in the present to 15 in the future (Fig. 2.51). There is a 167% increase in Type B Lasker events from 3 events in the present simulation to 8 in the future simulation (Fig. 2.52). At the Lamberts Bay Grid Cell there is an increase in Type A Lasker

events in the future in all the spawning months, except for November and December. September shows the largest increase in Type B Lasker events of 300% in the future.

At the Port Nolloth Grid Cell the model output data shows a 67% increase in the number of Type A Lasker events from 3 events in the present simulation to 5 events in the future simulation over a ten year period (Fig. 2.53). The number of Type B Lasker events remains the same in the present and future simulation, i.e. 2 events (Fig. 2.54). In the spawning months, December - February show no Lasker events in the future simulation. In September there is a 20% decrease in the number of Type B Lasker events in the future.

Table 2.1 A summary of the mean wind speed values, extreme events, mean turbulence values and Lasker events from the CSM results at the five grid cells in the southern Benguela system for the anchovy spawning season (i.e. September - February).

	Eastern Bank Grid Cell	**Western Bank Grid Cell**	**Cape Town Grid Cell**	**Lamberts Bay Grid Cell**	**Port Nolloth Grid Cell**
Mean wind speed value for the spawning season	Present: 7.0 $m.s^{-1}$ Future: 6.9 $m.s^{-1}$	Present: 7.4 $m.s^{-1}$ Future: 7.3 $m.s^{-1}$	Present: 7.7 $m.s^{-1}$ Future: 7.6 $m.s^{-1}$	Present: 8.0 $m.s^{-1}$ Future: 8.1 $m.s^{-1}$	Present: 9.9 $m.s^{-1}$ Future: 10.0 $m.s^{-1}$
Number of days showing extreme wind speeds (i.e. > 15 $m.s^{-1}$)	Present: 13 days Future: 12 days	Present: 23 days Future: 16 days	Present: 17 days Future: 17 days	Present: 2 days Future: 3 days	Present: 17 days Future: 11 days
Mean turbulence value for the spawning season	Present: 586.5 $m^3.s^{-3}$ Future: 528.1 $m^3.s^{-3}$	Present: 658.0 $m^3.s^{-3}$ Future: 596.1 $m^3.s^{-3}$	Present: 738.5 $m^3.s^{-3}$ Future: 670.2 $m^3.s^{-3}$	Present: 694.4 $m^3.s^{-3}$ Future: 712.8 $m^3.s^{-3}$	Present: 1234.7 $m^3.s^{-3}$ Future: 1268.6 $m^3.s^{-3}$
Number of days showing extreme turbulence values (i.e. > 5000 $m^3.s^{-3}$)	Present: 12 days Future: 6 days	Present: 15 days Future: 7 days	Present: 17 days Future: 7 days	Present: 0 days Future: 0 days	Present: 6 days Future: 3 days
The frequency of Type A Lasker events	Present: 25 events Future: 29 events	Present: 22 events Future: 16 events	Present: 12 events Future: 13 events	Present: 8 events Future: 15 events	Present: 3 events Future: 5 events
The frequency of Type B Lasker events	Present: 10 events Future: 16 events	Present: 10 events Future: 8 events	Present: 6 events Future: 8 events	Present: 3 events Future: 8 events	Present: 2 events Future: 2 events

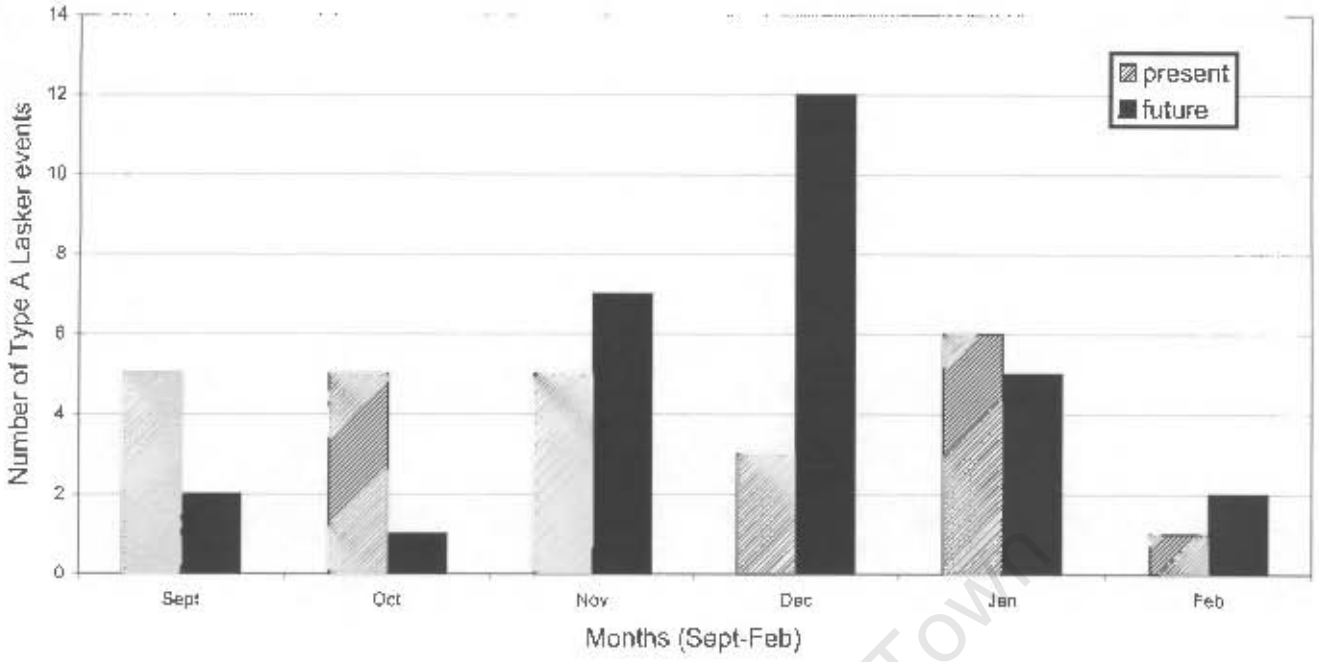

Figure 2-45 The number of Type A Lasker events for the spawning season in the present and future simulation at the Eastern Bank Grid Cell

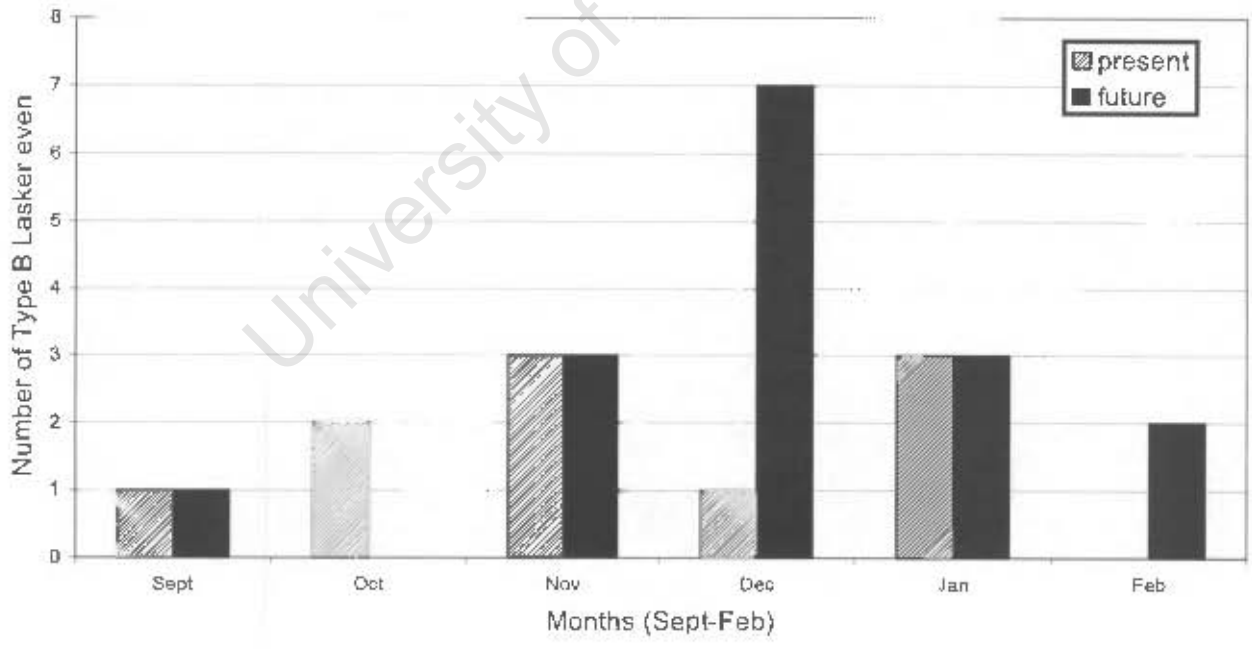

Figure 2-46 The number of Type B Lasker events for the spawning season in the present and future simulation at the Eastern Bank Grid Cell

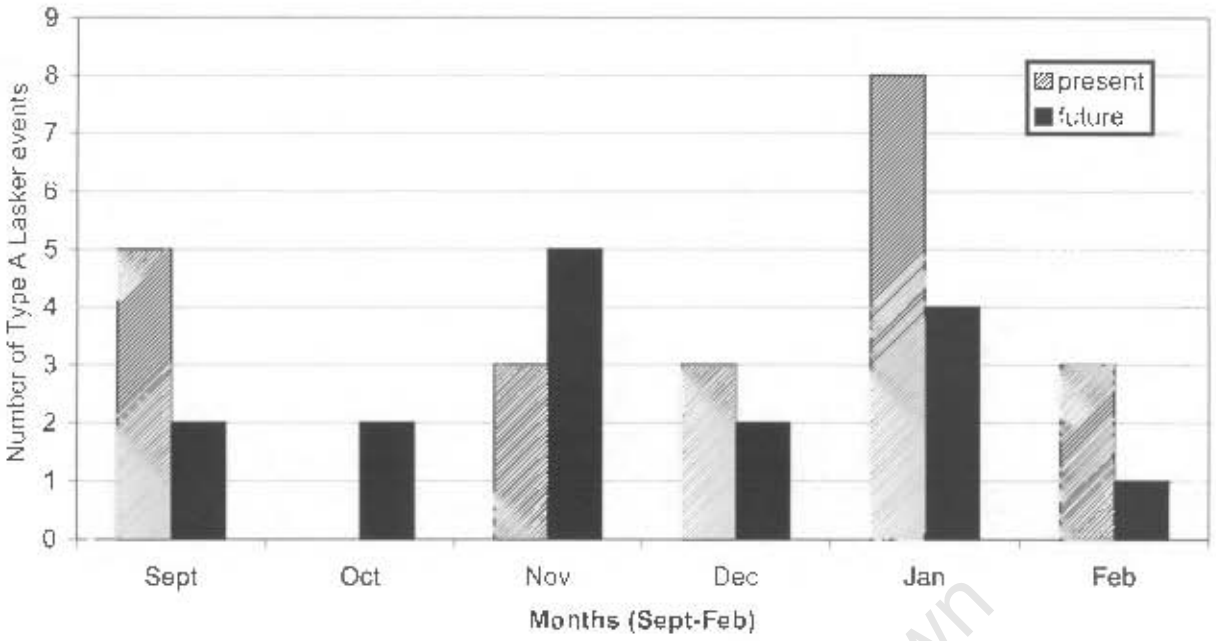

Figure 2-47 The number of Type A Lasker events for the spawning season in the present and future simulation at the Western Bank Grid Cell

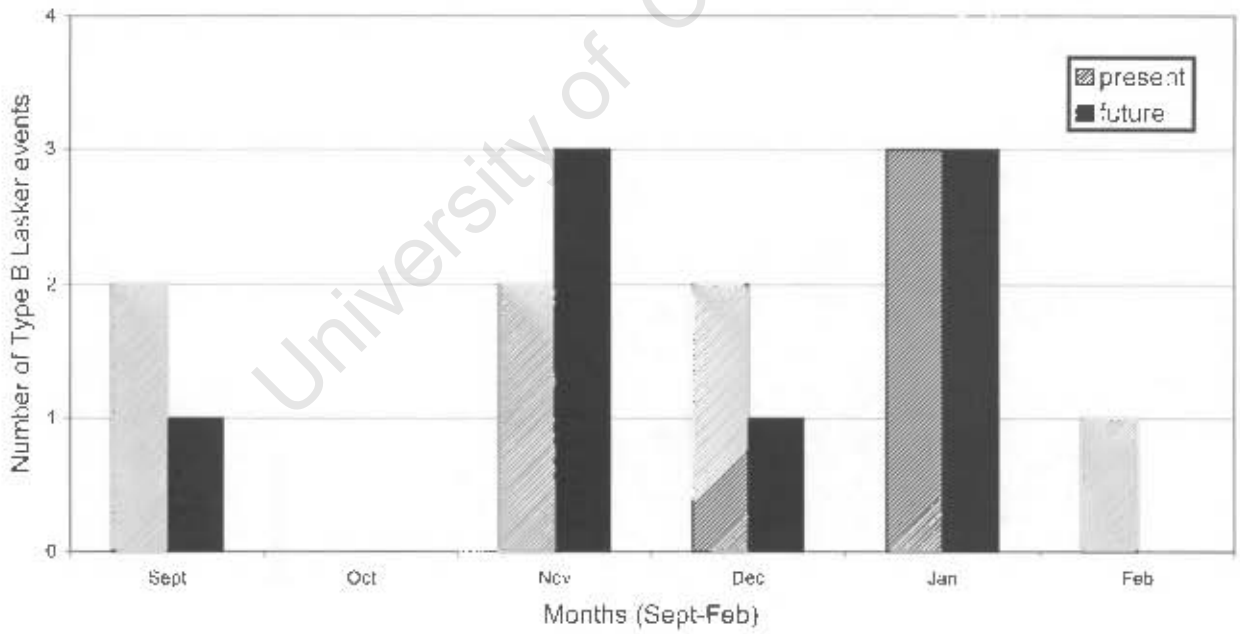

Figure 2-48 The number of Type B Lasker events for the spawning season in the present and future simulations at the Western Bank Grid Cell

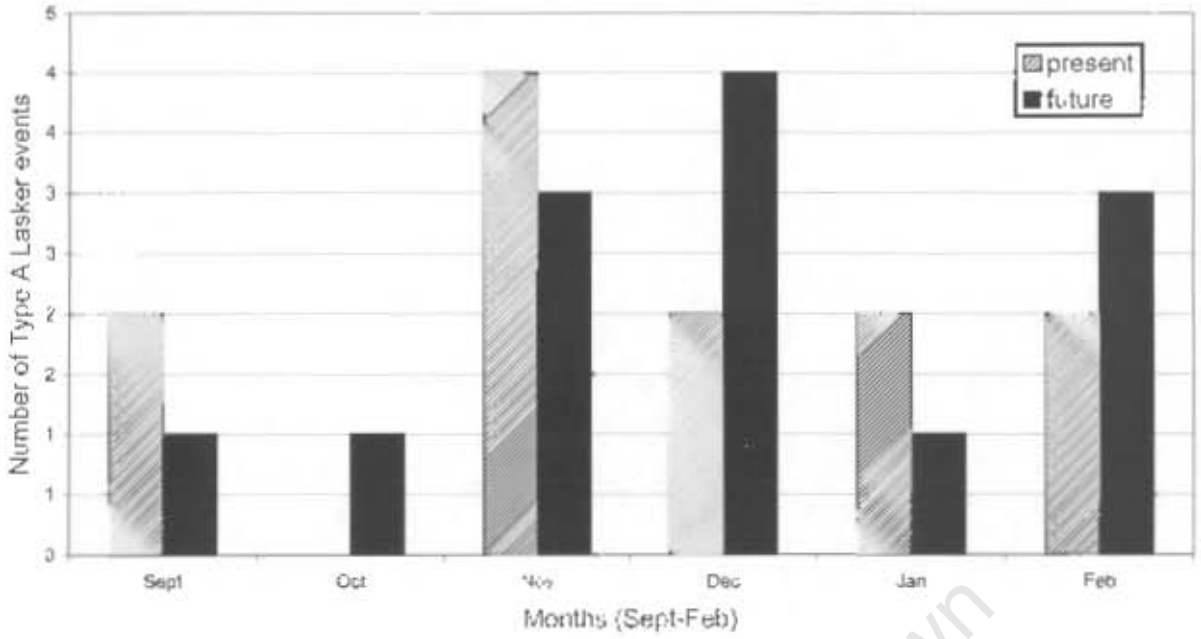

Figure 2-49 The number of Type A Lasker events for the spawning season in the present and future simulation at the Cape Town Grid Cell

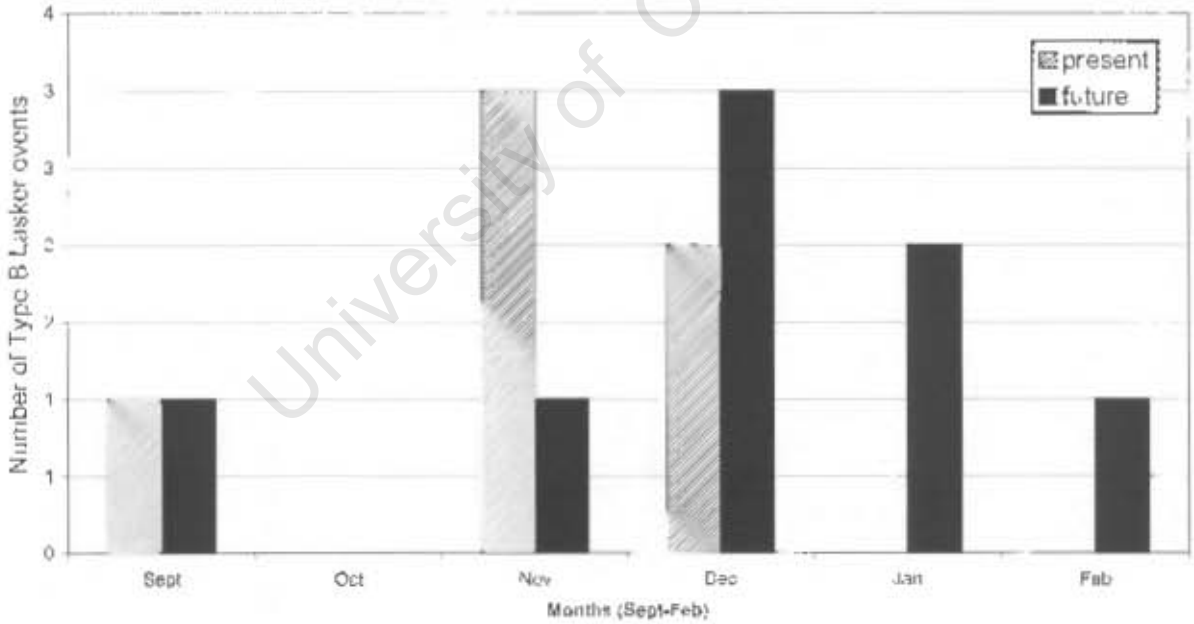

Figure 2-50 The number of Type B Lasker events for the spawning season in the present and future simulation at the Cape Town Grid Cell

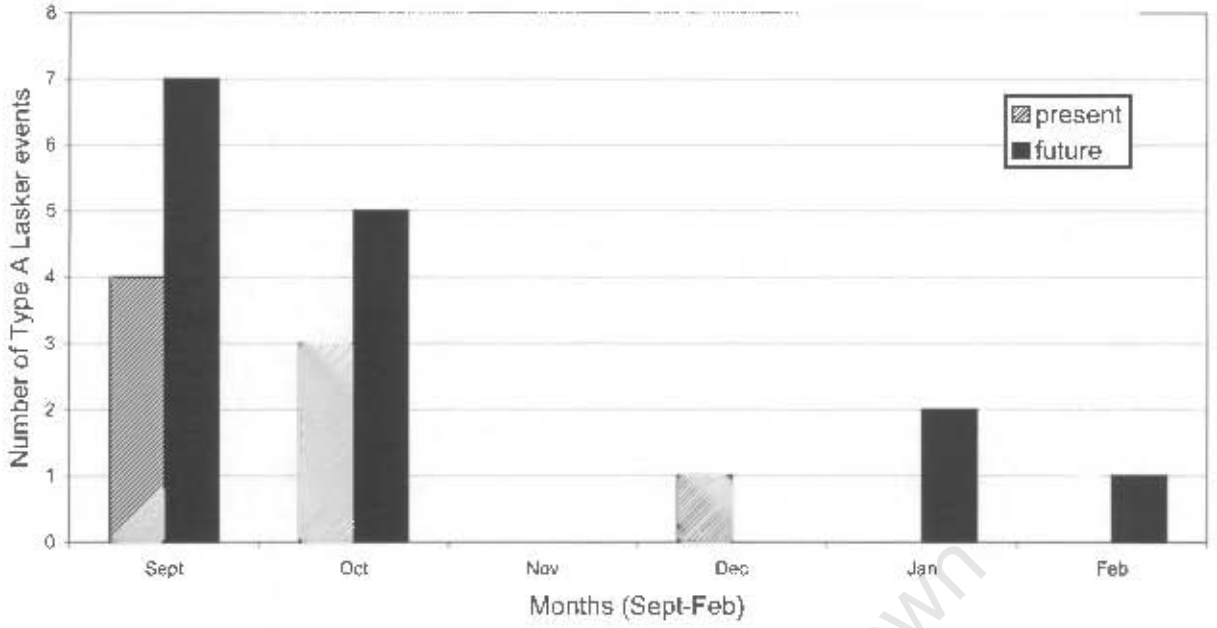

Figure 2-51 The number of Type A Lasker events for the spawning season in the present and future simulation at the Lamberts Bay Grid Cell

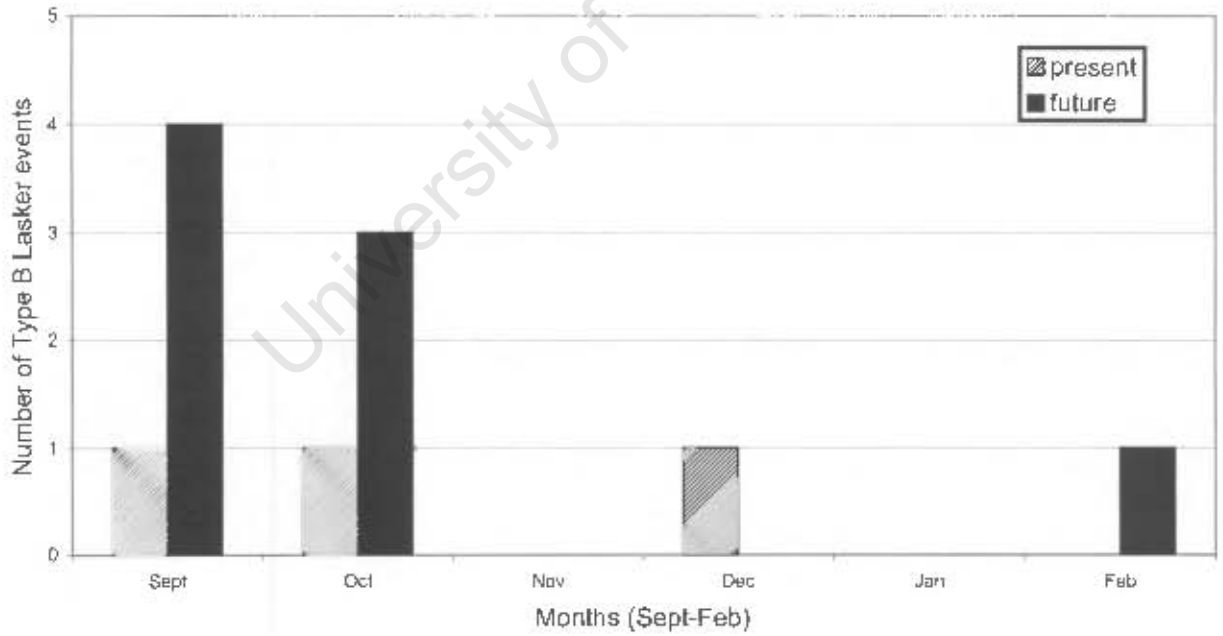

Figure 2-52 The number of Type B Lasker events for the spawning season in the present and future simulation at the Lamberts Bay Grid Cell

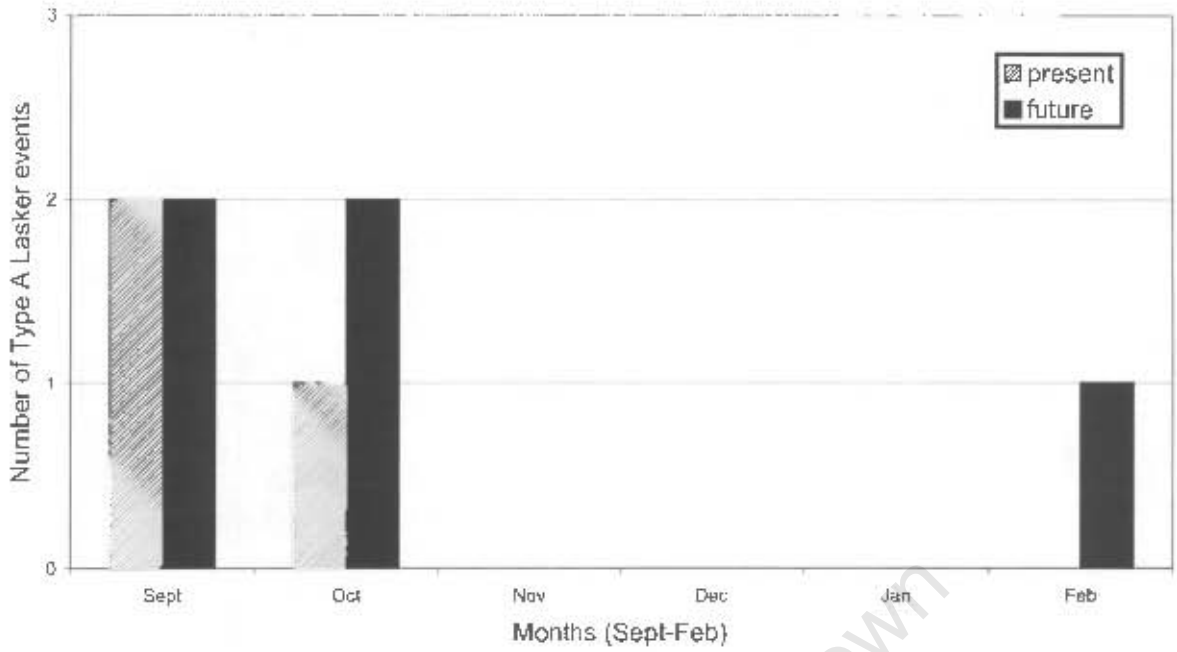

Figure 2-53 The number of Type A Lasker events for the spawning season in the present and future simulation at the Port Nolloth Grid Cell

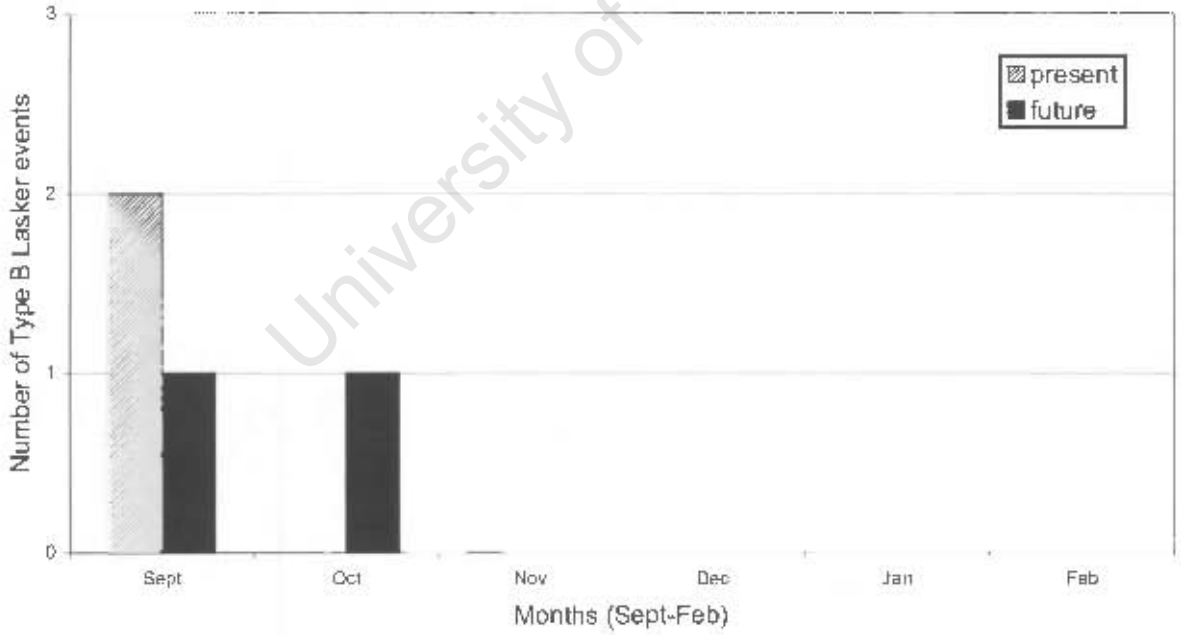

Figure 2-54 The number of Type B Lasker events for the spawning season in the present and future simulation at the Port Nolloth Grid Cell

2.3.6 Alongshore wind stress

At the Eastern Bank Grid Cell for the spawning season, November, December and February show decreases in mean alongshore wind stress in the future simulation (Fig. 2.55). November shows the largest decrease (14.2%) from 24.7 $m^2.s^{-2}$ in the present simulation to 21.2 $m^2.s^{-2}$ in the future. There is an increase in mean alongshore wind stress in September, October and January in the future simulation. October shows the largest increase (22.1%) at the Eastern Bank Grid Cell from 18.4 $m^2.s^{-2}$ in the present simulation to 22.5 $m^2.s^{-2}$ in the future.

At the Western Bank Grid Cell for the spawning season, September, November, December and February show decreases in alongshore wind stress (Fig 2.56). November shows the largest decrease (9.5%) from 40.2 $m^2.s^{-2}$ in the present simulation to 36.4 $m^2.s^{-2}$ in the future. October and January show increases in mean alongshore wind stress at the Western Bank Grid Cell in the future. January shows the largest increase (17.5%) from 39.5 $m^2.s^{-2}$ in the present simulation to 46.4 $m^2.s^{-2}$ in the future.

At the Cape Town Grid Cell there is a decrease in mean alongshore wind stress in September, November and December in the future for the spawning season (Fig. 2.57). November shows the largest decrease (12.0%) from 46.4 $m^2.s^{-2}$ in the present simulation to 40.8 $m^2.s^{-2}$ in the future. October, January and February show increases in mean alongshore wind stress in the future. January shows the largest increase in mean alongshore wind stress (22.6%) from 44.5 $m^2.s^{-2}$ to 54.5 $m^2.s^{-2}$ in the future.

The Lamberts Bay Grid Cells shows a decrease in mean alongshore wind stress in October (6.1%) from 34.4 $m^2.s^{-2}$ in the present simulation to 32.3 $m^2.s^{-2}$ in the future (Fig. 2.58). The remainder of the months in the spawning season show increases in mean alongshore wind stress. January shows the largest increase in mean alongshore wind stress (7.0%) at the Lamberts Bay Grid Cell from 74.8 $m^2.s^{-2}$ in the present simulation to 80.0 $m^2.s^{-2}$ the future.

At the Port Nolloth Grid Cell for the spawning season, there are decreases in alongshore wind stress in September and October (Fig. 2.59). September shows the larger decrease of the two (9.0%) from 72.3 $m^2.s^{-2}$ in the present simulation to 65.8 $m^2.s^{-2}$ in the future. There is an increase in mean alongshore wind stress for the remainder of the spawning months in the future simulation. The largest increase at the Port Nolloth Grid Cell is in November (10.6%), which

shows an increase from 102.6 $m^2.s^{-2}$ in the present simulation to 113.1 $m^2.s^{-2}$ in the future simulation.

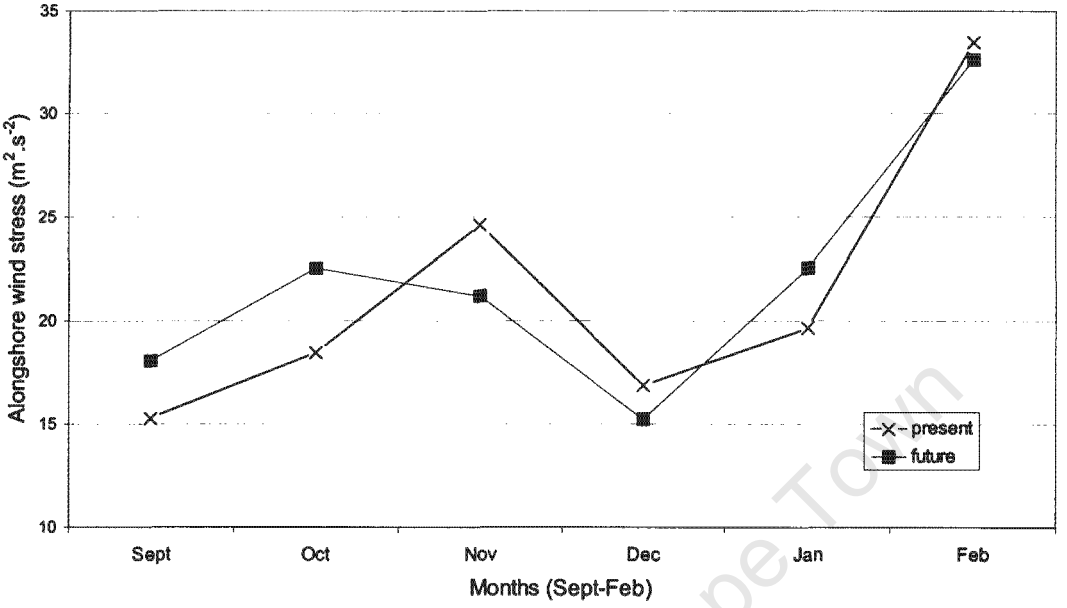

Figure 2-55 Present and future mean alongshore wind stress ($m^2.s^{-2}$) for the spawning season at the Eastern Bank Grid Cell

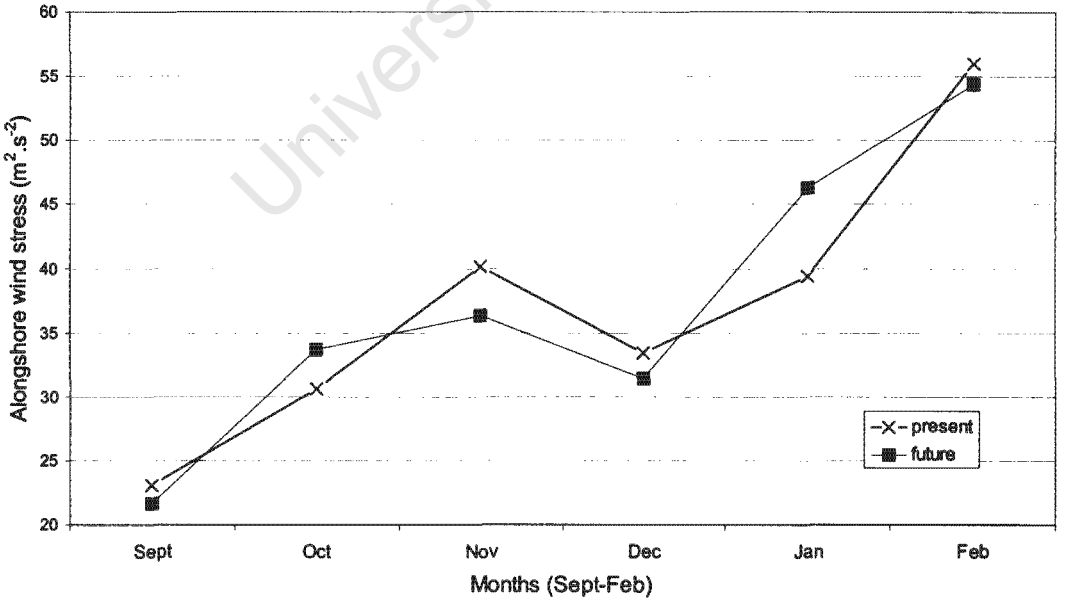

Figure 2-56 Present and future mean alongshore wind stress ($m^2.s^{-2}$) for the spawning season at the Western Bank Grid Cell

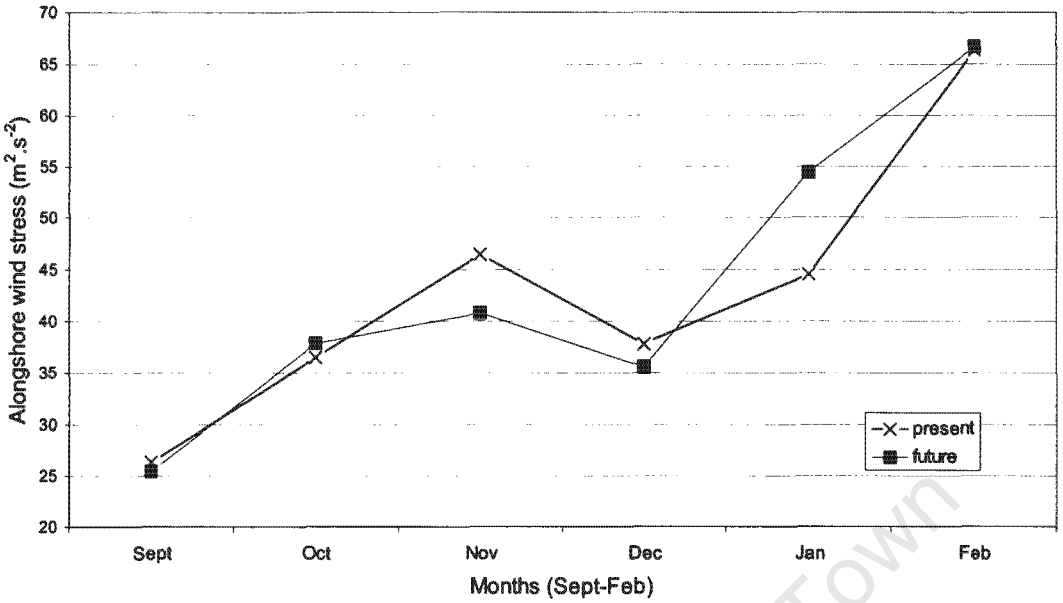

Figure 2-57 Present and future mean alongshore wind stress ($m^2.s^{-2}$) for the spawning season at the Cape Town Bank Grid Cell

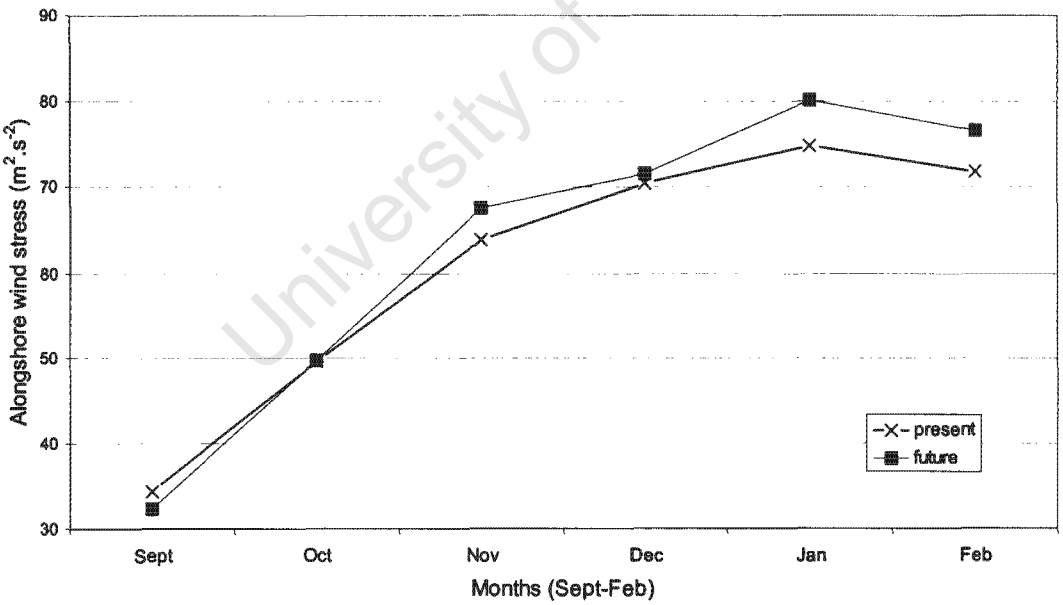

Figure 2-58 Present and future mean alongshore wind stress ($m^2.s^{-2}$) for the spawning season at the Lamberts Bay Grid Cell

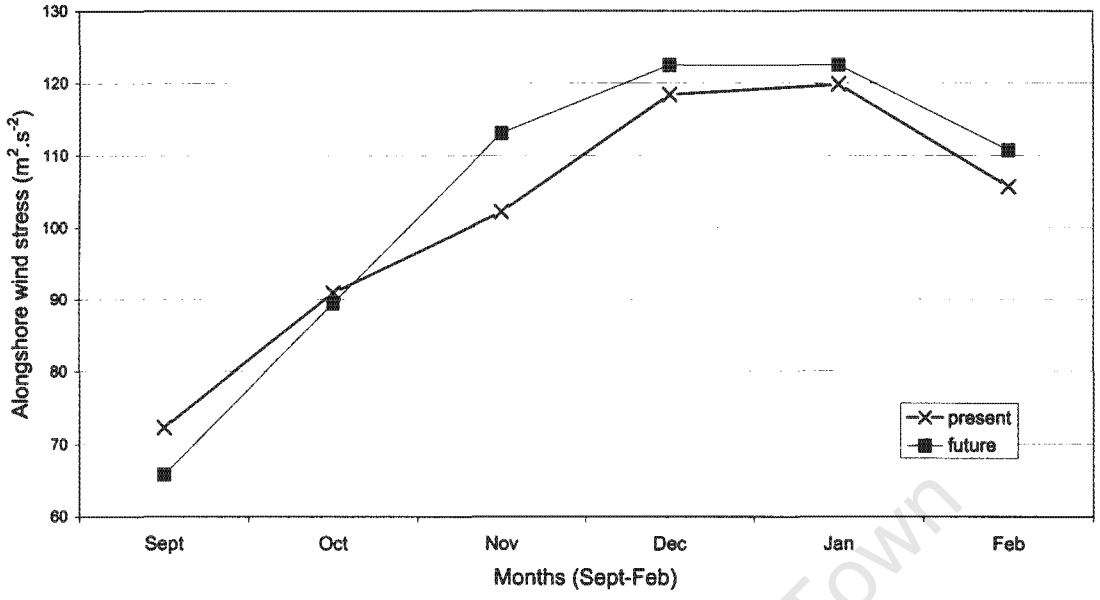

Figure 2-59 Present and future mean alongshore wind stress ($m^2.s^{-2}$) for the spawning season at the Port Nolloth Grid Cell

CHAPTER THREE

Discussion

3.1 Changes in wind speed values in the southern Benguela system

The Eastern Bank and Western Bank Grid Cells are the primary spawning localities for anchovy at present on the southern African coastline (Shelton 1981, 1986, Van Der Lingen *et al.* In press). Output from the Climate System Model shows that the Eastern Bank and Western Bank Grid Cells (see Figs 2.8 and 2.9) presently have mean wind speeds in the range of 5–8 $m.s^{-1}$ during the anchovy spawning season in the southern Benguela system. The Optimal Environmental Window, as described by Cury and Roy (1989) has not been applied to the southern Benguela system (C. Roy 2001 pers. comm.). Shin *et al.* (1998) also documented that there is no clear pattern of correspondence between wind speed values and spawning in the southern Benguela system, yet noted that anchovy spawning peaks when monthly mean wind speeds are between 5–8 $m.s^{-1}$ (Shin *et al.* 1998). Given the CSM data and the findings by Shin *et al.* (1998), it is hypothesised in this dissertation that optimal spawning takes place in the southern Benguela system when mean wind speeds are 5–8 $m.s^{-1}$.

The CSM wind vector maps show low wind vectors at the Eastern Bank and Western Bank Grid Cells (see Figs 2.10-2.12). The low magnitude of vectors suggests that the wind direction is not constantly unidirectional and that there is disturbance in the area. This is as a result of the two grid cells lying in the region of the mid latitudes, an area characterised by disturbance. The CSM data show an expected increase in alongshore wind stress from the present simulation to the future for the spawning months of September, October and January at the Eastern Bank Grid Cell and for October and January at the Western Bank Grid Cell (see Figs 2.55 and 2.56). As a result of the angle of the coastline at the Agulhas Bank area, the increase in alongshore wind stress is likely to produce an increase in upwelling at the Eastern Bank and Western Bank Grid Cells for the months mentioned above. This is likely to produce a concomitant increase in phytoplankton and thus food concentrations for anchovy larvae in the area, thereby increasing their survival rates. There is likely to be a decrease in food concentrations on the Eastern Bank Grid Cell in November, December and February and at the Western Bank Grid Cell in September, November, December and February due to the decrease in alongshore wind stress for these months. As is evident from the above discussion, the expected changes in upwelling at these grid cells is highly variable from month to month.

Anchovy spawning presently occurs when mean monthly wind speeds are within a window of 5-8 $m.s^{-1}$ in the southern Benguela system. It is suggested that lower or higher mean wind speeds

would have a negative effect on spawning and thus anchovy recruitment by detrimentally affecting food concentrations for anchovy larvae and the ease with which larvae are able to capture prey. The wind speed conditions at the Eastern Bank and Western Bank Grid Cells display similar future values in both magnitude and direction of wind to those in the present simulation (see Figs 2.8, 2.9, 2.22, 2.23, 2.25, 2.26). It is thus likely that wind speed values and wind direction at the Eastern Bank and Western Bank Grid Cells will continue to support successful anchovy spawning in the future.

The mean wind speeds from June - August for the present and future simulations at the Eastern and Western Bank Grid Cells are greater than 8 $m.s^{-1}$. Mean wind speeds in the present day simulation over this period for the Eastern Bank and Western Bank Grid Cells are 8.5 $m.s^{-1}$ and 8.7 $m.s^{-1}$ respectively. In the future simulation the mean wind speed values over this period for the Eastern Bank and Western Bank Grid Cells are both 8.4 $m.s^{-1}$. Therefore, it is likely, given the high wind speeds projected for the non-spawning months, that anchovy will continue to spawn on the Eastern and Western Agulhas Bank from September – February in the future.

Ecologists are increasingly recognising that extreme events often shape ecosystems and may cause ecological regime shifts (Done 1999). Schneider and Root (1996) suggest that extreme events are of particular importance at the intersection of disciplines, such as climatology and ecology, because of the large discontinuities that could occur with so many interactions between the biota and climate. Within the marine environment, extreme wind speeds could conceivably have dramatic effects on pelagic fish spawning, by removing eggs and larvae from coastal waters. An analysis of extreme wind events (defined as wind speeds >15 $m.s^{-1}$) in the CSM shows that at the Western Bank Grid Cell there is a 30% decrease in the number of days with extreme wind speeds in the spawning period in the future simulation (see Fig. 2.17). A reduction in extreme wind speed events is likely to enhance anchovy spawning at the Western Bank Grid Cell in the future.

Although the Cape Town Grid Cell is not the primary spawning locality for anchovy in the southern Benguela system (Shelton 1986), it is used as a spawning location by anchovy and especially sardine (Fowler and Boyd 1998). The CSM results show that both present and future wind speed values are within a range suitable for spawning i.e. 5–8 $m.s^{-1}$ during the period October - January. This area may thus conceivably be used as a 'backup' spawning location

when conditions are unsuitable on the Agulhas Bank, as suggested by Fowler and Boyd (1998) for sardine. The future simulation shows wind conditions very similar to the present. There is a non-significant increase ($p>0.05$) in mean wind speeds projected for September – January and all the means fall within the 5-8 $m.s^{-1}$ window. Alongshore wind stress values from the future simulation show an increase in upwelling and thus phytoplankton food supplies at the Cape Town Grid Cell in October, January and February. The largest increase is expected in January (22.6%). The month of February has, however, the highest mean wind stress values and is thus likely to be the month with the greatest food availability for larvae. Decreases in the alongshore wind stress for the remainder of the spawning months suggest that there may be a reduction in food concentrations during these months.

In terms of wind direction, the present and future simulations are also comparable, although there is an expected increase in the magnitude and frequency of south-easterly winds (see Fig. 2.27) during the spawning months. Boyd *et al.* (1998) graphed a negative correlation between anchovy recruitment and south-easterly winds at Cape Point (Cape Town Grid Cell) (Fig. 3.1). An increase in south-easterly winds results in an increase in turbulence and an increase in advective losses (Boyd *et al.* 1998). Therefore, according to Boyd's graph (1998), an increase in the magnitude and frequency of south-easterly winds may have a negative impact on anchovy recruitment through increased turbulence, a cooling of sea surface temperatures and by creating a marine environment too unstable for effective spawning. The small increase in south-easterlies, however, is unlikely to prevent successful spawning from taking place at the Cape Town Grid Cell. This upwelling increase warrants monitoring, although in general, the Cape Town Grid Cell is likely to remain a suitable 'back up' spawning location with respect to wind speed and direction.

The Lamberts Bay and Port Nolloth Grid Cells are not recorded as major anchovy spawning areas, although some authors have recorded sardine eggs off the West Coast (Painting *et al.* submitted). The West Coast is, however, used as a feeding ground for larvae and is consequently of importance for recruitment. Wind speeds are not projected to change significantly at either of these grid cells according to the CSM output data. Wind directions, in particular south-easterlies, also remain comparable (see Figs 2.30 and 2.35). The wind vector maps indicate that winds are predominantly southerly and that there is minimal fluctuation in wind direction, in both the present and future simulation. The alongshore wind stress at both

grid cells shows an increase from November – February (see Figs. 2.58 and 2.59). This translates into an increase upwelling in these areas for these months, which in turn results in an increase in phytoplankton and ultimately more food for anchovy on the West Coast. Alongshore wind stress at the Port Nolloth Grid Cell has higher monthly mean values than the Lamberts Bay Grid Cell in both the present and future simulations. For example in the future simulation mean monthly alongshore wind stress for January is 74.8 $m^2.s^{-2}$ at the Lamberts Bay Grid Cell and 119.8 $m^2.s^{-2}$ at the Port Nolloth Grid Cell. The Port Nolloth Grid Cell is thus likely to yield greater food concentrations for anchovy both in the present and as well as the future.

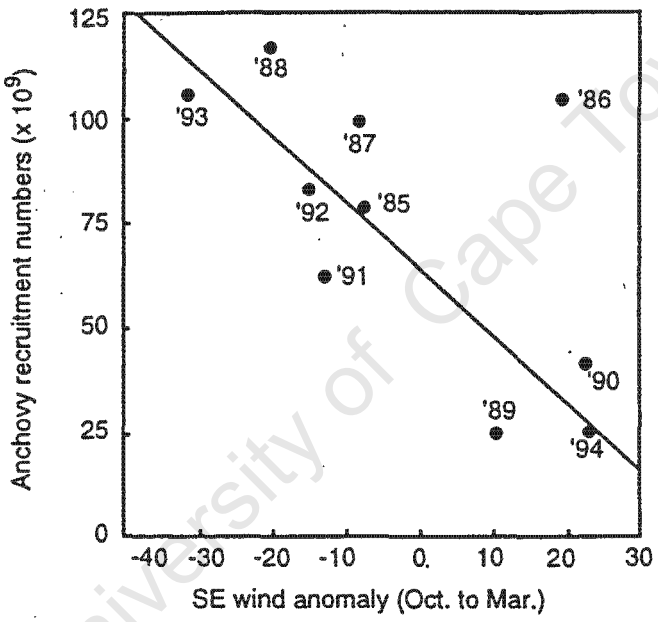

Figure 3-1 Correlation between anchovy recruit numbers and the spring/summer anomaly at Cape Point (Boyd *et al.* 1998)

Lamberts Bay and Port Nolloth Grid Cells presently provide anchovy with a food-rich environment on the West Coast. It is therefore suggested that this area will continue to be suitable for anchovy feeding because of the present and future simulation's comparable wind speeds and wind direction. It is feasible that the area may supply greater food concentrations in the future given the projected increase in alongshore wind stress from November – February. Although the waters are highly turbulent in this region, anchovy are apparently able to capitalise on the nutrient richness of the area as by the time they reach the West Coast they have to some extent matured. Although reasons for this are not fully understood, it has been suggested that stratification of the water column allows for anchovy feeding.

Successful anchovy spawning is probably presently precluded on the West Coast due to wind speeds exceeding the 5-8 $m.s^{-1}$ window and due to the unstable turbulent conditions associated with the higher wind speeds. As future wind speeds are comparable to present day wind speeds (e.g. mean wind speeds in October at the Port Nolloth Grid Cell are 9.40 $m.s^{-1}$ and 9.21 $m.s^{-1}$ for the present and future simulations respectively), it is unlikely that this area will be used as a spawning location in the future.

3.2 Changes in turbulence, stratification and temperature in the southern Benguela

3.2.1 Turbulence

The mean turbulence values on the Eastern Agulhas Bank calculated from the CSM are similar to those estimated by Bakun (1996), i.e. ~600-650 $m^3.s^{-3}$. The future simulation shows a 10% projected decrease in turbulence for the spawning season at the Eastern Bank Grid Cell, from 587 to 528 $m^3.s^{-3}$. These turbulence values are extremely high in comparison to other upwelling systems and anchovy may be limited to some extent by the effects of turbulence on larval feeding. MacKenzie *et al.* (1994) notes that low turbulence can also be detrimental to recruitment by reducing the encounter rate between larvae and food particles. Given, however, that anchovy spawn successfully off the California and Peru coastlines in turbulence conditions <250 $m^3.s^{-3}$, it is highly unlikely that a decrease in turbulence to 528 $m^3.s^{-3}$ will have deleterious consequences for anchovy in the future. This decrease is more likely to favour anchovy spawning by enabling more effective larval feeding.

The Western Bank Grid Cell experiences a turbulence regime similar to the Eastern Bank Grid Cell and is a probable reason for anchovy utilising both these localities for spawning. Bakun (1996) estimates that the mean turbulence in this region is ~600-650 $m^3.s^{-3}$ and the CSM data corroborates this estimate. The model projects a significant 9.4% decrease in turbulence from 658 $m^3.s^{-3}$ to 596 $m^3.s^{-3}$ ($p < 0.05$). It is not known at what turbulence intensity the beneficial effects of moderate turbulence (i.e. sufficient mixing of water for adequate interaction between larvae and food particles) and the negative effects of high turbulence (dispersed food and low larvae/food particle encounter rates) meet. It is hypothesised that this transition is a gradual one and may even stretch from 300 $m^3.s^{-3}$ (Fig 3.2).

It is also suggested that anchovy in the southern Benguela system are spawning in the outer limits of turbulence as depicted in Figure 3.2. Any decrease in turbulence is thus likely to improve spawning conditions and increase anchovy recruitment. The projected decreases in turbulence at both the Eastern Bank and Western Bank Grid Cells represent a possible increase in anchovy recruitment in the future.

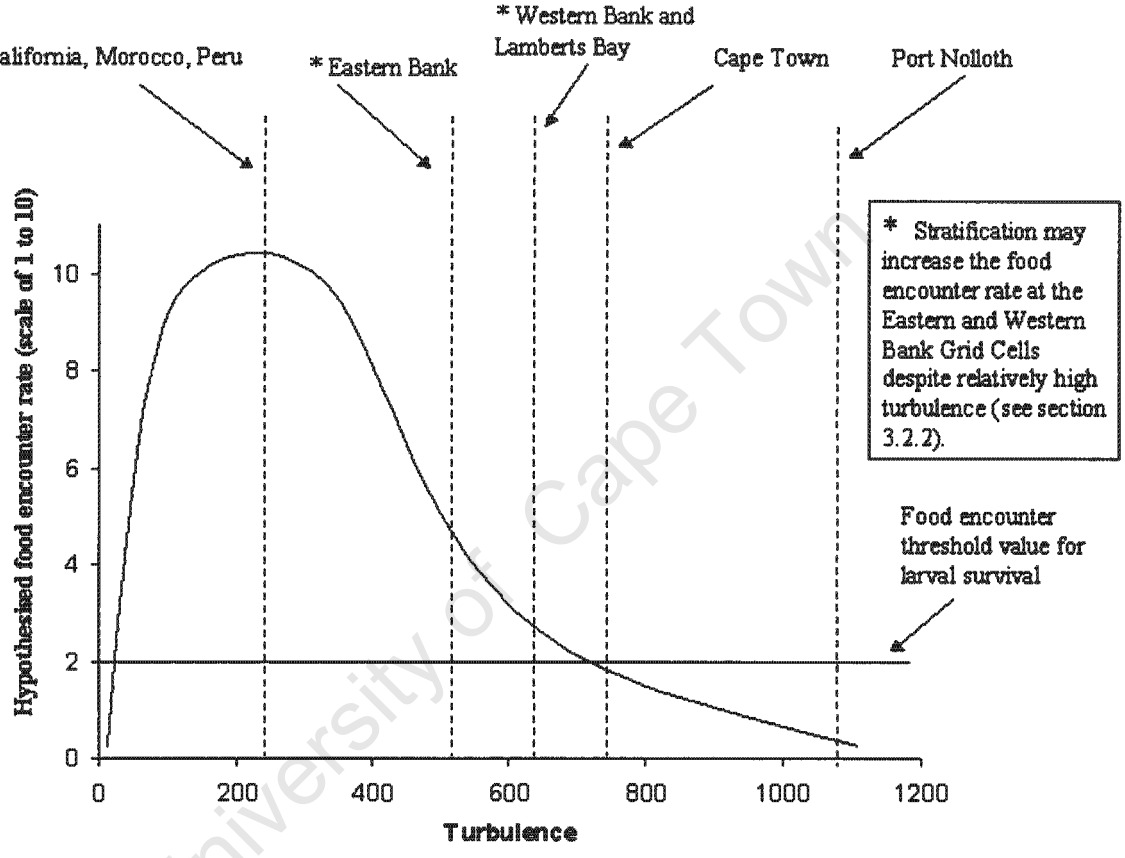

Figure 3-2 Hypothesised relationship between food encounter rate and turbulence in the southern Benguela System and at the California, Morocco and Peru Grid Cells

Turbulence is directly related to wind speed, hence an analysis of the number of extreme turbulence events reveals similar results to the analysis of days with extreme wind values. Extreme turbulence events (defined as days of turbulence >5000 $m^3.s^{-3}$) are projected to decrease at the Eastern Bank, Western Bank and Cape Town Grid Cells in the anchovy spawning months by 50%, 57% and 53% respectively. The literature does not contain studies on the effects of individual days of high turbulence on anchovy spawning but it is conceivable that extreme events could occasionally tip the survival scales against anchovy larvae, particularly in years

where larvae are already stressed due to unseasonally high turbulence or low food availability. An extreme event may push larvae beyond their stress resilience limits and greatly reduce survival of larvae. The projected decrease in extreme turbulent events is thus a further beneficial effect anticipated for anchovy recruitment in the future.

The Cape Town Grid Cell has been utilised as a spawning ground by anchovy (Fowler and Boyd 1998), and mainly sardine. A projected 9% significant decrease ($p < 0.05$) in mean turbulence for the spawning season from 739 $m^3.s^{-3}$ to 670 $m^3.s^{-3}$ may shift this grid cell into a range of turbulence more conducive for spawning. If the turbulence threshold for successful spawning is in the region of 700 $m^3.s^{-3}$ as hypothesised above (Fig. 3.2), then the projected decrease may represent a potential shift across a spawning threshold limit. This shift could improve this area as a spawning site for anchovy and sardine in the future.

The hypothesised shift in spawning locations discussed above is made more plausible by the apparent flexibility that pelagic fish show for spawning locations. Fowler and Boyd (1998) note that spawning sardine adults off the Agulhas Bank are able to relocate to near the Cape Peninsula if turbulence exceeds suitable levels. Painting *et al.* (submitted) also showed that at times there is a high concentration of sardine spawners off the West Coast. In 1962-1964, before the sardine collapse, sardine eggs were frequently found off Cape Columbine on the West Coast (Crawford 1981) and were recorded again in 1995 by Fowler and Boyd (1998). The West Coast has, despite its high turbulence, evidently been an alternative spawning ground for sardine. This may occur when the climate at other locations when other locations is unsuitable. Sardine and anchovy share similar spawning grounds in the southern Benguela system (Shin *et al.* 1998) and it has been suggested that anchovy are likely to be able to spawn in areas where sardine have been recorded. Sardine and anchovy may thus be effective at tracking changes in climate and utilising new areas that become favourable for spawning. The Cape Town Grid Cell is one such potential area, given the projected decrease in turbulence and events of extreme turbulence.

The Lamberts Bay and Port Nolloth Grid Cells have considerably higher turbulence values than the other three grid cells. Mean turbulence in the present and future simulations is 694 and 713 $m^3.s^{-3}$ for the spawning season at the Lamberts Bay Grid Cell and 1235 and 1267 $m^3.s^{-3}$ in the present and future simulations respectively at the Port Nolloth Grid Cell. This high turbulence regime is unlikely to favour spawning (Fig. 3.2) and indeed sardine spawning has been recorded

only rarely at the Lamberts Bay Grid Cell and not at all at the Port Nolloth Grid Cell. Projected turbulence values in the future simulation are similar to present values and thus climate change is unlikely to alter the suitability of this region for pelagic fish spawning.

3.2.2 Stratification

The CSM results show that the present mean turbulence values for the spawning months for the Eastern Bank and Western Bank Grid Cells are 586.1 $m^3.s^{-3}$ and 650.0 $m^3.s^{-3}$ respectively (see Figs 2.36 and 2.37). These turbulence values are greater than that of any other upwelling region in the world (Cury and Roy 1989) (Fig. 3.2). It is suggested that the reason anchovy are able to spawn successfully on the Agulhas Bank in turbulence values of this magnitude is because of the strong stratification of the water column (Parrish *et al.* 1983).

The southern Benguela system is unique in that it is the only upwelling system with a warm water current (the Agulhas Current) bounding it poleward (Shelton *et al.* 1985, Bakun 1996). Stratification is formed by the advection of warm Indian Ocean surface water, which counteracts the local wind mixing effects to produce stable conditions and a rich larval habitat (Parrish *et al.* 1983). This stable layer that forms during stratification in the upwelling region is an area of calmer conditions and has less intense upwelling and turbulence than the surrounding area. This translates into an abundance of food particles on which the fish can survive throughout the spawning season (Parrish *et al.* 1983). The stable layer provides the fish with a 'calm within the storm', enabling profitable feeding

At present, stratification of the water column occurs in spring and summer because of relatively light winds and solar heating. In the future, there is a projected 9.9% decrease at the Eastern Bank Grid Cell and a 9.4% decrease in turbulence at the Western Bank Grid Cell. Such decreases are unlikely to impact on the stratification in the water column. The beneficial effects of stratification in the water column at the Eastern Bank and Western Bank Grid Cells is thus likely to continue into the future.

3.2.3 Temperature

Both anchovy and sardine appear to have strict temperature requirements for spawning. Spawning anchovy are mostly absent from waters warmer than 20°C (Armstrong *et al.* 1988) and it has been suggested that anchovy are prevented from spawning in areas where water

temperatures are below 14°C (Boyd and Shillington 1994). Spawning anchovy and anchovy eggs are most commonly found within the temperature range of 16-19°C (Anders 1965, Painting *et al.* Submitted) and Shelton (1986) suggests that anchovy select locations within this range of temperatures for spawning and do not spawn outside this range.

Sea surface temperatures are dependent upon turbulence and upwelling. Turbulence results in greater mixing of surface water with deeper water and upwelling is, by definition, the movement of deep water to the surface. Deep water is substantially colder than surface waters and consequently both these processes result in a decrease in sea surface temperatures. The CSM did not generate temperature data, however, inferences can be made from alongshore wind stress and turbulence data as to how sea surface temperatures may be affected.

At the Western Bank and Cape Town Grid Cells, there are projected decreases in turbulence during the spawning season. Alongshore wind stress shows both projected increases and decreases at these grid cells (see Figs 2.56 and 2.57). This is likely to result in increases as well as decreases in upwelling. The projected decrease in turbulence, yet possible increases in upwelling result in conflicting effects on sea surface temperatures. The combined effect is difficult to estimate, but given that the decrease in turbulence (9%) and the increases in alongshore wind stress are relatively small, a dramatic change in sea surface temperatures is probably unlikely to happen. This effect, however, warrants monitoring in the future.

3.3 Lasker Events

The number and duration of calm periods or Lasker events is critical for anchovy larval survival (Lasker 1975). Lasker events at the Eastern Bank Grid Cell are expected to increase in the future (see Figs 2.45 and 2.46). Increases are not, however, uniformly distributed across the spawning season. December shows a considerable 300% increase in Type A events (see Fig. 2.45) and a 600% increase in Type B events (see Fig. 2.46), which suggests that this month may become a particularly favourable time for anchovy spawning in the future.

The Western Bank Grid Cell, in contrast, is expected to have fewer Lasker events in the future. The overall decrease in Type A events (20%) (see Fig. 2.47) and Type B events (27%) (see Fig. 2.48) may reduce the anchovy spawning potential of the area. The month of November, however, shows an expected increase in events and may offer anchovy spawners some respite.

Pelagic fish appear to be flexible spawners in time and space (Fowler and Boyd 1998). The increase in Lasker events at the adjacent Eastern Bank Grid Cell may result in a shift in spawning from the Western Bank Grid Cell to the Eastern Bank Grid Cell. The extent to which such a shift will occur is difficult, if not impossible, to model or estimate.

The Cape Town Grid Cell shows a projected overall increase in Lasker events during the spawning season (see Figs 2.49 and 2.50). The increases are expected to occur in the months of October, December and February. If the Cape Town Grid Cell is utilised as a 'backup' spawning location by anchovy in the future, it is likely that these months will be the most suitable for their spawning requirements.

The Lamberts Bay Grid Cell shows a projected 167% increase in Type B Lasker events during the spawning season in the future (see Fig. 2.52). September, in particular shows a considerable increase of 300%. Given that the West Coast has been used by spawning anchovy in the past as an apparently alternative spawning ground (Fowler and Boyd 1998), it is conceivable that this projected increase in Lasker events will make the area even more suitable. Further monitoring for detecting anchovy spawning on the West Coast should perhaps focus on the month of September, given the relatively high number of Lasker events projected for the future.

The Port Nolloth Grid Cell shows no projected change in Lasker events from the present to future simulation (see Figs 2.53 and 2.54). Given that this area is not presently utilised by anchovy for spawning and that conditions remain similar in the future, it is unlikely that the Port Nolloth Grid Cell will hold anything different for anchovy spawners in the future.

3.4 Currents as a means of transport

The model results show an expected 1.4% decrease in mean wind speeds for the spawning months at the Western Bank Grid Cell (see Fig. 2.9). A change in wind regimes in the future may affect the frontal jet current. The frontal jet, as a transport mechanism, is not fully understood and as a result suggestions made are speculative in their nature. It has been suggested that anchovy rely on a frontal jet current for bringing the spawned products around the Cape Peninsula to the West Coast in order to feed. Studies have shown that spawning in the early summer months (September - December) is most favourable for the transportation of eggs and larvae to the West Coast (Huggett *et al.* 1998). Late summer months (January and February)

showed complex flow patterns, which negatively affected the movement of eggs and larvae to the nursery grounds. Although the spawning grounds on the western Agulhas Bank provide food for the spawning adults (Richardson *et al.* 1998), it lacks the high concentrations of food particles for larvae that are abundant on the West Coast (Hutchings *et al.* 1995). Therefore, if the larvae do not reach the nursery grounds on the West Coast their survival rates are likely to decrease (Fowler and Boyd 1998).

Although very little literature exists on the frontal jet, a decrease in wind speeds is expected to result in a decrease in the strength of the frontal jet current. A decrease in the strength of the frontal jet current could cause the eggs and larvae to take longer to reach the feeding grounds, thus increasing the chances of predation and cannibalism (Valdés *et al.* 1987). An increase in strength could result in increased offshore flow conditions, thereby increasing the potential loss of spawned products. An increased current strength may also have a similar effect to increased turbulence, and prevent larvae from feeding effectively. This is a speculative comment and serves to highlight the importance of monitoring current strengths and anchovy spawning patterns over time.

The expected decreases in wind speed at the Western Bank Grid Cell (see Fig. 2.9) are, however, of such a small magnitude that it is unlikely that they will negatively impact the transportation of anchovy from the western Agulhas Bank to the West Coast.

Results show an expected increase in the southerly wind component for the spawning months in the future (see Fig. 2.26) over the Western Bank Grid Cell. This increase, however, does not show a large difference from the present simulation and is thus unlikely to have major implications for anchovy. If, however, the increases in southerly winds in the future are larger than anticipated by the Climate System Model, they could result in an increased strength of offshore winds along the West Coast. In other upwelling systems, such as the California Current, some fish stocks avoid spawning in periods of strong offshore flow (Bakun and Parrish 1982). Offshore flow can, however, potentially rejoin the frontal jet further up the coast as an onshore flow entrained with eggs and larvae (Fowler and Boyd 1998). In this way eggs and larvae can be transported back to the system. The expected changes in the Climate System Model's southerly wind component are, however, not likely to be strong enough to result in any significant changes to the offshore flow.

As is evident from the above discussion, there are numerous possible ways in which currents and the frontal jet may affect anchovy spawning if the wind speeds were to increase beyond the predicted values. The wind speed values at the five grid cells, however, show no significant differences (i.e. $p > 0.05$) in the future simulation to values at present. Thus it is likely that anchovy will continue spawning on the eastern and western Agulhas Bank, where conditions are favourable and there is effective transportation to the nursery grounds on the West Coast.

CHAPTER FOUR

Other Upwelling Systems

4.1 Introduction

Some of the most productive marine areas of the world are eastern boundary current systems, otherwise known as upwelling systems. The four largest in the world are the Benguela Current off southern Africa, the Californian Current off North America, the Humboldt Current off South America and the Canary Current off the North-West of Africa (Fig. 4.1). The two fisheries that contribute most to the worlds pelagic fish catch are the Peruvian and Chilean fisheries, which achieve fish catches of millions of tons per year (Cury *et al.* 1998). Other countries such as Morocco, California, South Africa and Ivory Coast-Ghana also contribute, although only achieve catches of several hundred thousands of tons (Cury *et al.* 1998). In this chapter, the changes in wind patterns from the present to the future simulation at the California Current, Canary Current and Humboldt Current systems are briefly examined. One grid cell from each system has been selected to represent the area. Data analysed include wind speed, turbulence and the number of Lasker events. These variables are extracted from the Climate System Model and show present and future simulated values. Table 4.1 displays the dominant species of anchovy found at each of the major upwelling areas and the spawning seasons associated with the species.

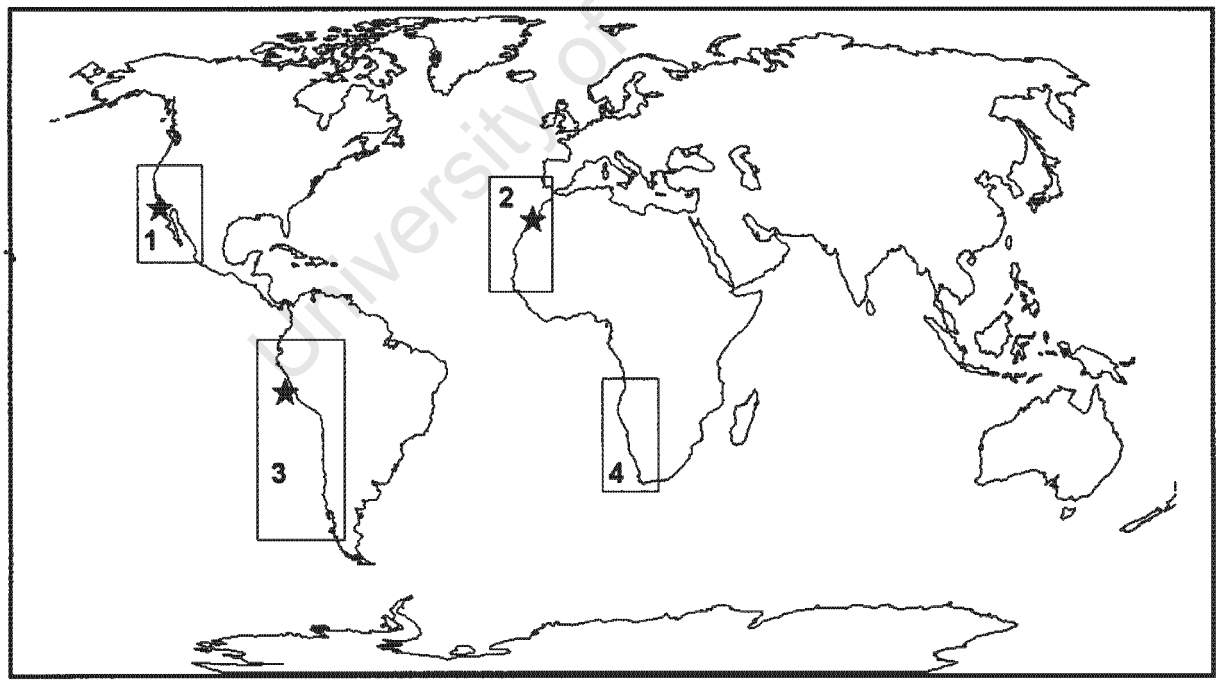

Figure 4-1 The four main upwelling systems of the world (blocked) and the specific grid cells (marked by a star) identified in the study. 1=California Current (California Grid Cell); 2=Canary Current (Morocco Grid Cell); 3=Humboldt Current (Peru Grid Cell); 4=Benguela Current

Table 4.1 Dominant sardine and anchovy species and their spawning seasons in the four major upwelling areas of the world (adapted from Shin *et al.* 1998).

Upwelling system/ current	Southern Benguela System	California Current	Canary Current	Humboldt Current
Spawning grounds	Western Agulhas Bank: 34-36°S and 18-20°S	Southern California Bight: 30-34°N Baja California: 26-30°N Southern Baja California 22-26°N	Spain: Bay of Biscay Portugal: 37-41°N Morocco: 28-30°N and 32-34°N Western Sahara: 22-26°N	Peru: 6-14°S Chile: 18-24°S
Specific grid cells identified in study within system	Eastern Bank Grid Cell (34.9°S, 22.5°E) Western Bank Grid Cell (34.9°S, 19.7°E) Cape Town Grid Cell (34.9°S, 16.9°E) Lamberts Bay Grid Cell (32.1°S, 16.9°E) Port Nolloth Grid Cell (29.3°S, 14.1°E)	California Grid Cell (32.1°N, 118.1°W)	Morocco Grid Cell (29.3°N, 11.3°W)	Peru Grid Cell (12.6°S, 78.8°W)
Dominant anchovy species	*Engraulis capensis*	*Engraulis mordax*	*Engraulis encrasicolus*	*Engraulis ringens*
Anchovy spawning season at specific grid cell	January*, February, September, October*, November* and December*	February*, March* and April*	June*, July* and August*	February, March, August*, September* and October*
Dominant sardine species	*Sardinops ocellatus*	*Sardinops caeruleus*	*Sardinops pilchardus*	*Sardinops sagax*
Sardine spawning season	January*, February*, September*, October, November and December	March, April*, May* and June*	January*, February* and December*	January, February, July*, August*, September* and October
References	Shelton and Hutchings 1982, Parrish *et al.* 1983, Hutchings 1992, Waldron *et al.* 1992	Ahlstrom 1960, Ahlstrom 1967, Hunter 1977, Parrish *et al.* 1983,	Fumestin and Fumestin 1959, Parrish *et al.* 1983	Sharp 1980, Alheit *et al.* 1984, Parrish *et al.* 1983, Pauly and Soriano 1987, Muck *et al.* 1987, Muck 1989

* Months corresponding to the peaks of reproduction

In upwelling systems, anchovy, sardine and sardinella populations are characterised by large annual fluctuations in their abundance (Sharp and Csirke 1983). For example, the Peruvian anchoveta (*Engraulis ringens*), the largest single fishery stock ever recorded, peaked in 1970 with an annual production of more than 12 million metric tons and collapsed in 1972/1973

(Pauly and Tsukayama 1987). The Pacific sardine (*Sardinops caerulea*), by contrast, collapsed in the 1950s and disappeared from the Californian fishery (Lasker and MacCall 1983). It has been suggested that these fluctuations are a result of recruitment failure (Shepherd *et al.* 1984). Recruitment success is likely to be influenced by increased fishing pressure (e.g. biomass depletion) and changes in the marine environment (e.g. changes in the mortality rates of eggs and larvae) (Lasker 1981, Beverton 1990). Climate change effects on the marine environment are thus likely to impact on the recruitment success of pelagic fish. Indeed Bakun (1990) has suggested that the increase in greenhouse gases in the earth's atmosphere is likely to result in an increase in upwelling intensity in major upwelling systems in the world with possible negative consequences for pelagic fish recruitment.

4.2 Optimal Environmental Window and upwelling systems

The Optimal Environmental Window has been applied to fish species in some of the world's main upwelling systems (Cury and Roy 1989). These systems are located in tropical or subtropical areas and where trade winds are responsible for the upwelling process (Roy *et al.* 1995). For example, it has been applied to the Peruvian anchoveta (*Engraulis ringens*), the Pacific sardine (*Sardinops sagax caerulea*) and West African sardine (*Sardina pilchardus*) and sardinella (*Sardinella aurita*). The hypothesis attempts to explain the non-linear relationship between pelagic fish recruitment and upwelling intensity by means of a dome-shaped relationship (Cury and Roy 1989) (see Fig. 1.6). It assumes that recruitment is influenced by factors related to wind such as offshore transport, wind mixing and biological production (Roy *et al.* 1995), with optimal wind speeds of 5-6 $m.s^{-1}$.

Important factors affecting larval survival are food availability and physical constraints (such as wind mixing and offshore transport). Sufficient food, associated with stable ocean conditions, is required for larval survival (Lasker 1981). A certain amount of turbulence is also required to increase the encounter rate between larvae and food particles (Rothschild and Osborn 1988) and thus increase larval survival. High wind speeds result in strong mixing of the water column, which has a negative effect on larvae by dispersing food patches (Peterman and Bradford 1987, Therriault and Platt 1981). The magnitude of the wind speed also determines the vertical input of nutrients into the system through upwelling. An increase in upwelling from weak to moderate intensity should have a positive effect on recruitment, since an increase in primary production, associated with increased upwelling, enhances food availability. Strong upwelling has a

negative effect on recruitment despite a potential increase in primary production because wind mixing is high.

Optimal environmental conditions for spawning in upwelling areas are a combination of a high upwelling index (~ 1.2 $m^3.s^{-1}$) and moderate wind mixing (~250 $m^3.s^{-3}$) (Cury *et al.* 1998). In the Canary, Humboldt and California Currents, spawning peaks occur at upwelling intensities ranging from 1 - 3.2 $m^3.s^{-1}$. Spawning peaks coincide with wind speeds of ~ 5-6 $m.s^{-1}$.

4.3 Examples of upwelling systems

4.3.1 California Current: *Engraulis mordax*

Off the coast of California, coastal upwelling is an important process (Reid *et al.* 1958). The California Current flows in an equatorward direction off the coast of western United States and northern Mexico. One of the major spawning grounds, the Southern California Bight (30-34°N), is located between the upwelling zones of northern California and Baja California (Bakun 1996). Spawning of anchovy (*Engraulis mordax*) takes place here from February - April (Hunter 1977, Parrish *et al.* 1981) (Table 4.1) and occurs at intermediate upwelling intensities (Shin *et al.* 1998).

The Southern California Bight is the main spawning ground of the pelagic fishes that dominate the California Current ecosystem (Bakun 1993). Within the Bight, eggs and larvae are retained by an enclosed circulation pattern and sheltered from strong coastal winds. As a result, the Ekman transport almost disappears and turbulent mixing by the wind is very low (Parrish *et al.* 1983). This area is therefore favoured as a spawning ground for pelagic fish as it is a natural larval retention area, where the loss of larvae from the coastal area is minimal and the low turbulence intensity allows for the concentration of food particles in a stratified layer (Lasker 1978). There is also a high concentration of food because of the advection of water from the upwelling region further north (Bakun 1996). Anchovy is the dominant species located within the reproductive area of the Bight, largely due to its small size and limited migration capabilities (Bakun 1993). During the spawning season, the turbulence in the area is less than 250 $m^3.s^{-3}$ in both the winter and summer seasons (Bakun 1993, 1996).

Results from studies in the California Current (Cury *et al.* 1995) suggest that the number of larval anchovy has a dome-shaped relationship with upwelling intensity (the Optimal

Environmental Window) (Fig. 4.2). High larval numbers were found at moderate upwelling intensities (~ 1.5 $m^3.s^{-1}$ per metre of coastline), whereas weak and strong upwelling intensities showed low larval numbers. Moderate turbulence has a positive impact on larval survival as it increases the encounter rate between the larvae and food particles in the water column (Rothschild and Osborn 1988). High turbulence on the other hand disperses food patches (Lasker 1975) and cause offshore loss of larvae from the favourable coastal area (Parrish *et al.* 1981).

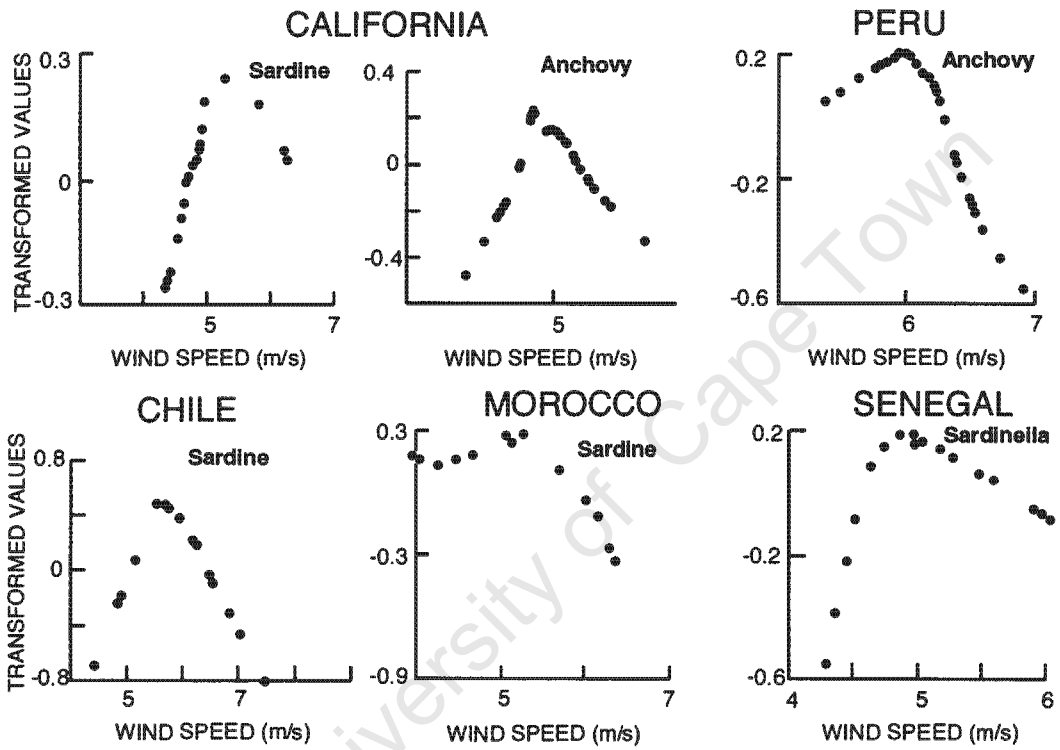

Figure 4-2 Optimal empirical transformations from the ACE algorithm for anchovy in the Californian ecosystem (adapted from Cury and Roy 1989, Roy *et al.* 1991, Cury *et al.* 1995 and Serra *et al.* 1998)

4.3.2 Canary Current (North-West Africa): *Engraulis encrasicolus*

Off the coast of Morocco, anchovy (*Engraulis encrasicolus*) and sardine (*Sardina pilchardus*) are the main catches. The dominant pelagic fish species in the Canary Current from 1970-1979 was sardine (*Sardina pilchardus*). Anchovy spawning off the coast of Morocco takes place from June - August (Furnestin and Furnestin 1959) (Table 4.1) and is out of phase with the upwelling process (upwelling intensity during spawning is in the range of 0.2-0.3 $m^3.s^{-1}$) (Shin *et al.* 1998). The Optimal Environmental Window has been applied to sardine off the coast of Morocco (Fig. 4.2) and shows optimal wind speeds values to be between ~5-6 $m.s^{-1}$. The Canary Current

system is the upwelling system with the least published information (Jarre-Teichmann and Christensen 1998).

4.3.3 Humboldt Current (Peru): *Engraulis ringens*

The dominant species of anchovy and sardine in the Humboldt Current, off Peru, are *Sardinops sagax* and *Engraulis ringens* respectively. Anchovy spawn from February - March and August - October, with peak spawning occurring from August - October (Parrish *et al.* 1983, Alheit *et al.* 1984, Pauly and Tsukayama 1987) (Table 4.1). Off Peru, spawning occurs below a maximum upwelling intensity (~1.8 $m^3.s^{-1}$) (Shin *et al.* 1998).

The Peruvian upwelling system is up to ten times more productive than other upwelling systems (Cury *et al.* 1998). Due to the latitudinal positioning of the Peru Current (i.e. ~9°), the area is characterised by relatively weak winds and low turbulence. The weak winds, however, promote relatively strong upwelling because of the high Coriolis parameter at the equator, which results in continuous enrichment for fish larvae (Bakun 1996). Studies have shown that upwelling is advantageous in the Humboldt Current for anchovy recruitment until wind speeds reach ~5-6 $m.s^{-1}$ (Fig. 4.2) (i.e. Optimal Environmental Window) (Cury and Roy 1989). The Peruvian upwelling system is the only system that has a combination of moderate turbulence (~224 $m^3.s^{-3}$) and high upwelling (1.2 $m^3.s^{-1}$) resulting in optimal conditions for spawning (Cury *et al.* 1998). As a result, anchoveta, which are not migratory, have remained the dominant species in the Peru Current (DeVries and Pearcy 1982). Recently, however, the sardine population has increased because of the over-fishing of anchoveta, (Bakun 1996).

The recruitment of Peruvian anchoveta depends both on the adult biomass (Csirke 1980) and environmental fluctuations (Mendelssohn and Mendo 1987). Studies show that high turbulence and low biomass may have played an important role in the collapse of the Peruvian anchoveta in 1972 and 1973. In these years there was low recruitment because of the high turbulence (>200 $m^3.s^{-3}$) and the parent stock was low (Cury and Roy 1989).

4.4 Results of the upwelling systems

4.4.1 California

A summary of the results from the Climate System Model for the California, Peru and Morocco Grid Cells is presented in Table 4.2. The California Grid Cell (32.092°N, 118.125°W) has future

wind projections that are similar to those in the present simulation (Fig. 4.5). For the spawning months (i.e. February - April) there is a decrease (of 7.2%) in mean wind speed values in February, identical mean wind speeds in March and an increase (of 2.9%) in mean values in April. The mean wind speed values for February and March in the present simulation fall within the optimal range, according to Cury and Roy (1989) (i.e. ~5-6 $m.s^{-1}$). The values projected for the future simulation continue to fall within this range. The mean wind speed values for April in the present and future simulations fall within 6-7 $m.s^{-1}$.

Table 4.2 Results from the Climate System Model for the California, Peru and Morocco Grid Cells.

	California Grid Cell	**Peru Grid Cell**	**Morocco Grid Cell**
Peak spawning months for anchovy	February, March and April	August, September and October	June, July and August
Mean wind speed value for the peak spawning season	Present: 6.1 $m.s^{-1}$ Future: 6.0 $m.s^{-1}$	Present: 6.3 $m.s^{-1}$ Future: 6.3 $m.s^{-1}$	Present: 6.0 $m.s^{-1}$ Future: 6.1 $m.s^{-1}$
Mean turbulence value for the peak spawning season	Present: 358. 2 $m^3.s^{-3}$ Future: 356.8 $m^3.s^{-3}$	Present: 304.6 $m^3.s^{-3}$ Future: 303.2 $m^3.s^{-3}$	Present: 293.9 $m^3.s^{-3}$ Future: 292.5 $m^3.s^{-3}$
The frequency of Type A Lasker events	Present: 32 events Future: 31 events	Present: 25 events Future: 27 events	Present: 33 events Future: 42 events
The frequency of Type B Lasker events	Present: 20 events Future: 20 events	Present: 15 events Future: 19 events	Present: 28 events Future: 34 events

The turbulence values from October - January at the California Grid Cell show large deviance from the mean turbulence values in both the present and future simulations (Fig. 4.6). May - September show a smaller deviance from the mean turbulence value in both simulations. The mean turbulence in February and March in the present simulation is 304 $m^3.s^{-3}$ and 349 $m^3.s^{-3}$ respectively. In the future simulation the mean turbulence values decrease to 284 $m^3.s^{-3}$ in February and 319 $m^3.s^{-3}$ in March, showing a decrease of 7% and 9.4% respectively.

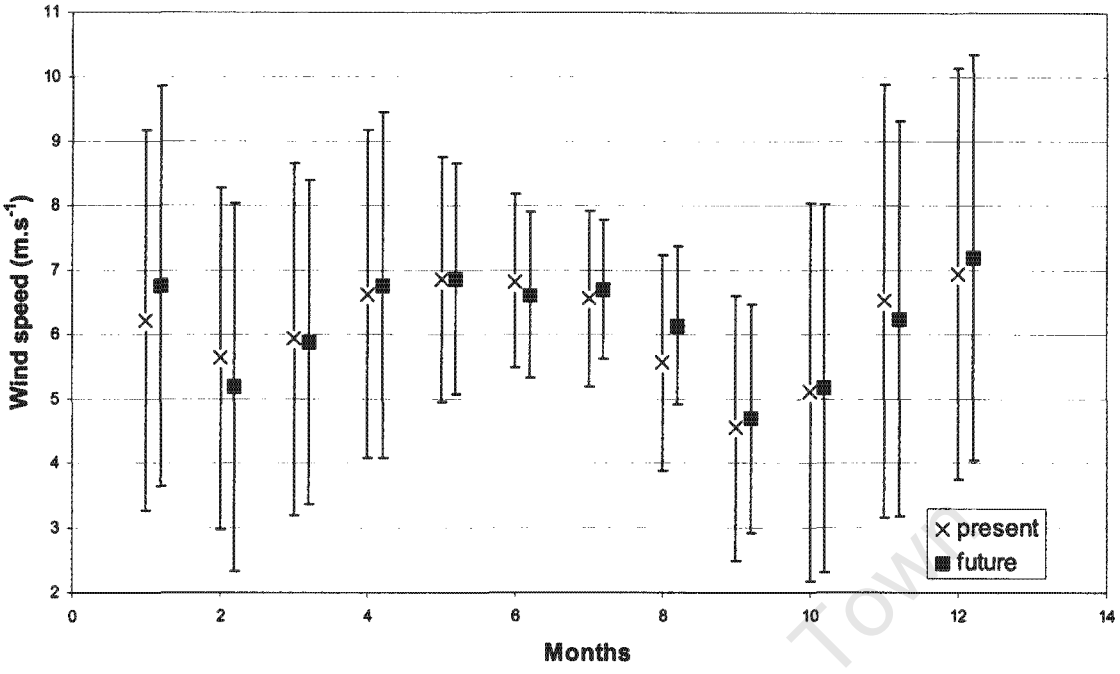

Figure 4-3 Mean wind speeds (+- standard deviation) in the present and future simulation at the California Grid Cell

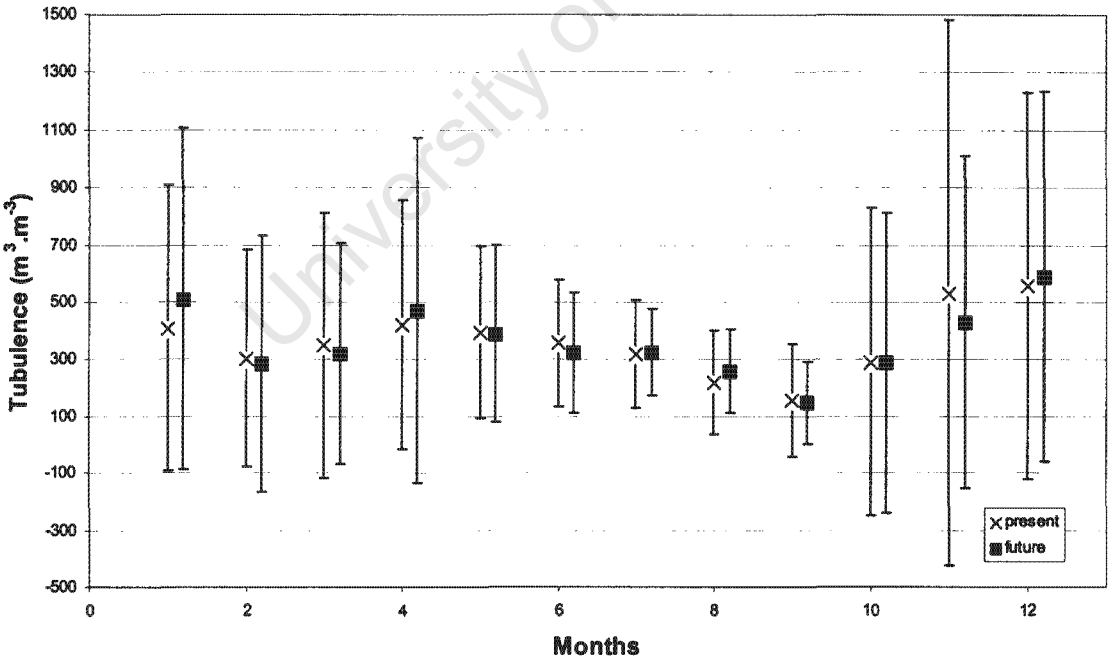

Figure 4-4 Mean turbulence values (+- standard deviation) in the present and future simulation at the California Grid Cell

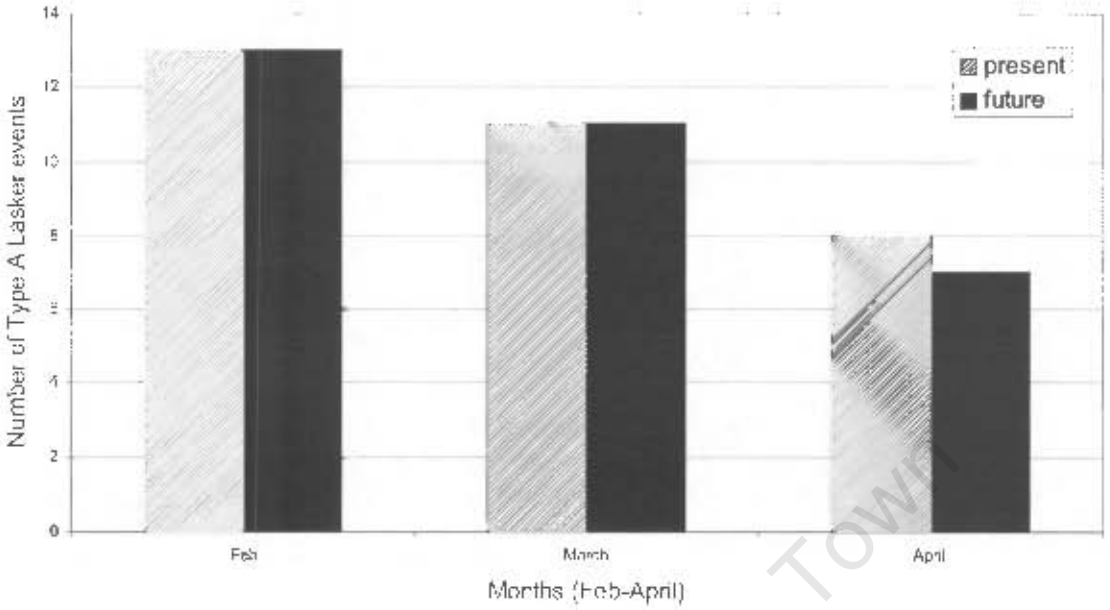

Figure 4-5 The number of Type A Lasker events for the spawning season in the present and future simulation at the California Grid Cell

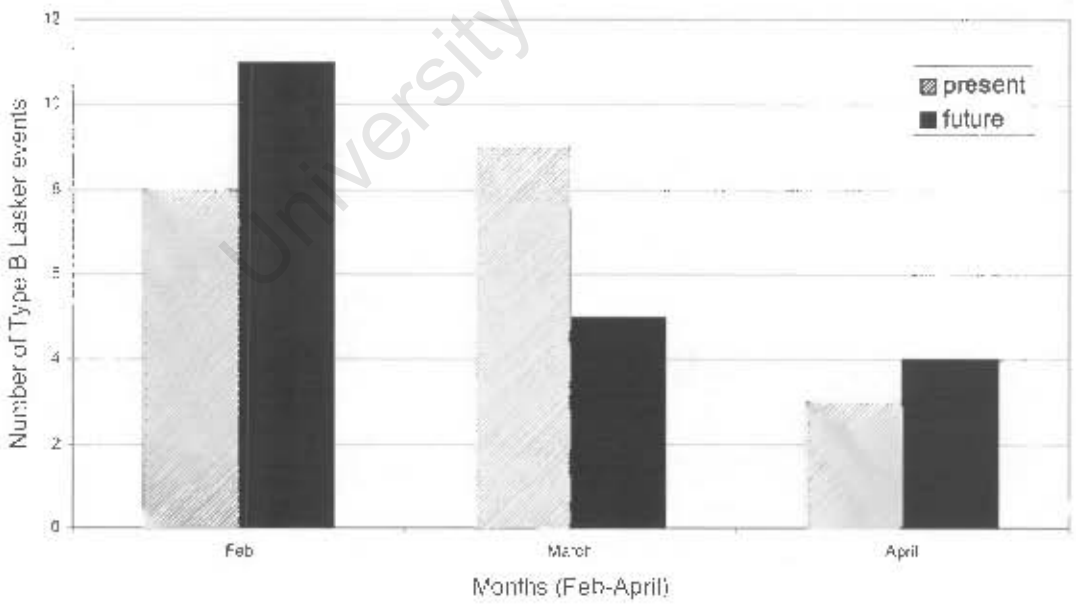

Figure 4-6 The number of Type B Lasker events for the spawning season in the present and future simulation at the California Grid Cell

Bakun (1996) suggests that the average turbulence value for the California Current at present does not exceed 250 $m^3.s^{-3}$ (Bakun 1996). April has turbulence values in the present and future simulations that exceed optimal turbulence (~ 422 $m^3.s^{-3}$ in the present and 467 $m^3.s^{-3}$ in the future).

There is a 3% decrease in Type A Lasker events for the spawning season from the present simulation to the future (Fig. 4.7). There is no change in the number in Type B Lasker events from the present to the future simulation (Fig. 4.8).

4.4.2 Peru

At the Peru Grid Cell (12.558°S, 78.75°W) the mean wind speeds are similar in magnitude in the present and future simulations (Fig. 4.9). Although anchovy spawning does occur in February and March, the peak spawning months are August - October. In the present simulation, mean wind speeds from August - October fall within 6-7 $m.s^{-1}$. These winds show similar values in the future simulation. There is a decrease of 1.6% in August and an increase of 1.6% in mean wind speeds for September and October.

At the Peru Grid Cell the peak spawning months (August - October) show a large deviance from the mean turbulence value in both the present and future simulations (Fig. 4.10). From December - April, the deviance from the mean is considerably smaller. The mean turbulence shows a 5.7% decrease in August in the future and a 3.4% and 1% increase in turbulence for September and October respectively. The mean turbulence values for the peak spawning months fall within the range of 250-350 $m^3.s^{-3}$ in the present simulation and continue to fall within this range in the future simulation.

There is an overall increase in the frequency of Lasker events at the Peru Grid Cell in the future simulation for the spawning months (February, March, August, September and October) (Figs 4.11 and 4.12). The future simulation shows a 4% increase in Type A Lasker events and an 8% increase in Type B Lasker events. For the peak spawning months there is an 8% increase in Type A events and 13% increase in Type B events. The largest increase in the frequency of Lasker events in the future occurs in August.

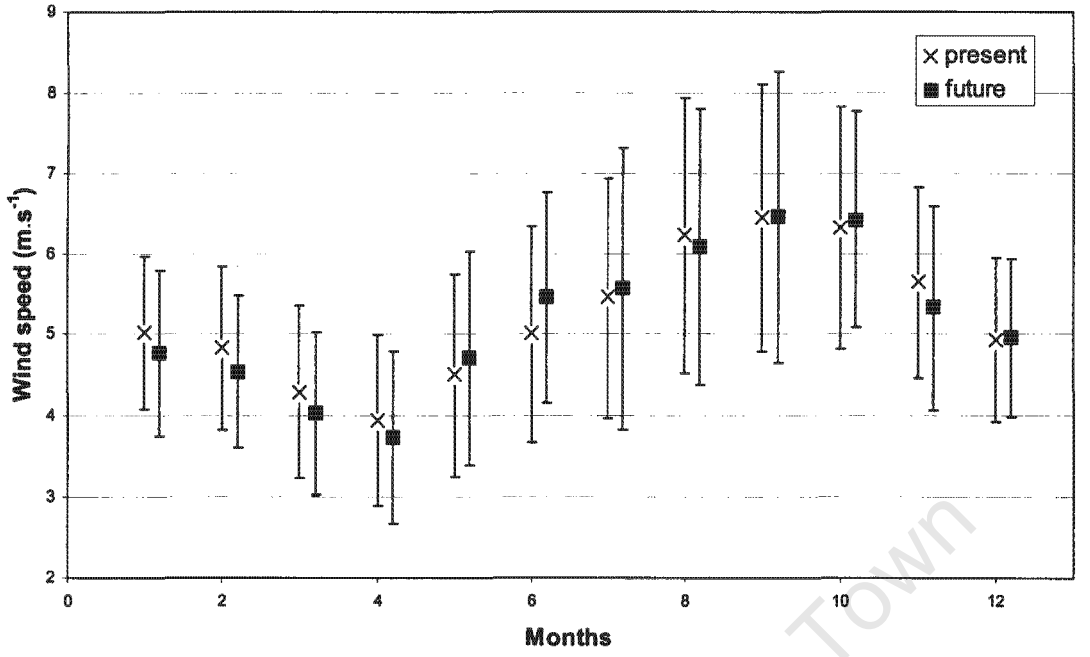

Figure 4-7 Mean wind speeds (+- standard deviation) in the present and future simulation at the Peru Grid Cell

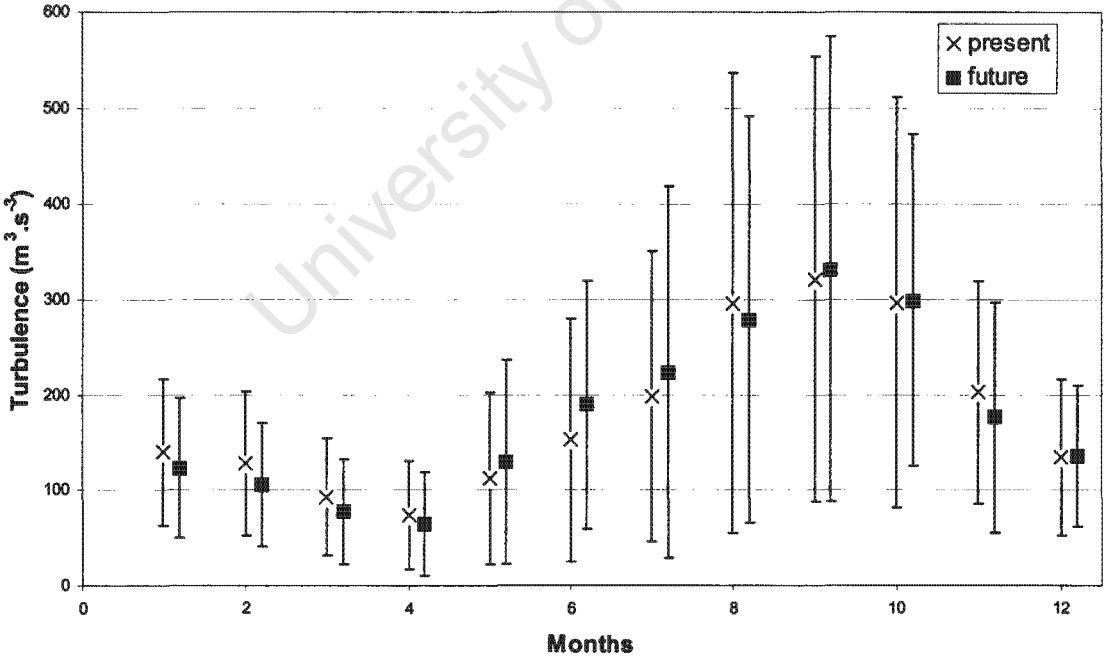

Figure 4-8 Mean turbulence values (+- standard deviation) in the present and future simulation at the Peru Grid Cell

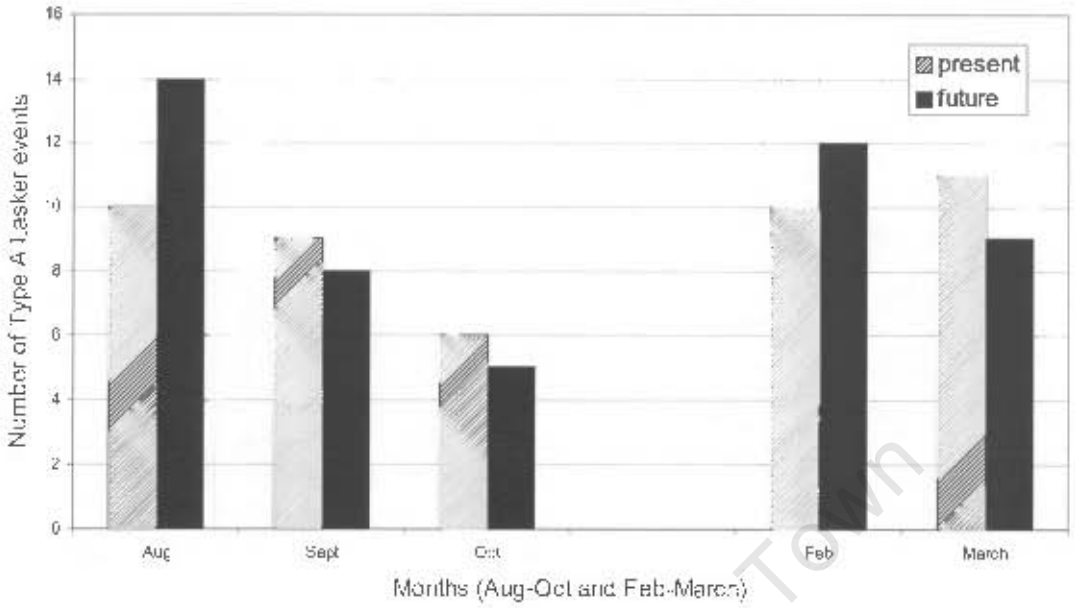

Figure 4-9 The number of Type A Lasker events for the spawning season in the present and future simulation at the Peru Grid Cell

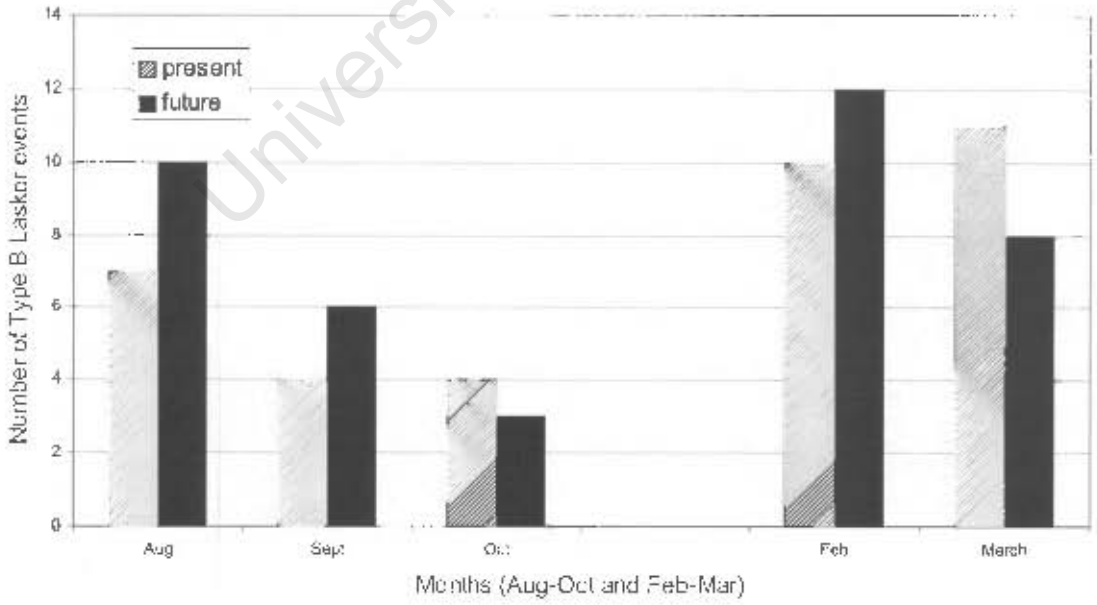

Figure 4-10 The number of Type B Lasker events for the spawning season in the present and future simulation at the Peru Grid Cell

4.4.3 Morocco

At the Morocco Grid Cell (29.301°N, 11.25°W) mean wind speeds in the present and future simulations are similar (Fig. 4.13). In all months in both simulations, the standard deviation of the wind is large. Mean wind speeds in July and August in the present simulation fall within the range of 5-6 $m.s^{-1}$. In the future simulation there is a 5.3% and 1.9% increase in mean wind speeds for July and August and wind speeds continue to fall within the 5-6 $m.s^{-1}$ range.

At the Morocco Grid Cell for June there is a 13% decrease in turbulence values from the present to the future simulation (Fig. 4.14). July and August show increases in turbulence of 21% and 1.4% respectively. The average turbulence at the Morocco Grid Cell is ~250 $m^3.s^{-3}$ (Bakun 1996). July and August show turbulence values in the future, which fall between 200-300 $m^3.s^{-3}$.

There is an overall increase in the frequency of Lasker events at the Morocco Grid Cell in the spawning season in the future simulation (Fig. 4.15 and 4.16). There is a 27% increase in Type A events and 21% increase in Type B events in the future from June - August. June shows an increase of 500% in Type A events in the future simulation.

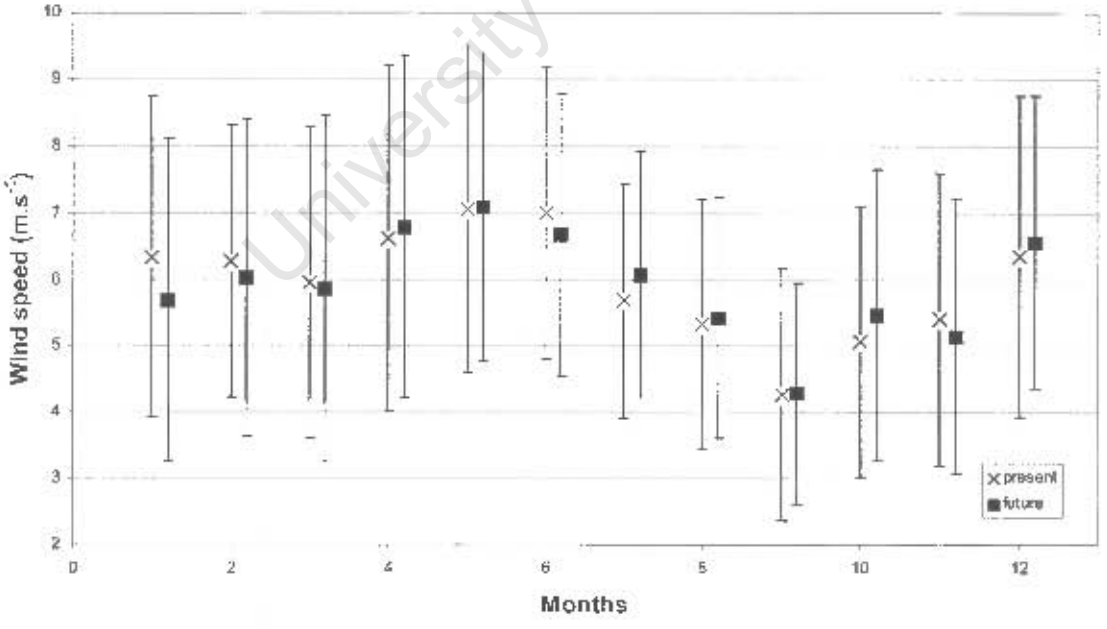

Figure 4-11 Mean wind speeds (+- standard deviation) in the present and future simulation at the Morocco Grid Cell

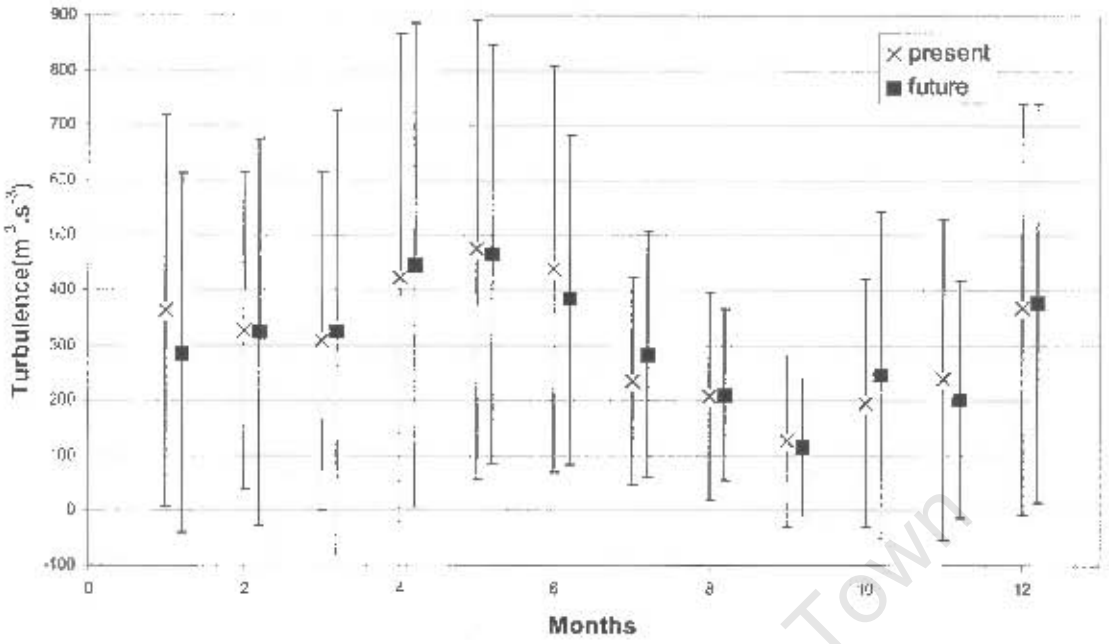

Figure 4-12 Mean turbulence values (+- standard deviation) in the present and future simulation at the Morocco Grid Cell

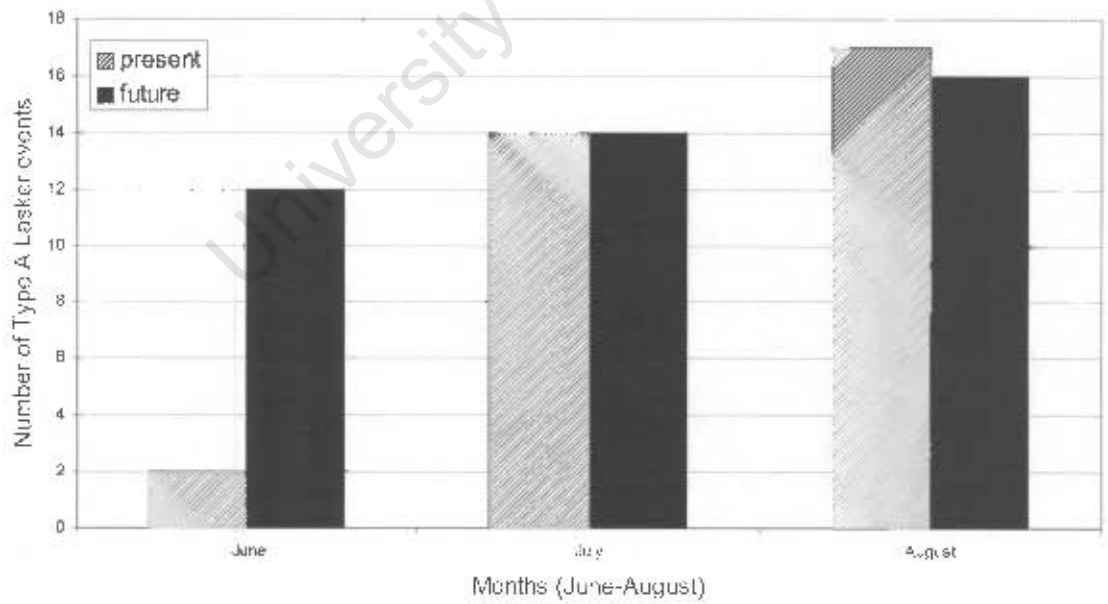

Figure 4-13 The number of Type A Lasker events for the spawning season in the present and future simulation at the Morocco Grid Cell

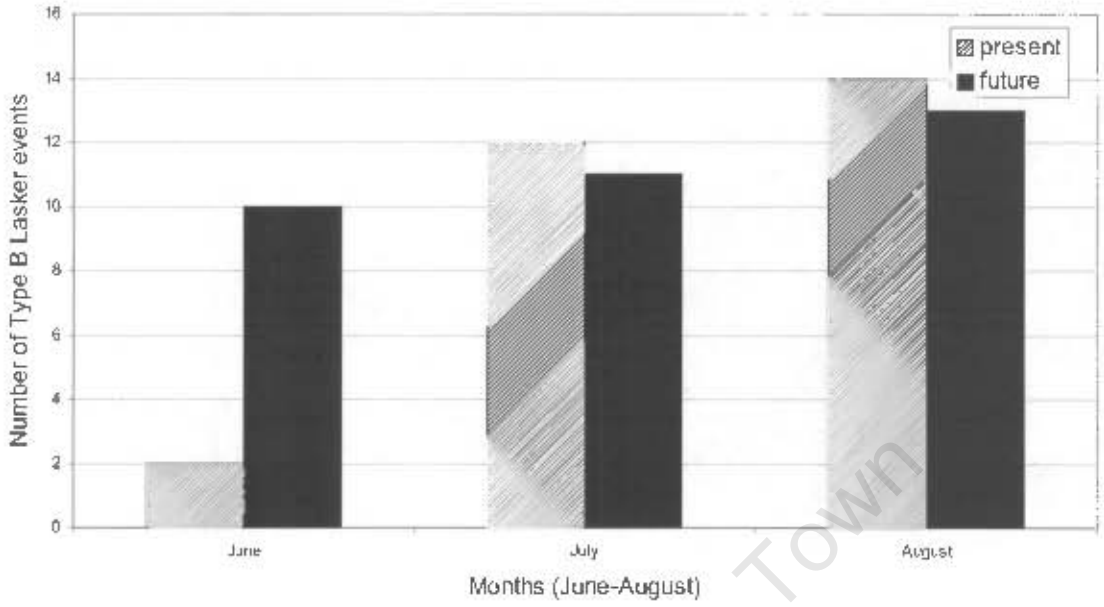

Figure 4-14 The number of Type B Lasker events for the spawning season in the present and future simulation at the Morocco Grid Cell

4.5 Discussion

4.5.1 California

The CSM output shows that the California Grid Cell (Fig. 4.5) supports optimal wind speeds at present as delineated by Cury and Roy (1989) (i.e. ~5-6 $m.s^{-1}$) for the peak spawning months. Wind speeds in the future show a 2% decrease from present day values and continue to fall within the optimal range in the peak spawning months (February - March). The present and future mean wind speeds for the spawning season from the CSM are also comparable with the Optimal Environmental Window for anchovy in the California Current (Fig. 4.2), which shows optimal wind speeds to be ~5-6 $m.s^{-1}$ (Roy *et al.* 1991, Cury *et al.* 1995, Serra *et al.* 1998). According to the Optimal Environmental Window (Cury and Roy 1989), projected wind speeds at the California Grid Cell in the future are optimal for anchovy larvae survival. At this wind speed (~5-6 $m.s^{-1}$) there is moderate upwelling, which allows for sufficient concentrations of nutrients (nitrate and phosphate) to be upwelled into the euphotic layer. This results in an increase in phytoplankton and thus an increase in food particles for larvae.

At the California Grid Cell the mean monthly turbulence during the spawning months in the present simulation ranges between 284 $m^3.s^{-3}$ and 467 $m^3.s^{-3}$. These values are in a higher range

than that suggested by Bakun (1996). Bakun (1996) stipulates a threshold value of 250 $m^3.s^{-3}$ for successful recruitment in the California Current. The decrease in turbulence projected for February and March in the future (Fig. 4.6) may produce a more stable environment and result in the increased formation of patches of food particles (Peterman and Bradford 1987). This may have a positive impact on first feeding larvae, which require high concentrations of food at a critical time in their life cycle. These potential improvements in recruitment conditions may be offset to some extent by the increase in turbulence projected for April from 422 $m^3.s^{-3}$ to 467 $m^3.s^{-3}$.

The California Grid Cell does not show a large change in the number of Lasker events for the spawning season in the future simulation (Figs 4.7 and 4.8). It is unlikely that the 3% decrease in Type A events will have any major influence on larval survival.

4.5.2 Morocco

Output data from the CSM shows that the Morocco Grid Cell (Fig. 4.13) supports optimal wind speeds of ~5-6 $m.s^{-1}$ as suggested by Cury and Roy (1989) for the peak spawning months. In the future simulation, wind speeds show a 2% increase and continue to fall within the optimal range in the peak spawning months (July - August). As occurs at the California Grid Cell, projected wind speeds at the Morocco Grid Cell in the future are optimal for anchovy larvae survival, in terms of the Optimal Environmental Window Hypothesis.

At the Morocco Grid Cell the mean monthly turbulence during the spawning months in the present simulation ranges between 207 $m^3.s^{-3}$ and 440 $m^3.s^{-3}$. These values are in a higher range than that suggested by Bakun (1996). Bakun (1996) stipulates a threshold value of 250 $m^3.s^{-3}$ for successful recruitment in the Canary Current. The decrease in turbulence projected for June (Fig. 4.14), may thus have a positive impact on anchovy through increasing the encounter rate between first feeding larvae and food particles. In July there is an increase from 235 $m^3.s^{-3}$ to 284 $m^3.s^{-3}$. This value of 284 $m^3.s^{-3}$ is, however, low in comparison to the other spawning months values and is thus unlikely to have adverse effects on anchovy recruitment.

The Morocco Grid Cell shows a 27% increase in the frequency of Type A Lasker events in the future simulation for the spawning season (Fig. 4.15). This increase in Lasker events in the future is likely to have a positive effect on anchovy larval survival in this upwelling system. An increase in events signifies an increase in the number of 'calm' days, implying increased water

column stability. This allows for the concentration of food particles in a stratified layer and thus a greater supply of food for anchovy larvae. This in turn increases the chances of larval survival in the upwelling area. The 500% increase in Type A Lasker events in June in the future simulation is likely to result in June being the most successful month in the spawning season in the future.

4.5.3 Peru

At the Peru Grid Cell, wind speeds in the present and future simulations for the peak spawning months fall between 6-7 $m.s^{-1}$ (Fig. 4.9). According to the Optimal Environmental Window, optimal wind speeds are 5-6 $m.s^{-1}$ (Cury and Roy 1989). Studies done on anchovy in the Peru Current, however, show optimal wind speeds to be ~6 $m.s^{-1}$ (Fig. 4.3, Roy *et al.* 1991, Cury *et al.* 1995, Serra *et al.* 1998). Therefore wind speeds from the CSM do not compare with suggested optimal wind speeds for the Peru Current in both the present and future simulations and exceed these values. As the dominant wind in the Humboldt Current is equatorward, strong winds lead to the offshore movement of the Ekman layer which can result in eggs and larvae being removed from their preferred food-rich coastal habitat (Bakun and Parrish 1980, Sinclair 1988). Also, strong winds enhance turbulent mixing in the surface layer, which causes the desegregation of food patches (Lasker 1978, Theriault and Platt 1981). This makes it more difficult for larvae to obtain sufficient food and thus increases their chances of starvation. Furthermore, strong winds inhibit the ability of larvae to capture food particles (MacKenzie *et al.* 1994). Future mean wind speeds are similar to present mean wind speeds. As successful spawning presently takes place at the Peru Grid Cell, it is likely that future wind speeds will continue to support anchovy spawning.

The turbulence values at the Peru Grid Cell for the peak spawning months in the present simulation fall within the range of 250-350 $m^3.s^{-3}$ (Fig. 4.10). As was reported for the California and Morocco Grid Cells, the turbulence values from the model are higher than those presented by Bakun (1996). Average turbulence in the Humboldt Current has been estimated to be 250 $m^3.s^{-3}$ (Bakun 1996). The future simulation shows turbulence values that are similar to those in the present simulation, suggesting that the projected turbulence values are likely to continue supporting spawning.

There is a projected increase of 4% in the frequency of Type A Lasker events and an 8% increase in Type B events (Figs 4.11 and 4.12) in the spawning months in the future at the Peru Grid Cell. This change is likely to be beneficial for first feeding larvae and hence recruitment. The wind speed values, turbulence values and the frequency of Lasker events suggest that successful spawning is likely to continue in this area.

CHAPTER FIVE

Conclusions

5.1 General

Large annual variations in population sizes are common for many pelagic fish species. Although over-fishing has in recent years depleted many fish populations, environmental changes from year to year also play a major role in fluctuations of fish stocks. Owing to the commercial importance of pelagic fish, short-term fluctuations in pelagic fish stocks have been the subject of much ecological research.

Anchovy (*Engraulis capensis*) is presently the mainstay of the South African pelagic fishing industry. The successful recruitment of this species is dependent upon climatic conditions and thus a shift in climate, as predicted by many climatologists worldwide, could potentially limit or even improve recruitment, which is important for the fishing industry. Physical and biological factors contributing to fish population variability are numerous and interrelated, resulting in a very complex system. Two factors appear to be critical for successful recruitment of anchovy in southern African waters, namely: transport of spawned products and food availability for larvae. Transport is important because the southern Benguela system is the only major upwelling system in the world where the spawning and nursery grounds are separate and spawned products are transported to the nursery grounds via currents. The north-flowing jet current is of particular importance in this process. The second factor of food availability is largely a function of upwelling intensity (alongshore wind stress) and the number of calm days (Lasker events). Wind speed has a direct impact on upwelling and Lasker events and is thus a critical factor for anchovy recruitment success.

Empirical attempts to relate recruitment to environmental factors have not been successful, partly due to the short time series available for analysis (Bakun 1985). Mathematical modelling has been used with some success to deal with environmental uncertainties in recruitment processes (Shannon *et al.* 1996).

In this dissertation, output data from the NCAR Climate System Model has been used to infer how changes in climate variables in the future may affect the recruitment success of anchovy in the southern Benguela system. This dissertation has focussed on wind speed, equatorward wind stress (as a proxy for upwelling) and turbulence in

the southern Benguela system, as they are understood to be some of the key abiotic factors affecting anchovy spawning success. Other major upwelling systems are briefly examined and include the California Current, the Humboldt Current and the Canary Current.

The Climate System Model used to generate a future climatic simulation was validated using the NCEP reanalysis. The NCEP and CSM present simulation data over South Africa and the surrounding oceans were closely related and confirmed that the CSM is comparable with other leading GCMs. The CSM future simulation assumes a transient growth at 1% per annum to a doubling of atmospheric CO_2 (i.e. 2 x CO_2).

Results from CSM show a future intensification and ridging of the South Atlantic High Pressure Cell south and east of southern Africa for late summer months (January and February). A consequence of this intensification is an increase in the pressure gradient and an increase in the frequency of south-easterly winds. As a result of the angle of the coastline, an increase in frequency of south-easterly winds will produce an increase in upwelling on the West Coast and a concomitant increase in food concentrations for anchovy larvae. An increase in upwelling may, however, change sea surface temperatures, with possible negative consequences for anchovy.

Anchovy presently spawn on the eastern and western Agulhas Bank (Eastern Bank Grid Cell and the Western Bank Grid Cell) during spring and summer (September-February). It is suggested that in general, both grid cells will continue to be suitable spawning locations in the future, and that spawning conditions may even improve. The reasons for this conclusion are as follows:

- Decreases in wind speeds projected for the future at the Eastern and Western Bank Grid Cells continue to fall within average wind speeds for the southern Benguela system (i.e. 5-8 $m.s^{-1}$). As successful anchovy spawning presently takes place within this range of wind speed values, it is suggested that within the range of 5-8 $m.s^{-1}$ there is suitable upwelling and turbulence conditions for larval survival and hence recruitment.

- At the Eastern Bank Grid Cell, there is a comparable frequency of extreme wind speeds in the present and future simulations and a 50% decrease in the frequency of extreme turbulence in the future simulation. At the Western Bank Grid Cell there is a 30% decrease in the frequency of extreme wind speeds and a 56% decrease in the frequency of extreme turbulence in the future simulation. Extreme events are often fundamental to ecosystem functioning because of the periodic catastrophic effect on the survival of biota. In the case of anchovy, extreme turbulence or wind speed may greatly reduce larval recruitment. A reduction in the number of extreme events at both grid cells is thus likely to have a positive impact on spawning success.

- Turbulence values at both grid cells in the spawning season in the future do not exceed suggested mean turbulence values for the southern Benguela system (i.e. ~600-650 $m^3.s^{-3}$, Bakun 1996). There is a 10% projected decrease in average turbulence at the Eastern Bank Grid Cell and a 9% decrease at the Western Bank Grid Cell for the spawning season in the future simulation. Strong turbulence is detrimental to spawning as it inhibits the ability of larvae to capture food particles in the water column. Also, turbulent mixing in the upper surface layer disperses larval prey organisms, which aggregate in the water column. Thus strong turbulence can lead to starvation of larvae. The projected decreases in turbulence for the future will in all likelihood favour anchovy spawning by enabling more effective larval feeding.

- There is an 81% increase in the expected frequency of Type A Lasker events in the CSM future simulation at the Eastern Bank Grid Cell. The output data shows an average of 1.6 Type A Lasker events per year at the Eastern Bank Grid Cell in the present simulation and an average of 2.9 per year in the future. There is a 300% increase in the frequency of Type A Lasker events in December in the future simulation. Lasker events during the spawning season may enhance anchovy recruitment as they result in a greater concentration of food particles and thus enable fish larvae to feed effectively in calm, food-rich waters. Lasker events allow for rapid growth and provide larvae with some measure of resilience against the difficult feeding conditions during more turbulent conditions. The

large increase in the frequency of Lasker events in December at the Eastern Bank Grid Cell suggests that this month may become a more favourable time for anchovy spawning in the future.

One exception, however, to the Western Bank Grid Cell continuing to be a suitable spawning location, is a 27% decrease in the expected frequency of Type A Lasker events in the CSM future simulation. As the future simulation shows more Lasker events at the Eastern Bank Grid Cell, this grid cell may have better spawning conditions in the future than the Western Bank Grid Cell.

The conditions at the Cape Town Grid Cell projected by the future simulation, suggest that this grid cell may be used as an alternative spawning location if conditions were to become unsuitable on the Agulhas Bank. The spawning season shows optimal wind speeds (5-8 $m.s^{-1}$), a decrease in turbulence from present values, and an increase in Lasker events in the future simulation. As sardine and anchovy have been known to spawn in this region in the past, it is conceivable that this grid cell may be an alternative spawning location in the future.

The projected increases in the alongshore wind stress on the West Coast of southern Africa from November - February in the future simulation indicate that there will be increased upwelling in this area. Anchovy larvae that migrate to the West Coast to feed are thus likely to encounter even greater food concentrations in the future. Wind speed and turbulence at the Lamberts Bay and Port Nolloth Grid Cells exceed average values for successful spawning (wind speeds of >8 $m.s^{-1}$; and turbulence >650 $m^3.s^{-3}$, Bakun 1996) in the present and future simulations. These grid cells do not presently support optimal conditions for spawning and it is thus unlikely that they will be suitable spawning locations in the future.

Along with the Benguela Current, the California Current, Humboldt Current and Canary Currents are the four main upwelling systems in the world. The latter three have been examined briefly (the California Grid Cell, Morocco Grid Cell and Peru Grid Cell) in an attempt to understand how a change in climate in the future will affect anchovy recruitment. The variables extracted from the CSM output data

include wind speed, turbulence and Lasker events for both the present and future simulations.

In all three upwelling systems, optimal spawning takes place when mean wind speeds are between 5-6 $m.s^{-1}$ (Optimal Environmental Window). At the California and Morocco Grid Cells, future mean wind speeds continue to fall within the optimal range (5-6 $m.s^{-1}$). This will in all likelihood result in similar recruitment in the future. There are both increases and decreases in turbulence projected for the spawning months at both grid cells. The California Grid Cell shows no major change in the frequency of Lasker events in the future, whereas the Morocco Grid Cell shows a 27% increase in the frequency of Lasker events in the future simulation. This increase is likely to result in increased stabilisation of the water column and an increase in the concentration of food particles for the larvae, which could enhance recruitment. The month of June shows a 500% increase in the frequency of Lasker events in the future simulation at the Morocco Grid Cell and is thus likely to be the most successful spawning month in the future.

At the Peru Grid Cell, mean wind speeds in the spawning season fall within the range of 6-7 $m.s^{-1}$ in both the present and future simulations. Mean turbulence and frequency of Lasker events are also similar in the two simulations. Anchovy spawning is thus unlikely to be adversely affected by future wind regimes off the Peru coastline.

The ecological complexity in the web of interacting environmental and biological factors affecting pelagic fish recruitment is immense. Output data from the Climate System Model show that to the best of our present knowledge and understanding of climate change, successful spawning will continue to occur at the California, Morocco and Peru Grid Cells and that the western Agulhas Bank (i.e. the Western Bank Grid Cell) and eastern Agulhas Bank (i.e. the Eastern Bank Grid Cell) will remain suitable areas for anchovy spawning in the southern Benguela system in the future.

5.2 Constraints and Caveats

There are a number of constraints that are presented by the nature of the data. Perhaps the most obvious constraint in this study is the resolution of the model used. The resolution of the CSM is relatively low at ~2.8°, and the grid cell data generated thus represent an extensive area (~280 km x 280 km). This creates some limitation for predicting impacts of climate change on anchovy (which spawn in specific locations) as processes operating on a finer scale are also likely to affect anchovy recruitment. The vertical resolution of the boundary layers is also low, which may affect features. The low horizontal resolution does not resolve land-ocean interface with the resolution of the real world. Any increase in resolution is, however, constrained by current modelling limitations and the future simulation presented in this thesis thus typifies current abilities. Another caveat associated with GCM used is that the model only uses 10 years of data for a simulation and there is great interdecadal variability. A model that incorporates a larger time scale may produce a more realistic representation of the climate variables.

A further caveat to the study is that although the Optimal Environmental Window applies well to other upwelling systems (California Current, Peru Current and Humboldt Current), it has not been successfully applied to the southern Benguela system, due to insufficient data. Furthermore, in the southern Benguela system the spawning grounds and recruitment areas are spatially distinct. The transportation of anchovy larvae from the one area to the other and the return migration is therefore an important component to the recruitment success of anchovy. The transportation mechanism of anchovy is presently speculative and warrants further investigation.

Anchovy were the main focus of the study. Yet, in the upwelling systems, both anchovy and sardine are important pelagic fish and show alternating trends in species dominance. Currently, however, the cause of regime shifts between these species is unknown. The Optimal Environmental Window applies to both anchovy and sardine (Cury and Roy 1989). It could thus be argued that both species should been examined in this thesis.

Global climate models are continually being upgraded and replaced with new models. Future research could utilise the latest models for generating climatic predictions and run comparisons with the data presented in this thesis. In this way, the fisheries industry can keep track of the best available predictions for climate change as well as the possible implications for anchovy recruitment.

REFERENCES

AHLSTROM, E.H. 1960 – Synopsis on the biology of the Pacific sardine (*Sardinops caerulea*). In: *Proceedings of the World Scientific Meeting on the Biology of Sardines and Related Species*, Rome FAO, II, Species Synopses: 415-451.

AHLSTROM, E.H. 1967 – Co-occurences of sardine and anchovy larvae in the California Current region off California and Baja California. *Calif. Coop. Oceanic Fish. Invest. Rep.* **11:** 117-135.

ALHEIT, J., V.H. ALARCON AND B.J. MACEWICZ 1984 – Spawning frequency and sex ratio in the Peruvian anchovy, *Engraulis ringens*. *Calif. Coop. Oceanic Fish. Invest. Rep.* **25:** 43-52.

AGENBAG, J.J. 1992 - A procedure for the computation of sea surface advection velocities from satellite thermal band imagery, with applications to the south-east Atlantic Ocean. PhD thesis, University of Cape Town: 394 pp.

ANDERS, A.S. 1965 - Preliminary observations on anchovy spawning off the South African coast. *S. Afr. Shipp. News Fishg Ind. Rev.* **20(11):** 103-107.

ANDERSON, J.T. 1988 - A review of size dependent survival during pre-recruit stages of fishes in relation to recruitment. *J. NW. Atl. Fish. Sci.* **8:** 55-66.

ARMSTRONG, M.J., P. CHAPMAN, S.F.J. DUDLEY, I. HAMPTON AND P.E. MALAN 1991 - Occurrence and population structure of pilchard *Sardinops ocellatus*, round herring *Etrumeus whiteheadi* and anchovy *Engraulis capensis* off the east coast of southern Africa. *S. Afr. J. mar. Sci.* **11:** 227-249.

ARMSTRONG, D.A., B.A. MITCHELL-INNES, F. VERHEYE-DUA, H. WALDRON AND L. HUTCHINGS 1987 - Physical and biological features across an upwelling front in the southern Benguela. In: *The Benguela and Comparable Ecosystems*. Payne, A.I.L., J.A. Gulland and K.H. Brink. (Eds). *S. Afr. J. mar. Sci.* **5:** 171-190.

ARMSTRONG, M.J., P.A. SHELTON, I. HAMPTON, G.M. JOLLY AND Y.C. MELO 1988 - Egg production estimates of anchovy biomass in the southern Benguela system. *Calif. Coop. Oceanic Fish. Invest. Rep.* **29:** 137-157.

ARMSTRONG, M.J. AND R.M. THOMAS 1989 - Clupeoids. In: *Oceans of Life off Southern Africa.* Payne, A.I.L. and R.J.M. Crawford (Eds). Cape Town, Vlaeberg: 105-121.

BAKUN, A. 1985 - Comparative studies and the recruitment problem: searching for generalizations. *Calif. Coop. Oceanic Fish. Invest. Rep.* **26:** 30-40.

BAKUN, A. 1990 - Global climate change and intensification of coastal ocean upwelling. *Science.* **247:** 198-201.

BAKUN, A. 1993 – The California Current, Benguela Current and Southwestern Atlantic Shelf Ecosystems: A comparative approach to identifying factors regulating biomass yields. In: *Large Marine Ecosystems – Stress, Mitigation, and Sustainability.* Sherman, K., L.M. Alexander and B. Gold (Eds). American Association for the Advancement of Science. Washington, D.C.: 199-224.

BAKUN, A. 1996 - Patterns in the Ocean: Ocean Processes and Marine Population Dynamics. University of California Sea Grant Program, San Diego, California, USA, in co-operation with Centro del Investigaciones Biológicas del Noroeste, La Paz, Mexico: 323pp.

BAKUN, A. AND R.H. PARRISH 1980 - Environmental inputs to fishing population models for eastern boundary current regions. In: *Workshop on the Effects of Environmental Variation on the survival of larval pelagic fishes.* Sharp, G.D. (Ed.). Lima, Peru, April 20- May 5, 1980, 67-104, IOC Workshop Rep. **28:** 323pp.

BAKUN, A. AND R.H. PARRISH 1982 - Turbulence, transport, and pelagic fish in the California and Peru Current systems. *Calif. Coop. Oceanic Fish. Invest. Rep.* **23:** 99-112.

BANG, N.D. AND W.R.H. ANDREWS 1974 - Direct current measurements of a shelf-edge frontal jet in the southern Benguela system. *J. mar. Res.* **32(3):** 405-417.

BERGH, M.O., J.G. FIELD, AND L.V. SHANNON. 1985 - A preliminary carbon budget of the southern Benguela pelagic ecosystem. *Int. Symp. Upw. W. Afr., Inst. Inv. Pessq.*, Barcelona. **1:** 281-304.

BERNAL, P.A. 1991 - Consequences of Global Climate Change for Oceans: A Review. *Climate Change.* **18:** 339-359.

BEVERTON, R.J.H. 1990 – Small marine pelagic fish and the threat of fishing: are they endangered? *J. Fish. Biol.* **37:** 5-16.

BLAXTER, J.H.S. AND J.R. HUNTER 1982 - The Biology of the Clupeoid Fishes. *Adv. mar. Biol.* **20:** 1-223.

BOOTH, A.J. AND T. HECHT 2000 – Utilisation of South Africa's living marine resources. In: *Marine Biodiversity Status Report for South Africa Summary.* Durham, B.D. and J.C. Pauw (Eds). National Research Foundation, Pretoria: 57-67.

BOVILLE, B.A. AND P.R. GENT 1998 – The NCAR Climate System Model, version one. *J. Climate.* **11:** 1115-1130.

BOVILLE, B.A., J.T. KIEHL, P.J. RASCH AND F.O. BRYAN 2000 – Improvements to the NCAR CSM-1 for transient climate simulations. *J. Climate.* Accepted.

BOYD, A.J. AND G. NELSON 1998 - The variability of the Benguela current off the Cape Peninsula. In: *Benguela Dynamics: Impacts of Variability on Shelf-Sea*

Environments and their living resources. Pillar, S.C., C.L. Moloney, A.I.L. Payne, and F.A. Shillington (Eds). *S. Afr. J. mar. Sci.* **3:** 145-168.

BOYD, A.J., L.J. SHANNON, F.H. SCHÜLEIN AND J. TAUNTON-CLARK 1998 - Food, transport and anchovy recruitment in the southern Benguela upwelling system of South Africa. In: *Global versus Local Changes in Upwelling Systems*. Durand M., P. Cury, R. Mendelssohn, C. Roy, A. Bakun and D. Pauly (Eds). Editions de l'Orstom, Paris: 195-209.

BOYD, A.J. AND F.A. SHILLINGTON 1994 - Agulhas Bank synthesis: physical forcing and circulation patterns *S. Afr. J. mar. Sci.* **90:** 114-122.

BOYD, A.J., J. TAUNTON-CLARK AND G.P.J. OBERHOLSTER 1992 - Spatial features of the near-surface and mid-water circulation patterns off western and southern South Africa and their roles in the life histories of various commercially fished species. In: *Benguela Trophic Functioning*. Payne, A.I.L., K.H. Brink, K.H. Mann and R. Hilborn. (Eds). *S. Afr. J. mar. Sci.* **12:** 189-206.

CAMPBELL, D.E. AND J.J. GRAHAM 1991 - Herring recruitment in marine coastal waters: an ecological model. *Can. J. Fish. Aquat. Sci.* **48:** 448-471.

COCHRANE, K.L. AND L. HUTCHINGS 1995 – A structured approach to using biological and environmental parameters to forecast anchovy recruitment. *Fish. Oceanogr.* **4:** 102-127.

CRAWFORD, R.J.M. 1980 - Seasonal patterns in South Africa's western cape purse-seine fishery. *J. Fish. Biol.* **16:** 649-664.

CRAWFORD, R.J.M. 1981 - Distribution, availability and movements of pilchard *Sardinops ocellata* off South Africa. 1964-1976. *Fish. Bull. (S. Afr.).* **14:** 1-46.

CRAWFORD, R.J.M. 1987 - Food and Population variability in five regions supporting large stocks of anchovy, sardine and horse mackerel. In: *The Benguela and*

Comparable Ecosystems. Payne, A.I.L., J.A. Gulland and K.H Brink (Eds). *S. Afr. J. mar. Sci.* **5:** 735-757.

CRAWFORD, R.J.M., L.V. SHANNON AND D.E. POLLOCK 1987 - The Benguela Ecosystem. Part 4. The Major Fish and Invertebrate Resources. *Oceanogr. Mar. Biol. Ann. Rev.* **25:** 353-505.

CSIRKE, J. 1980 – Recruitment of the Peruvian anchovy and its dependence on the adult population. In: *The Assessment and management of pelagic fish stocks.* Saville, A. (Ed.). *J. Cons. Int. Explor. Mer.* **177:** 307-313.

CULLEN, J.J. AND M.P. LESSER 1991 – Inhibition of photosynthesis by ultraviolet radiation as a function of dose and dosage rate: results for a marine diatom. *Mar. Biol.* **111:** 183-190.

CULLEN, J.J., P.J. NEALE AND M.P. LESSER 1992 – Biological weighting function for the inhibition of phytoplankton photosynthesis by ultraviolet radiation. *Science.* **258:** 1314-1316.

CURY, P. AND C. ROY 1989 - Optimal Environmental Window and pelagic fish recruitment success in upwelling areas. *Can. J. Fish. Aquat. Sci.* **46:** 670-680.

CURY, P., C. ROY, R. MENDELSSOHN, A. BAKUN, D.M. HUSBY AND R.H. PARRISH 1995 – Moderate is better: exploring nonlinear climatic effect on Californian anchovy. In: *Climate and northern fish populations.* Beamish, R.J. (Ed.). *Can. Spe. Pub. Fish. Aquat. Sci.* **121:** 417-424.

CURY, P., C. ROY AND V. FAURE 1998 – Environmental constraints and pelagic fisheries in upwelling areas: the Peruvian puzzle. In: *Benguela Dynamics.* Pillar, S.C., C.L. Moloney, A.I.L. Payne and F.A. Shillington (Eds). *S. Afr. J. mar. Sci.* **19:** 159-167.

CURY, P., A BAKUN, R.J.M. CRAWFORD, A JARRE, R.A. QUIÑONES, L. SHANNON AND H. VERHEYE 2000 - Small pelagics in upwelling systems: patterns of interaction and structural changes in "wasp-waist" ecosystems. *ICES J. mar. Sci.* **57:** 603-618.

CUSHING, D.H. 1969 - Upwelling and fish production. *FAO Fish. Tech. Pap.* **84:** 40pp.

DANABASOGLU, G. 1998 – On the wind-driven circulation of the uncoupled and coupled NCAR climate system ocean model. *J. Climate.* **11:** 1442-1454.

DE VRIES, T.J. AND W.G. PEARCY 1982 – Fish debris in sediments of the upwelling zone off central Peru: A late Quarternary record. *Deep-Sea Res.* **28:** 87-109.

DONE, T.J. 1999 – Coral community adaptability to environmental change at the scales of regions, reefs and reef zones. *Am. Zool.* **39(1):** 66-79.

DONEY, S.C., W.G. LARGE AND F.O. BRYAN 1998 – Surface ocean fluxes and water-mass transformation rates in the coupled NCAR Climate System Model. *J. Climate.* **11:** 1420-1441.

ELSBERY, R.L. AND R.W. GARWOOD 1978 – Sea-surface temperature anomaly generation in relation to atmospheric storms. *Bull. Am. Meteor. Soc.* **59(7):** 786-789.

FAURE, V. AND P. CURY 1998 – Pelagic Fisheries and Environmental Constraints in Upwelling Areas: How much is possible? In: *Global versus Local Changes in Upwelling Systems.* Durand, M., P. Cury, R. Mendelssohn, C. Roy, A. Bakun and D. Pauly (Eds). Editions de l'Orstom, Paris: 391-407.

FOWLER, J.L. AND A.J. BOYD 1998 – Transport of anchovy and sardine eggs and larvae from the western Agulhas Bank to the West Coast during the 1993/94 and 1994/95 spawning seasons. In: *Benguela Dynamics: Impacts of variability on Shelf-*

Sea Environments and their Living Resources. Pillar, S.C., C.L. Moloney, A.I.L. Payne and F.A. Shillington (Eds). *S. Afr. J. mar. Sci.* **19:** 181-195.

FURNESTIN J. AND M.L. FURNESTIN 1959 – La reproduction de la sardine et de l'anchois des cotes atlantiques du maroc. *Rev. Trav. Inst. Peches marit.* **23(1):** 79-104.

GENT, P., G. BRYAN, G. DANABASOGLU, S. DONEY, W. HOLLAND, W. LARGE AND J. MCWILLIAMS 1998 – The NCAR Climate System Model ocean component. *J. Climate.* **11:** 1287-1306.

GORNITZ, V., S. LEBEDEFF AND J. HANSEN 1982 - Global Sea level Trends in the Past Century. *Science.* **215:** 1611-1614.

HAMPTON, I. 1987 - Acoustic survey on the abundance and distribution of anchovy spawners and recruits in South African waters. In: *The Benguela and Comparable Ecosystems*. Payne, A.I.L., J.A. Gulland and K.H. Brink. (Eds). *S. Afr. J. mar. Sci.* **5:** 901-917.

HAMPTON, I. 1992 - The role of acoustic surveys in the assessment of pelagic fish resources on the South African continental shelf. In: *Benguela Trophic Functioning.* Payne, A.I.L., K.H. Brink, K.H. Mann and R. Hilborn (Eds). *S. Afr. J. mar. Sci.* **12:** 1031-1050.

HARDY, J.T. 1997 – Biological effects of chemicals in the sea-surface microlayer. In: *The Sea Surface and Global Climate Change.* Liss, P.S. and R.A. Duce (Eds). Cambridge, University Press: 339-370.

HENDERSON-SELLERS, A AND K. MCGUFFIE 1987 – A Climate Modelling Primer. John Wiley and Sons, Suffolk: 217 pp.

HUGGETT, J.A., A.J. BOYD, L. HUTCHINGS AND A.D. KEMP 1998 – Weekly variability of clupeoid eggs and larvae in the Benguela jet current: implications for

recruitment. In: *Benguela Dynamics.* Pillar, S.C., C.L. Moloney, A.I.L. Payne and F.A. Shillington (Eds). *S. Afr. J. mar. Sci.* **19:** 197-210.

HUNTER, J.R. 1977 – Behavior and survival of northern anchovy *Engraulis mordax* larvae. *Calif. Coop. Oceanic Fish. Invest. Rep.* **14:** 138-146.

HUNTER, J.R. AND B.J. MACEWICZ 1985 - Sexual maturity, batch fecundity, spawning frequency, and temporal pattern of spawning for the northem anchovy, *Engraulis mordax*, during the 1979 spawning season. *Calif. Coop. Oceanic Fish. Invest. Rep.* **21:** 139-149.

HUNTER, J.R. AND S.R. GOLDBERG 1980 - Spawning incidence and batch fecundity in northern anchovy, *Engraulis mordax. Fish Bull. (Wash.).* **77(3):** 641-652.

HUNTSMAN, S.A. AND R.T. BARBER 1977 - Primary production off northwest Africa: the relationship to wind and nutrient conditions. *Deep-Sea Res.* **24:** 25-33.

HUTCHINGS, L. 1992 - Fish harvesting in a variable productive environment – searching for rules or searching for exceptions? In: *Benguela Trophic Functioning* Payne, A.I.L., K.H. Brink, K.H. Mann and R. Hilborn. (Eds). *S. Afr. J. mar. Sci.* **12:** 297-318.

HUTCHINGS, L. 1994 - The Agulhas Bank: a synthesis of available information and a brief comparison with the other east-coast shelf regions. *S. Afr. J. Sci.* **90:** 179-185.

HUTCHINGS, L. AND A.J. BOYD 1992 - Environmental Influences on the Purse-seine Fishery in South Africa. *Investigacion Pesquera* (Chile). **37:** 23-43.

HUTCHINGS, L., M.J. GIBBONS AND R.J.M. CRAWFORD 2000 – Functional ecosystems: The pelagic open ocean. In: *Marine Biodiversity Status Report for South Africa Summary.* Durham, B.D. and J.C. Pauw (Eds). National Research Foundation, Pretoria: 16-19.

HUTCHINGS, L., H.M. VERHEYE, B.A. MITCHELL-INNES, W.T. PETERSON, J.A. HUGGETT AND S.J. PAINTING 1995 - Copepod production in the southern Benguela system. *ICES J. mar. Sci.* **52:** 439-455.

IPCC (Intergovernmental Panel on Climate Change) 1990 – Climate Change: The IPCC Scientific Assessment. Houghton, J.T., G.J. Jenkins and J.J. Ephraums (Eds). Cambridge University Press, Cambridge, UK. 365 pp.

IPCC (Intergovernmental Panel on Climate Change) 1992 - Climate Change 1992. The Supplementary Report to the IPCC Scientific Assessment. Houghton, J.T., B.A. Callander and S.K. Varney (Eds). Cambridge University Press, Cambridge, UK. 200 pp.

IPCC (Intergovernmental Panel on Climate Change) 1996 - Climate Change 1995. The Science of Climate Change: Contribution of Working Group 1 to the Second Assessment Report of the Intergovernmental Panel on Climate Change. Houghton, J.T., L.G. Meira Filho, B.A. Callander, N. Harris, A. Kattenberg and K. Maskell (Eds). Cambridge University Press, Cambridge, UK. 572 pp.

IPCC (Intergovernmental Panel on Climate Change) 2001 - Climate Change 2001. The Scientific Basis: Contribution of Working Group 1 to the Third Assessment Report of the Intergovernmental Panel on Climate Change. Houghton, J.T. and D. Yihui (Eds). Cambridge University Press, Cambridge, UK.

JAMES, A.G. 1987 - Feeding ecology, diet and field-based studies on feeding selectivity of the Cape anchovy, *Engraulis capensis* Gilchrist. In: *The Benguela and Comparable Ecosystems*. Payne, A.I.L., J.A. Gulland and K.H. Brink. (Eds). *S. Afr. J. mar. Sci.* **5:** 673-692.

JAMES, A.G. AND K.P. FINDLAY 1989 - Effect of particle size and concentration on feeding behaviour, selectivity, and rates of food ingestion by the Cape anchovy, *Engraulis capensis. Mar. Ecol. Prog. Ser.* **50:** 275-294.

JAMES, A.G., T.A. PROBYN AND L. HUTCHINGS 1989 - Laboratory-derived carbon and nitrogen budgets for the omnivorous planktivore, *Engraulis capensis* Gilchrist. *J. expl. mar. Biol. Ecol.* **131:** 125-145.

JARRE-TEICHMANN, A. AND V. CHRISTENSEN 1998 – Comparative Modelling of Tropic Flows in four Large Upwelling Ecosystems: Global versus Local Effects. In: *Global versus Local Changes in Upwelling Systems.* Durand, M., P. Cury, R. Mendelssohn, C. Roy, A. Bakun and D. Pauly (Eds). Editions de l'Orstom, Paris: 423-443.

KARENTZ, D. 1994 – Ultraviolet tolerance mechanisms in Antarctic marine organisms. In: *Ultraviolet Radiation in Antarctica: Measurements and Biological Effects.* Weiler, C.S. and P. Penhale (Eds). *American Geophysical Union Antarctic Research Series.* **62:** 93-775.

KAWASAKI, T., S. TANAKA, Y. TOBA, AND A. TANIGUCHI (Eds) 1991 - Long-term Variability of Pelagic Fish Populations and Their Environment. Pergamon Press, Oxford, New York, Beijing, Frankfort, Seoul, Sydney, Tokyo: 402 pp.

KERR, R.A. 1990 - Global Warming Continues in 1989. *Science.* **247:** 521.

KULLENBERG, G. 1971 - Vertical Diffusion in shallow waters. *Tellus.* **23:** 129-135.

LALLI, C.M. AND T.R. PARSONS 1993 - Biological Oceanography: An introduction. Buttterworth-Henemann Ltd., Oxford, England: 301 pp.

LARGIER, J.L., P. CHAPMAN, W.T. PETERSON AND V.P. SWART 1992 - The western Agulhas Bank: circulation, stratification and ecology. In: *Benguela Trophic Functioning.* Payne, A.I.L., K.H. Brink, K.H. Mann and R. Hilborn. (Eds). *S. Afr. J. mar. Sci.* **12:** 319-339.

LASKER, R. 1975 – Field criteria for survival of anchovy larvae: The relation between inshore chlorophyll maximum layers and successful first feeding. *Fish. Bull. (U.S.).* **73:** 453-462.

LASKER, R. 1978 - The relation between oceanographic conditions and larval anchovy food in the California Current: identification of factors contributing to recruitment failure. *J. Cons. Int. Explor. Mer.* **173:** 212-230.

LASKER, R. 1981 (Ed.) – Marine fish larvae. Morphology, ecology, and relation to fisheries. University of Washington Press, Seattle, WA: 131 pp.

LASKER, R., H.M. FEDER, G.H. THEILACKER AND R.C. MAY 1970 – Feeding, growth and survival of *Engraulis mordax* larvae reared in the laboratory. *Mar. Biol. (Berl.).* **5:** 345-353.

LASKER, R. AND A. MACCALL 1983 – New ideas on the fluctuations of the clupeoid stocks off California. In: *Proceedings of the Joint Oceanographic Assembly 1982*, General Symposia, Can. National Committee, Sc. Committee on Oceanic Research, Ottawa: 110-120.

LASKER, R. AND K. SHERMAN (Eds) 1981 – The early life history of fish: recent studies. The second ICES symposium, Woods Hole, April 1979. *J. Cons. Int. Explor. Mer.* **178:** 607 pp.

LLUCH-BELDA, D., R.A. SCHWARTZLOSE, R. SERRA, R.H. PARRISH, T. KAWASAKI, D. HEDGECOCK AND R.J.M. CRAWFORD 1992 - Sardine and anchovy regime fluctuations of abundance in four regions of the world oceans: a workshop report. *Fish. Oceanogr.* **1(4):** 339-347.

MACKENZIE, B.R., T.J. MILLER, S. CYR AND W.C. LEGGETT 1994 - Evidence for a dome-shaped relationship between turbulence and larval fish ingestion rates. *Limnol. Oceanogr.* **39:** 1790-1799.

MANN, K.H. AND J.R.N. LAZIER 1991 - Dynamics of marine ecosystems: biological physical interactions in the oceans. 1st Edition, Blackwell Scientific Publications, Boston: 466 pp.

MARUYAMA, K., H. HIRAKUCHI, J. TSUTSUI, N. NAKASHIKI, S, KADOKURA AND M. KADOYU 1997 - Global warming projection for 125 years using NCAR CSM coupled model. *CRIEPI Tech. Per. U97834*, Central Research Institute of Electric Power Industry, Tokyo, Japan: 24 pp.

MEEHL, G.A, W.D COLLINS, B.A. BOVILLE, J.T. KIEHL, T.M.L. WIGLEY AND J.M. ARBLASTER 2000 – Response of the NCAR Climate System Model to increased CO_2 and the Role of Physical Processes. *J. Climate.* **13(11):** 1879-1898.

MELO, Y.C. 1994a - Spawning frequency of the anchovy *Engraulis capensis*. *S. Afr. J. mar. Sci.* **14:** 321-332.

MELO, Y.C. 1994b - Multiple spawning of the anchovy *Engraulis capensis*. *S. Afr. J. mar. Sci.* **14:** 313-320.

MENDELSSOHN, R. AND P. CURY 1987 – Forecasting a fortnightly abundance index of the Ivoirian coastal pelagic species and associated environmental conditions. *Can. J. Fish. Aquat. Sci.* **44:** 408-421.

MENDELSSOHN, R. AND J. MENDO 1987 – Exploratory analysis of anchoveta recruitment off Peru and related environmental series. In: *The Peruvian Anchoveta and Its Upwelling Ecosystem: Three Decades of Change.* Pauly, D. and I. Tsukayama (Eds): 294-306. ICLARM Studies and Reviews 15. Instituto del Mar del Peru (IMARPE), Callao, Peru; Deutsche Gesellschaft für Technische Zusammenarbeit (GTZ), GmbH, Eschborn, Federal Republic of Germany; and International Center for Living Aquatic Resources Management (ICLARM), Manila, Philippines: 351 pp.

MUCK, P. 1989 – Relationships between anchoveta spawning strategies and the spatial variability of sea surface temperature off Peru. In: *The Peruvian upwelling ecosystem: dynamics and interactions.* Pauly, D., P. Muck and I. Tsukayama (Eds). *ICLARM Conf. Proc.* **18:** 168-173.

MUCK, P., O. SANDOVAL DE CASTILLO AND S. CARRASCO 1987 – Abundance of sardine, mackerel and horse mackerel eggs and larvae and their relationship to temperature, turbulence and anchoveta biomass off Peru. In: *The Peruvian anchoveta and its upwelling ecosystem: three decades of change.* Pauly D, and I. Tsukayama (Eds). *ICLARM Stud. Rev.* **15:** 268-275.

NEFTEL, A., H OESCHGER, T. STAFFELBACH AND B. STAUFFER 1988 – CO_2 record in the Byrd ice core 50,000-5,000 years BP. *Nature.* **331:** 609-611.

NELSON, G. AND L. HUTCHINGS 1983 - The Benguela upwelling area. *Progr. Oceanogr.* **12(3):** 333-356.

PAINTING, S.J., J. COETZEE AND J.L. FOWLER (submitted) - Factors contributing to variability in anchovy and sardine spawning in the southern Benguela. III. Fish distribution and anchovy success. *Fish. Oceanogr.*

PARRISH, R.H., A. BAKUN, D.M. HUSBY AND C.S. NELSON 1983 - Comparative climatology of selected environmental processes in relation to eastern boundary current pelagic fish reproduction. In: *Proceedings of the Expert Consultation to Examine Changes in Abundance and Species Composition of Neritic Fish Resources, San José, Costa Rica, April 1983.* Sharp, G. D. and J. Csirke (Eds). *FAO Fish. Rep.* **291(3):** 731-777.

PARRISH, R.H., C.S. NELSON AND A. BAKUN 1981 – Transport mechanisms and reproductive success of fishes in the California Current. *Biol. Oceanogr.* **1:** 175-203.

PAULY, D. AND M. SORIANO 1987 – Monthly spawning stock and egg production of peruvian anchoveta (*Engraulis ringens*), 1953 to 1982. In: *The Peruvian anchoveta and its upwelling ecosystem: three decades of change.* Pauly, D. and I. Tsukayama (Eds). *ICLARM Stud. Rev.* **15:** 167-178.

PAULY, D. AND I. TSUKAYAMA (Eds) 1987 – The Peruvian anchoveta and its upwelling ecosystem: three decades of change. *ICLARM Stud. Rev.* **15:** 351 pp.

PEIXOTO, J.P. AND A.H. OORT 1992 – Physics of Climate. American Institute of Physics, New York: 520 pp.

PETERMAN, R.M. AND M.J. BRADFORD 1987 – Wind speed and mortality rate of a marine fish, the northern anchovy *(Engraulis mordax). Science.* **235:** 354-356.

PETERSON, W.T., L. HUTCHINGS, J.A. HUGGETT AND J.L. LARGIER 1992 – Anchovy spawning in relation to the biomass and the replenishment rate of their copepod prey on the western Agulhas Bank. In: *Benguela Trophic Functioning*. Payne A.I.L., K.H. Brink, K.H. Mann and R. Hilborn (Eds). *S. Afr. J. mar. Sci.* **12:** 487-500.

REID, J.L., G.I. RODEN AND J.G. WYLLIE 1958 – Studies of the California current system. *Calif. Coop. Oceanic Fish. Invest. Rep.* **23:** 219-226.

RICHARDSON, A.J., B.A. MITCHELL-INNES, J.L. FOWLER, S.F. BLOOMER, H.M. VERHEYE, J.G. FIELD, L. HUTCHINGS AND S.J. PAINTING 1998 - The effect of sea temperature and food availability on the spawning success of the Cape anchovy *Engraulis capensis* in the southern Benguela. In: *Benguela Dynamics: Impacts of variability on Shelf-Sea Environments and their Living Resources.* Pillar, S.C., C.L. Moloney, A.I.L. Payne and F.A. Shillington (Eds). *S. Afr. J. mar. Sci.* **19:** 275-290.

ROTHSCHILD, B.J. AND T.R OSBORN 1988 – The effects of turbulence on planktonic contact rates. *J. Plankton Res.* **10:** 465-474.

ROY, C., P. CURY AND S. KIFANI 1991 - Optimal Environmental Window and pelagic fish reproductive strategy in upwelling areas. *International Symposium on Benguela Trophic Functioning, Resource Utilization from an Ecosystem Perspective.* 8-13 September 1991, Cape Town, South Africa.

ROY, C., C. PORTEIRO AND J. CABANAS 1995 – The Optimal Environmental Window Hypothesis in the ICES Area: The example of the Iberian sardine. *ICES Co-operative Research Report.* **206:** 57-65.

SARAVANAN, R. 1998 – Atmospheric low-frequency variability and its relationship to mid-latitude SST variability: Studies using the NCAR climate system model. *J. Climate.* **11:** 1386-1404.

SCHNEIDER, S.H. AND T.L. ROOT 1996 – Ecological implications of climate change will include surprises. *Biodivers. Conserv.* **5(9):** 1109-1119.

SERRA, R., P. CURY, AND C. ROY 1998 - The recruitment of the Chilean Sardine (*Sardinops sagax*) and the 'Optimal Environmental Window'. In: *Global versus Local Changes in Upwelling Systems.* Durand, M., P. Cury, R. Mendelssohn, C. Roy, A. Bakun and D. Pauly (Eds). Editions de l'Orstom, Paris: 267-274.

SHANNON, L.V. 1985 - The Benguela Ecosystem. Part 1. Evolution of the Benguela, physical features and processes. In: *Oceanography and Marine Biology. An Annual Review.* Barnes, M. (Ed.). Aberdeen, University Press. **23:** 105-182.

SHANNON, L.J., G. NELSON, R.J.M. CRAWFORD, AND A.J. BOYD 1996 - Possible impacts of environmental change on pelagic fish recruitment: modelling anchovy transport by advective processes in the southern Benguela. *Glob. Change Biol.* **2:** 407-420.

SHARP, G.D. 1980 - Report of the workshop on the effects of environmental variation on survival of larval pelagic fishes. In: *Workshop on the Effects of Environmental Variation on Survival of Larval Pelagic Fishes.* Lima, 20 April-5 may 1980. *IOC Workshop Report.* **28:** 15-66.

SHARP, G.D. AND J. CSIRKE 1983 – Proceedings of the expert consultation to examine changes in abundance and species composition of neritic fish resources. *FAO Fish. Rep.* **291:**1224 pp.

SHELTON, P.A. 1981 - Research on pelagic fish in the southern Benguela region. *Trans. Roy. Soc. S. Afr.* **44(3):** 365-371.

SHELTON, P.A. 1986 - Fish spawning strategies in the variable southern Benguela Current region. PhD thesis, University of Cape Town: 327 pp.

SHELTON, P.A., A.J. BOYD AND M.J. ARMSTRONG 1985 - The influence of large scale environmental processes on neritic fish populations in the Benguela Current system. *Calif. Coop. Oceanic Fish. Invest. Rep.* **26:** 72-92.

SHELTON, P.A. AND L. HUTCHINGS 1982 - Transport of anchovy, *Engraulis capensis* Gilchrist, eggs and early larvae by a frontal jet current. *J. Cons. Int. Explor. Mer.* **40 (2):** 185-198.

SHELTON, P.A. AND L. HUTCHINGS 1990 - Ocean stability and anchovy spawning in the southern Benguela Current region. *Fish. Bull.* **88(2):** 323-338.

SHEPERD, J.G, J.G. POPE AND R.D. COUSENS 1984 – Variations in fish stocks and hypotheses concerning their links with climate. *J. Cons. Int. Explor. Mer.* **185:** 225-267

SHIN, Y., C. ROY AND P. CURY 1998 - Clupeoids reproductive strategies in upwelling areas: a tentative generalization. In: *Global versus Local Changes in Upwelling Systems.* Durand, M., P. Cury, R. Mendelssohn, C. Roy, A. Bakun and D. Pauly (Eds). Editions de l'Orstom, Paris: 409-422.

SINCLAIR, M. 1988 - Marine Populations. An essay on population regulation and speciation. Washington Sea Grant Program. Univ. Washington Press, Seattle and London: 252 pp.

STEELE, J.H. 1974 - Kinds of variability and uncertainty affecting fisheries, 245-263. In: *Exploitation of Marine Communities*. Dahlem Konferenzen 1984. May, R.M. (Ed.). Springer-Verlag, Berlin, Heidelberg, New York, Tokyo: 366 pp.

THERIAULT, J.C. AND T. PLATT 1981 - Environmental control of phytoplankton patchiness. *J. Fish. Res. Board Can.* **38(6):** 368-641.

TSUTSUI, J.I. AND A. KASAHARA 1996 – Simulated tropical cyclones using the National Center for Atmospheric Research Community climate model. *J. Geophys. Res.* **101(D10):** 15013-15032.

TSUTSUI, J.I., A. KASAHARA AND H. HIRAKUCHI 1999 – The impacts of global warming on tropical cyclones – a numerical experiment with the T42 version of NCAR CCM2, Preprint volume of the 10th Symposium on Global Change Studies. J16B.3, 10-15 January 1999, Dallas, Texas.

VALDÉS, E.S., P.A. SHELTON, M.J. ARMSTRONG AND J.G. FIELD 1987 - Cannibalism in South African anchovy: egg mortality and egg consumption rates. In: *The Benguela and Comparable Ecosystems*. Payne, A.I.L., J.A. Gulland and K.H Brink (Eds*). S. Afr. J. mar. Sci.* **5:** 613-622.

VAN DER LINGEN, C.D., L. HUTCHINGS, D. MERKLE, J.J. VAN DER WESTHUIZEN AND J. NELSON (In press) – Comparative spawning habitats of anchovy (*Engraulis capensis*) and sardine (*Sardinops sagax*) in the southern Benguela upwelling ecosystem. In: *Proceedings of the Symposium on Spatial Processes and the Management of Fish Populations.* (Editors unknown). University of Alaska Sea Grant.

VAREKAMP, J.C., E. THOMAS, AND O. VAN DE PLASSCHE 1992 – Relative sea level rise and climate change over the last 1500 years. *Terra Nova.* **4:** 293-304.

WALDRON, M.E., M.J. ARMSTRONG AND B.A. ROEL 1992 – Birth date distribution of juvenile anchovy *Engraulis capensis* caught in the southern Benguela

ecosystem. In: *Benguela Trophic Functioning*. Payne, A.I.L., K.H. Brink, K.H. Mann and R. Hilborn (Eds). *S. Afr. J. mar. Sci.* **12:** 865-871.

WILLIAMSON, D.L., J.J. HACK AND J.T. KIEHL 1995 – Climate sensitivity of the NCAR Community Climate Model (CCM2) to horizontal resolution. *Clim. Dyn.* **11:** 377-397.

WOOSTER, W.S. AND J.L. REID 1963 – Eastern boundary currents. In: *The Sea.* Hill, M.N. (Ed.). Interscience Pub., New York. **2:** 253-280.

WROBLEWSKI, J.S AND J.G RICHMAN 1987 – The non-linear response of plankton to wind mixing events – implications for survival of larval northern anchovy. *J. Plankt. Res.* **9(1):** 103-123.

ZHANG, M.H., W.Y. LIN AND J.T. KIEHL 1998 – Bias of atmospheric short-wave absorption in the NCAR community climate models 2 and 3: Comparison with monthly ERBE/GEBA measurements. *J. Geophys. Res.* **103:** 8919-8925.

Personal Communications

Associate Professor Bruce C. Hewitson. 2001. Climate Systems Analysis Group. Environmental and Geographical Science Department. University of Cape Town.

Dr Carl Van Der Lingen. 2001. Marine and Coastal Management. Cape Town.

Dr Claude Roy. 2001. Oceanography Department. University of Cape Town.